UNIVERSITA' DEGLI STUDI DI PARMA

Dipartimento di Chimica

Ph.D. in Science and Technology of
Innovative Materials
Cycle XXV

Sensing bitterness in bakery and beverage food products

Alessandro Bedini

Coordinator:

Prof. Enrico Dalcanale

Supervisors:

Dr. Michele Suman

Prof. Enrico Dalcanale

Author :

Alessandro Bedini

Alla mia Famiglia

e

a Greta

CONTENTS

Introduction : Taste Chemistry and common industrial procedures for taste evaluation

1

1.1 Taste Physiology and Chemistry

Most of the human senses, including hearing, touch or thermoception, are based on the detection of physical events like sounds wave, pressure and temperature variation respectively. Taste and smell senses are dedicated to the detection of hydrosoluble and volatile molecules respectively and they are true chemical sensing systems constituted by thousands of cells that work as chemoreceptors inside the nose mucosa and the oral cavity. Scientists started to study the functioning of the human taste rationalizing the ability of the human tongue to distinguish four different basic tastes: sweet, bitter sour and salty. In the early years of the XXth century the Japanese scientist K. Ikeda [1] reported the discovery of a fifth taste called umami, referred to the ability to sense L-glutamate.

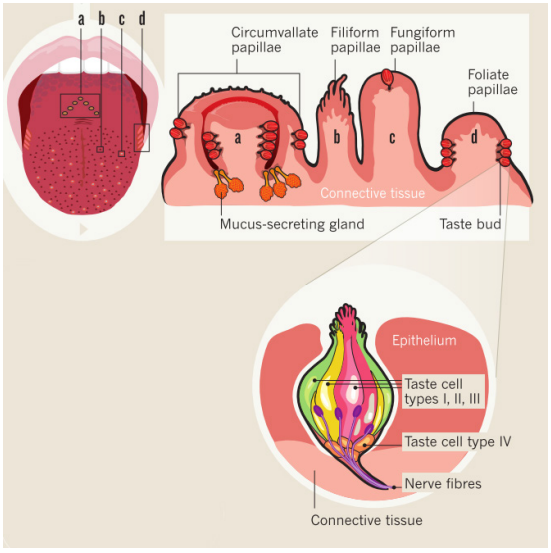

Figure 1 – Human tongue, papillae types and taste buds structure.

All five tastes are sensed by specific receptors cells present on the surface of the human tongue as shown in figure 1. Taste receptor cells, which are assembled into taste buds that are distributed across different papillae on the tongue and palate epithelium, are dedicated to the detection of molecular markers specific for a specific taste.

Taste perception is used by living for the detection of foodstuff that ensures the correct intake of energy and to avoid the ingestion of potential poisonous molecules. Sweet taste regulate the correct intake of high-energy carbohydrates, salty taste

detect sodium inside foodstuff, umami sense the presence of protein. Sour and bitter taste are used for another purpose, they are used principally to sense potential threat for the body like microbiological adulteration or presence of xenobiotical and potentially dangerous molecules.

The study of the molecular basis of the human sense of tasting started in the XXth century after the discovery of synthetic molecules with a particular intense taste : Saccharin discovered by C. Fahlberg in 1878 (approximately 200 times sweeter than sucrose) and phenilthiocarbammide discovered by Fox in 1931 [2].

1.2 Receptors analysis

Only in recent years, thanks to the large advances made in molecular biology, it has been possible to hypothesize the mechanism by which the human tongue operates in the detection of the five tastes [3].

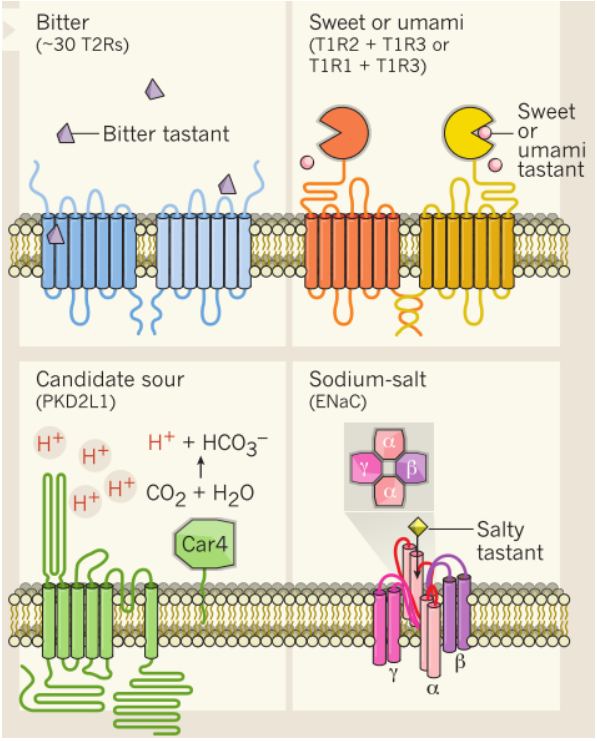

Figure 2 – Taste receptor's types: Bitter taste (T2R's family), Sweet taste (T1R2 + T1R3 dimer), and Umami taste (T1R1 + T1R3 dimer), Sour Taste (PKD2L1 receptor), Salty taste (ENaC receptor).

In figure 2 the five main classes of trasmembrane proteins known to play a role as taste receptors on the human tongues papillae are summarized. Only sweet and umami taste receptors are fully characterized and their mechanism of transduction is completely understood. This is due to their structural affinities (they share one protein in the binding site and also they have similar structures) and to the importance that they have in the dairy food industry. Studies on umami and sweet detection led to the development of artificial sweeteners and umami enhancers widely used in the last decades.

Sour and salty tastes are related to two different receptors (PKD2L1 and EnaC respectively) which are, for the moment, not completely known and there are only hypothesis on their action. The bitter taste is the most complicated, due to the presence of more than 30 different receptor dedicated to its detection. For the moment only few information are known about how this taste detection works.

1.3 Sweet taste

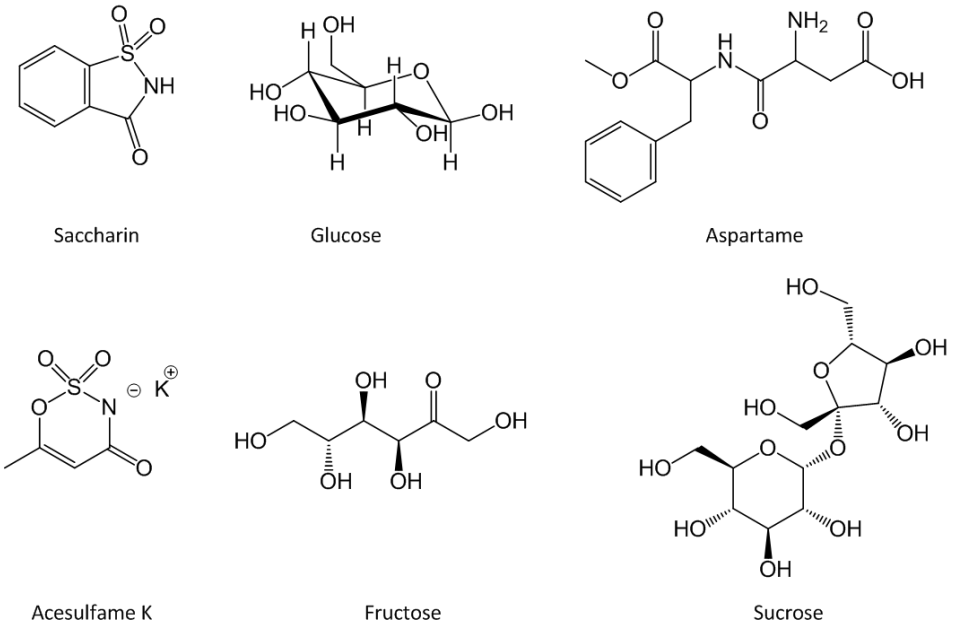

Figure 3 – Typical sweet molecole : i) Saccharin; ii) Glucose; iii) Aspartame; iv) Acesulfame K; v) Fructose; vi) Sucrose.

The perception of taste is commonly used by mammals to identify foodstuffs with a high throughput of energy. The sweet taste is used for the identification of

carbohydrates that are one of the main molecular classes used for the synthesis of ATP in mammals (figure 3). Humans has a high threshold level to sense this class of molecules due to the fact that this sense is used to collect large quantities of carbohydrates inside the body to have more energy at our disposal; so foodstuffs with a high content of sugars are sensed with a limited sweet taste. There is a big and appreciable difference between the taste intensity of the carbohydrates; for example fructose is sweeter than sucrose in a water solution even if the last one has one unit of fructose inside its structure. In the last decades of the nineteenth century new molecules sweeter than sucrose were discovered by chance like aspartame or Saccharin (known to be ~ 400 times sweeter than sucrose), and this posed the basis for the artificial sweeteners industry. In spite of this discovery no model for the sweet taste detection mechanism was proposed until the sixties. Shallenberger and Acree [4] proposed in 1967 the so called AH-B model (figure 4) that described the requisite that a molecule necessitates to have in order to elicit a sweet taste.

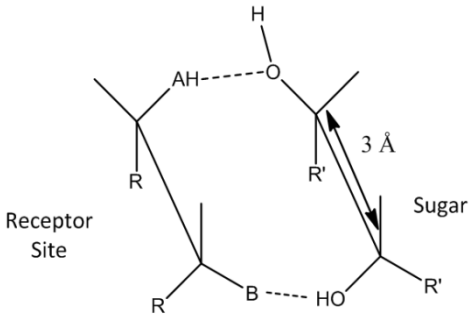

(1)

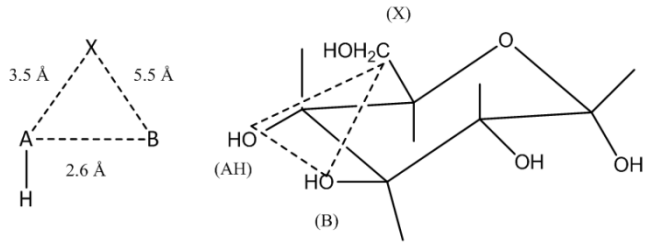

(2)

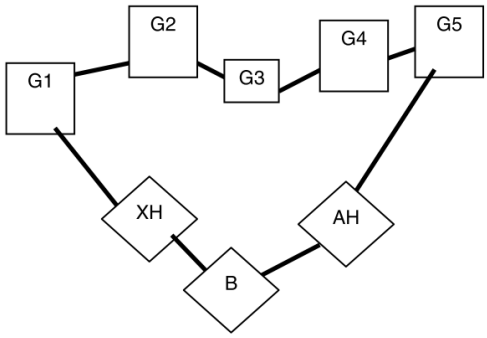

Figure 4 – 1) AH-B model (1967); 2) Kier AH-B-X model (1972); 3) Tinti and Nofri multi-site model (1996).

From this point of view a sweetener need an hydrogen bond donor group spaced by 3 Å from an hydrogen bond acceptor group. With these simple 3 elements is possible to describe the taste of carbohydrates and some artificial sweetener like Saccharin and Acesulfame K but other sweetener like the Aspartame cannot be fully described with this model: another interaction is needed to better describe it. In the 1972 Kier (figure 4) expanded the model [5] proposing the interaction with a third group (commonly referred as X group, so the model became AH-B-X model) that modulate the bound between ligand and receptor by a hydrophobic interaction. The presence of this group enhances the interaction. With the introduction of this 3rd interaction Aspartame sweet taste can be fully described. The interest in the exploitation of the sweet taste recognition mechanism grown over the last three decades due to the interest in lowering the sugars contents inside the foodstuffs for diet oriented products. The recent advances in molecular biology made possible to fully describe the sweet taste receptor structure. The sweet receptor is defined as a class C GPCR that exists as a heterodimer of the T1R2 and T1R3 subunits; these membrane proteins compose the so called “Venus flytrap” receptor. The binding of glucophore generate a chemical cascade signal that stimulate the releasing of Ca^{2+} ions outside the tastant cell and the subsequent neural impulse transmission that end with the taste perception by the human brain. Tinti an Nofri [6] (figure 4) fully described for the first time the exact structure of the Venus flytrap binding site making possible the rational synthesis of artificial sweeteners like Neotame (~7000 times sweeter than sucrose, figure 5).

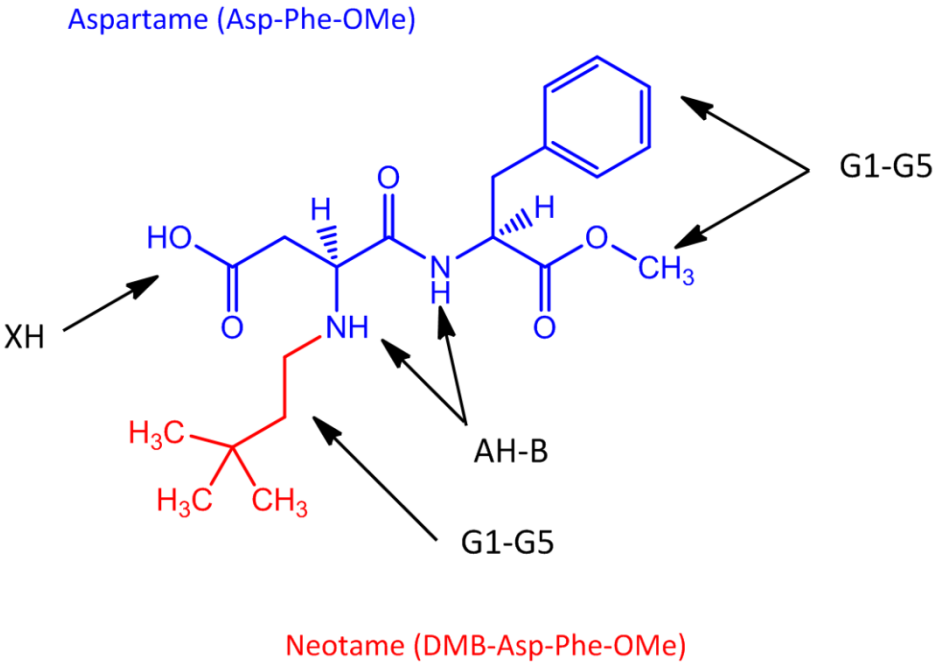

Figure 5 – Neotame structure Vs Aspartame in the Tinti-Nofri model of interaction.

In this model is possible to recognize the same binding site previously proposed by the AH-B model and the Kier model. It is possible to identify another hydrogen donor group (XH in figure 4) and several hydrophobic interaction points labeled as G, for a total of 8 interaction points. On the basis of these consideration is now possible to explain why sweetener like Neotame are able to elicit a so intense sweet taste also at low concentrations. This molecule is similar to the aspartame (a widely used sweeter largely diffused as food additive) with which has in common the peptide Asp-Phe-OMe; the only difference is represented by the presence of dimethyl-butyl group alkylated to the nitrogen of the aspartame moiety. This group is responsible of the enhanced interaction of the binding site via multiple interactions with lipophilic aminoacids inside the Venus flytrap.

The receptor for sweet taste was fully characterized by a biochemical point of view in 2006 by Nelson [7], demonstrating the mechanism of transduction.

1.4 Umami taste

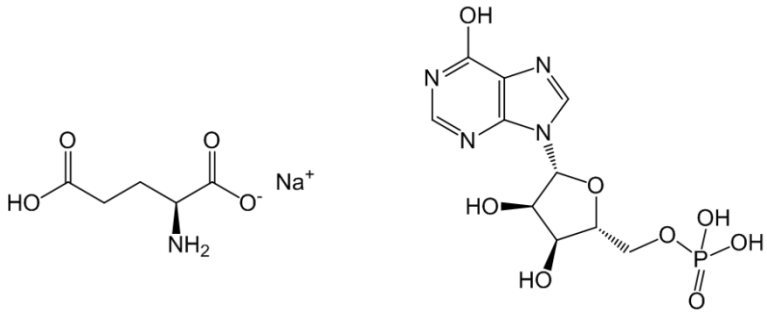

Sodium glutamate Inosine monophosphate

Figure 6 – The main umami molecular marker (Sodium glutammate) and the umami taste enhancer (Inosine monophosphate, IMP).

The umami taste was introduced as a fifth basic taste in the early years of the twentieth century but it is demonstrated only in recent years that there is a specific receptor dedicated to the detection of umami molecular markers [8]. Umami sensing is related to the detection of amino acid in foodstuffs and in particular it is generated by the presence of mono- and di-sodiumglutammate. The choice of this molecule is related to the fact that it is largely present in almost every protein in different amounts, so the presence of this amino acid can be related with the presence of proteins in large quantities and this taste is commonly perceived in fish or meat based product. Also vegetables, like soy shoots that elicit a particular intense umami taste. The receptor identified has a structure similar to the one of sweet taste, it is also a heterodimeric protein composed by two subunit T1R1/T1R3 with a binding site working in the same way of the one dedicated to the sweet taste detection.

The umami taste can be enhanced when there is sodium glutamate in presence of 5'-ribonucleotides such as inosine-5'-monophosphate (IMP) and guanosine-5'-monophosphate (GMP), and this synergy is a hallmark of this taste quality [9]. This two molecules cannot interact alone with the receptor but they enhance the interaction between the amino acid and the receptor when the last one is inside the binding site positioning on the top of it and determining a stronger closure of the receptor; this interaction determine a more intense chemical cascade in the G-coupled protein that enhance the intensity of the perceived umami taste [10]. With 5'-ribonucleotides it is possible to obtain a strong umami taste without using large quantities of sodium glutamate and limiting the concentration of sodium inside products.

1.5 Sour taste

The mechanism of transduction of the sour taste appears to be related only to the detection of carboxylic acids [10]. First attempt of rationalization of this taste linked it directly to the concentration of hydronium ions present in water [12]. This hypothesis disappeared when it was clear that only organic acids were able to stimulate a sour taste response. Also including other variables like the dissociation constants and the tritable acidity, the sour taste intensity cannot be completely explained. Recent hypothesis directly correlate the molar concentration of all the species present in solution that posses at least one carboxylic group [13].

From a structural point of view the requisite to elicit sour taste is the presence of one or more carboxylic groups, in addition to other functional groups.

The transduction mechanism is not still clear and it is also not clear how many receptors are involved in this type of transduction. The main candidate, as sour taste receptor, is the transmembrane protein PKD2L1 [14]. Recent studies indicate that this protein is involved, in collaboration with another ion cell, in the detection of sour taste molecular markers.

1.6 Salty taste

One of the principal cations, essential for the correct function of every cell in our body and present in every fluid compartment of the body, is sodium. Its exceptional role forced mammalians to develop dedicated sensing system oriented to its detection also at low concentration levels. The sensitivity of this cation has a double role serving simultaneously as a warning system against hyper salty foodstuff and to satisfy the daily intake of sodium necessary for the correct functioning of the human body. The salt taste sensation is affected by systemic conditions that result in increased levels of aldosterone (a corticosteroid that regulate the sodium and water absorption); this suggests that salt taste perception may involve one of that hormone's cell sodium transporter targets. The involved receptor is the epithelial-sodium channel (ENaC) a trasmembrane protein constituted by 3 different subunits (α,β,γ ENaC) recently attributed to the salty taste detection [15] in the mammalian.

1.7 Bitter taste

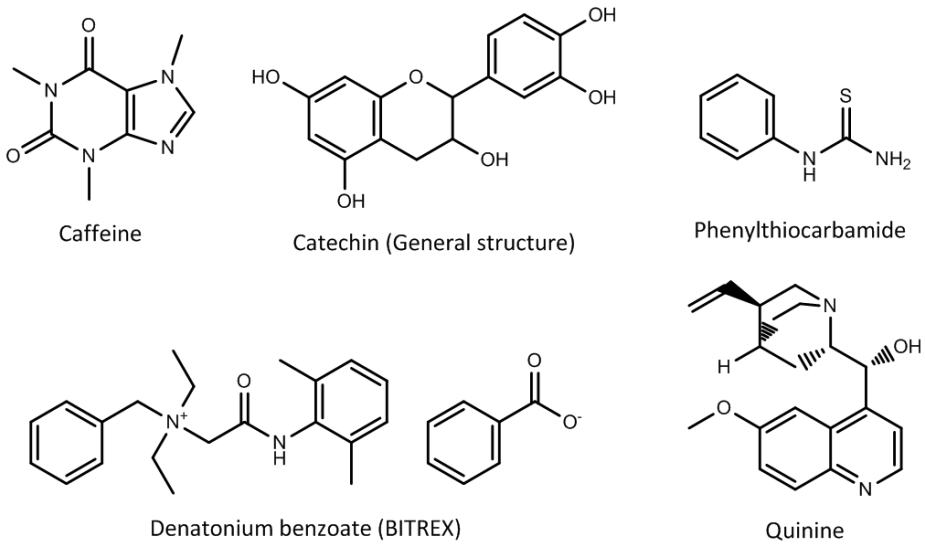

Figure 7 – Some examples of the differences between the structures of bitter taste molecular markers.

The ability to sense poisonous and potentially threatening substances is elicited by bitter taste. Generally alkaloids are all sensed as bitter and they also express a pharmacological effect on the body. Despite these considerations bitter taste is also known to be a pleasant taste and it can be found in a large variety of foodstuff that are based on cocoa, coffee and tea. Molecules like caffeine are largely used in the food industry as a common additive in particular in cola based drinks; also polyphenols elicit a bitter taste note. Bitter taste can be expressed by a large variety of molecular markers. The most important, from a storical point of view is phenylthiocarbamide (PTC), discovered by Fox. This molecule posed the basis for the start of the research about how the gustatory system works. Fox discovered that some subjects sense the PTC as strongly bitter instead others are insensitive towards this molecule. Due to the large structural variety of toxic molecules that can be ingested, mammalians are able to sense as bitter molecules with, apparently, no structural affinity like the ones shown in figure 7. This large number of molecular targets is reflected in the large numbers of receptor (up to 30 named as TAS2R's) that are used by the tongue for bitter taste detection [16]. The effective mechanism of sensing is still unknown. From a structural point of view it is known that they are glycoproteins [17] and have the ability to form both homo- and hetero-oligomers [18]. The sensibility of this class of receptor is high with a general low threshold limit, necessary to avoid the introduction of potentially

poisonous compounds [19] even at low concentrations. Recent experiments suggested that the same TAS2Rs respond to several different bitter taste compounds [20]. This means the this receptor class posses a low specificity toward a particular class of substances and the response toward a large number of molecule suggest a shape recognition driven detection [21]. There are a lot of different information about the TAS2R receptor family [22] but not an harmonized mechanism of interaction that explain deeply the binding site involved with a particular functional group.

1.8 Profile attribute analysis (PAA)

The taste determination is commonly made, in the food industry, using sensorial analysis. In this type of measures a group of people try to correlate the intensity of a taste to a particular foodstuff. This type of correlation between particular tastant molecules and their concentration inside foodstuffs was firstly exploited by Beidler. In 1954 Beidler [23] proposes, after an intense work on animals, an equation were the human physcophysical response is proportional to neurophysical response:

$$\frac{\boldsymbol{R}}{\boldsymbol{R_{max}}} = \frac{\boldsymbol{C}}{\boldsymbol{k + C}}$$

Were R is the response of the consumer and R_{max} is maximum response obtainable and C is the logarithmic function of the molar concentration of the tastant used in the experiment. The Beidler equation to psychophysical data allows determination of stimulus parameters (the binding constant, *K*, and the maximum response, R_{max}) for human taste perception. It may also open the way to express taste intensities in terms of a universal Taste Coefficient, a potentially more tractable way of quantifying the taste response. Objectify this sense in measurable and reproducible scale is a hard task, commonly exploited by panel groups. A panel group is formed by a trained or not trained personal (it depends by the method used) that taste foodstuff and describe their overall experience in terms of attributes on a previously defined scale of intensity. Descriptive sensory tests are focused on the examination of a product through the evaluation of the attributes perceptible by the five sense organs (organoleptic attributes), such as colour, odour, taste, touch, texture and noise. They involve the detection (discrimination) and description of both the qualitative and quantitative sensory components in a consumer product by panels of judges. The construction of an organoleptic profile of the target product allows the judges to discriminate product each one from the others and also to quantify some of these differences. Until 1960's the sensory analysis techniques used in quality control assurance were based on the personal experience of the expert assessors deputed.

This operational methodology was not much reproducible in order to be considered a standardizable technique due to the lack of reproducibility from one manufacturing site to the other. Therefore more standard procedures were developed to achieve the same goal but in a more reproducible way, that can be used as analytical tool to evaluate the quality of products. Descriptive methodology used in sensory allow the panel test to compare reference of standard with daily produced products and allow the comparison between prototypes to understand the possible responses by the consumers. It can be also used for the monitoring and the evaluation of changes in the product during time due to aging, shelf life, modifications induced by packaging on the final perception made by the consumer. There are different approaches to the application of sensory analysis to quality control (flavour profile method, quantitative descriptive method, quantitative flavour profiling, spectrum method...) but all of these methodologies are based on the use of a panel of judges with a certain degree of training or a particular orientation toward the investigated product. In almost all methodologies it is required that panellist have a certain degree of sensitivity toward the sensorial aspects investigated. In order to obtain reproducible and precise data from the panel test, the panelist must be trained on the evaluation of certain sensorial aspects to develop something that can be called a "common language" : describe the investigates products attributes with great precision. During this "learning stage" the panel is exposed to a wide variety of different products in order to experience as much variability as possible to detect the main differences with products and become as more descriptive as possible. At this stage it is also important that the products chosen are representative of the one that later will be investigated. Once the team of panellist is selected it is important to train it to the description of the main product attributes and determine a scale of intensity which is representative of the product explored. The procedure used during this stage is commonly chosen as function of the method used for the sensory analysis.

In the following paragraph different techniques for sensory analysis were listed but not all of them were used directly in the food industry for quality control of flavour. Generally the description of flavours using a panel test can be achieved in different ways such as:

1. Flavour Profile Method (FPM) and Profile Attribute Analysis (PAA)
2. Quantitative Descriptive Analysis Method (QDA)
3. Texture profile method (TPM)
4. Spectrum Method

1.8.1 FPM and PAA

The Flavour Profile Method was one of the first tries to develop an analytical descriptive method for the food industry [24]. In FPM the panel group discuss about the different aspects detectable of the product's flavour. Commonly the panel is composed by 4-6 judges who are firstly trained to define precisely the flavour aspects. The original FPM method used numbers and symbols which replace the numerical scales that allowed the use of statistical methods to describe the results obtained by the panel. With the introduction of the numerical scale this method became Profile Attribute Analysis (PAA). An advantage in this method is that assessors are highly trained on the detection of a specific attribute and it raises the efficiency in the detection of small variation of a single attribute. Furthermore it can be done with a small group of panellists, making possible a easily coordination; this is also the drawback of this method because the departure of a single member of the panel has a deep impact on the final response made by the whole panel.

1.8.2 QDM

In QDM is used every day, non technical, language with a larger panel that the one used in PAA. Panelists are selected from a large group of candidates and selection is made according to the ability of the candidate to discriminate the differences among the proposed samples. [24]. The selected panellists are trained using reference products to develop the appropriate terminology to describe the samples. There is a relatively freedom of choice in the terminology and each panellist develop his own terminology.
In QDA the information about the product's attributes are provided by the relative differences in the responses showed by the judges. In this case there is the huge problem in comparing the results obtained between different laboratories and in a different time. This technique has a low reproducibility in respect of PAA but it does not require high trained panellist to be done.

1.8.3 TPM (Texture Profile Method)

The texture profile method was developed for the classification of the texture of foodstuffs to fill a gap between consumers and producers in the terminology commonly used for the description.

Three groups of attributes are used for the description:

- Mechanical
- Geometric
- Others

The panellist are chosen only by their ability to discriminate by the attributes used. All the attributes are measured on a scale developed by Szczsmiak that cover a large number of tastes and attributes like textures commonly sensed in the food and each point of the scale is referred to a specific food.
With this method, panellists are able to describe the sensation perceived during the mastication by the consumer. The main drawback of this technique is the large amount of hours spent in performing the training session of the panel group and the limitation to the textural aspects of the food described.

1.8.4 Spectrum Method

In the spectrum method the panel group is not focused only on the textural aspect in the description of the samples but they use also a huge list of different attributes to describe products with a complete "spectrum". The panel group is focused only on one type of product and develops its terminology using technical language in term of taste, flavour, color or appearance for example. The scale at which each panel refers is based on an extensive use of standards samples. This operation dramatically reduces the use variability and errors done by the panel. The drawback of this technique is the large amount of time spent in the training session, in the development of an appropriate terminology and in the introduction to scaling that can be in the order of tens of hours. In addition, common standards used for the Spectrum method are not available outside the USA and the analysis cannot be done without appropriate standards because the scales used for the attributes are absolute and not relative.

These four techniques have the same objective, to describe the final consumer experience in an objective scale that can be used to make comparisons between different foodstuffs made by the same company and also made by competitors. QDM is a methodology that allows the panel to describe the overall sensation, its interlaboratory reproducibility is very low. TPM is a sensorial analysis that can be used only to describe the product texture for the description of flavour it is a very limited technique. This gap is filled by the Spectrum Method that allow a deeper description of different attributes in foodstuff, but the unavailability of the standards used as reference outside the USA make impossible to apply this methodology. FPM/ PAA

instead are the best compromise between the number of attributes that can be used and their variability sensed by the panellist and the time spent to make a measure.

1.9 Artificial taste sensors: the electronic tongue

Panel tests are able to detect every minimal difference in a sample and they can be updated with new definition with a dedicated training session. Furthermore, they can describe the same taste sensed by the customer and they are very useful in the detection of particular issues like the presence of disliked off-taste. Even if this technique is largely used in the development of new products and in tracking particular problems, the food industry has a great interest in developing standard measure systems focused on the detection of taste. The standardization of this operation makes possible to check a large quantities of products for quality control purposes avoiding the major limit in using a trained panel test: the number of samples checked daily. Monitoring the final product that exit from the production plant is a daily analysis performed by the workers directly on the manufacturing site. The main problem of this check is that it is performed by personnel with experience but not trained on an objective a reproducible scale, so the response that they give back on the product quality cannot be measured over the time. All the information about problems on the production line (like overcooking or undercooking, for example) is not easily tracked; also the effect of unwanted changing in ingredients is lost and the possible impact on the final product cannot be tracked rationally. To overcome these problems, in the last decades, a lot of different devices were developed aimed to exploit the taste task in different media. The idea behind electronic tongue is the same of electronic noses: the number of molecular target is too high to develop a specific sensor for each taste molecular marker. With a reduced amount of sensors, with partial specificity toward classes of analytes or completely aspecific, it may be possible to draw a map of the taste. This principle is called “blind analysis”. The biggest limit of this analysis is that, for the moment, it is possible to analyze only liquid samples because all these systems are based on electrodes (using amperometric or voltammetric measures). Obviously the best operative environment is based on water solutions and in literature there are reported a lot of works focused, for example, on detection of taste in wine [25-26], beer [27-28] fruit juice [29] and even oil [30]. For solids an analysis is still possible but the introduction of an extraction is needed to obtain an analyzable sample: in this case the time for data collection rise. The electrodes can be simple naked electrodes [31], polymer covered [32] or enzyme covered [33] arranged in array. The signal recorded by every electrode is commonly processed using multivariate methods like PCA (Principal Component Analysis). This type of analysis returns a fingerprint typical for the investigated sample that can be

correlated with a library of fingerprints (recorded in the same condition) of the samples known to be reference standard. In this case all the information about the specific molecular target is lost. The system is able to sense the analytes all together with one measure but it is not able to tell us if a particular molecules changed concentration and it is responsible for a particular taste changing. Another limitation of this technique is the calibration phase, the instrument need to be trained to detect which samples have the desired taste and which have one or more particular defect or adulteration in respect to the standard ones. One array of sensors can be used for the analysis of different matrices; a proper calibration is needed for each group of samples. For example it is not possible to make a measure of the sweetness of a fruit juice using a calibration for the same taste developed on smoothies. The two matrices are characterized by the presence of fruit in large quantities and in some cases can be made with the same ingredients. However there are differences in the consistency , in the viscosity and also in the final composition of the beverage. Array sensors analysis is focused on the measure of the overall environment not simply on a specific target. Even if some sensors are targeted to a specific marker the response still depends on the matrix explored. So a specific training session is needed every time the sample matrix is changed in order to obtain information about the taste of the new foodstuff.

In conclusion, this technique provides a powerful tool to investigate taste with a standardized and reproducible method, as needed for quality control in industry. In special cases this system can be used to detect particular defects in foodstuff as an alternative to the panel test (despite a panel is still needed for the development of the library of standards). The difficulty to analyze solid samples in short times limits the number of samples that can be done daily making less easy to use this technique for quality control purposes in the food industry.

References

[1] "*New Seasonings*"; Ikeda K.; Journal of the Chemical Society of Tokyo; Vol. 30, Pg. 820-836 (1909). Translated in English: "*New Seasonings*"; Ogiwara Y., Ninomiya Y.; Chemical Senses; Vol. 27 Pg. 847-849 (2002).

[2] "*The relationship between chemical constitution and taste*"; Fox A. L.; Proceedings of the National Academy of Science; Vol. 18, Pg. 115-120 (1932)

[3] "The finer points of taste"; Trivedi B. P.; Nature; Vol. 486, Pg. S2-S3 (2012).

[4] "*Molecular theory of the sweet taste*"; Shallenberger R. S. , Acree T. E.; Nature, Vol. 216, Pg. 480-482, (1967).

[5] "*Molecular theory of sweet taste*"; Kier L.B.; Journal of Pharmaceutical Science, Vol. 61,Pg. 1394–1397, (1972).

[6] "*Sweetness reception in man: the multipoint attachment theory*"; Nofri C., Tinti J.; Food Chemistry, Vol. 563, Pg. 263–274, (1996).

[7] "*Mammalian sweet taste receptors*"; Nelson, G. et al.; *Cell*, Vol.106, Pg. 381–390, (2001).

[8] "*An amino acid receptor*"; Nelson G. et al.; Nature, Vol. 416, Pg.199–202, (2002).

[9] "*Measurement of the relative taste intensity of some l-α-amino acids and 5'-nucleotides*"; Yamaguchi S., et al.; Journal of Food Science; Vol.36, Issue 6, Pg. 846-849, (1971)

[10] "*Molecular mechanism for the umami taste synergism*"; Zhanga F., Klebanskyb B., Fineb R. M., Xua H., Pronina A., Liua H., Tachdjiana C. and Xiaodong L.; Proceedings of the National Academy of Science; Vol.105, Issue 52, Pg. 20930-20934, (2008).

[11] "*The Chemistry and Physiology of Sour Taste—A Review";* E. Ramos Da Conceicao Neta, S. D. Johanningsmeier And R. F. Mcfeeters ; Journal Of Food Science Vol. 72, Issue 2, (2007).

[12] "*The relation of the taste of acids to their degree of dissociation*" ; T.W.Richards ; Journal of the American Chemical Society, Vol. 20, Issue 6, Pg. 121, , (1898).

[13] "*Time-intensity evaluation of acid taste in subjects with saliva high flow and low flow rates for acids of various chemical properties*"; O. Lugaz , A.M. Pillias, N. Boireau-Ducept , A. Faurion, Chem. Senses, Vol. 30 Pg. 89, 2005.

[14] "*The candidate sour taste receptor, PKD2L1, is expressed by type III taste cells in the mouse*"; S. Kataoka, R. Yang, Y. Ishimaru, H. Matsunami, J.C. Kinnamon, T. E. Finger; Chem. Senses, Vol. 33, Issue 3, Pg. 243, 2008.

[15] "*The cells and peripheral representation of sodium taste in mice*"; J. Chandrashekar et al.; Nature Vol. 464, Pg. 297, 2010.

[16] "*T2Rs Function as Bitter Taste Receptors*", J. Chandrashekar et al.; Cell,Vol. 100, Pg. 703–711 (2000).

[17] "*Functions of human bitter taste receptors depend on N-glycosylation*"; Reichling C., Meyerhof W., Behrens M.; Journal of Neurochemistry; Vol.106, Pg. 1138–1148, (2008).

[18] "*Oligomerization of TAS2R bitter taste receptors*"; Kuhn C., Bufe B., Batram C., Meyerhof W.; Chemical Senses,Vol.35, Pg. 395–406 (2010).

[19] "*Genetics of taste and smell: poisons and pleasures*"; Reed D.R., Knaapila A., Progress in Molecular Biology and Translational Science,; Vol.94, Pg.213–240, (2010).

[20] "*The molecular receptive ranges of human TAS2R bitter taste receptors*"; Meyerhof W., Batram C., Kuhn C., Brockhoff A., Chudoba E., Bufe B., et al.; Chemical Senses, Vol.35, Pg.157–170 (2010).

[21] "*Structural requirements of bitter taste receptor activation*"; Brockhoff A., Behrens M., Niv M.Y., Meyerhof W.; Proceedings of the National Academy of Science, Vol.107,Pg. 11110–11115, (2010).

[22] "*Bitter taste receptor research comes of age: From characterization to modulation of TAS2Rs*"; Behrens M., Meyerhof W.; Seminars in Cell & Developmental Biology (2012), DOI : 10.1016/j.semcdb.2012.08.006. In press

[23] "*A theory of taste stimulation*"; Beidler L.M., Journal of General Physiology, Vol., Pg. 133-139 (1954).

[24] "*Descriptive sensory analysis: past, present and future*"; Murray J.M., Delahunty C.M, Baxter I.A., Food Research International, Vol. 34, Pg. 461-471 (2001).

[25] "*State of the Art in the Field of Electronic and Bioelectronic Tongues – Towards the Analysis of Wines*"; Zeravik J., Hlavacek A., Lacina K., Skladal P.; Electroanalysis, Vol.21, Issue 23, Pg. 2509 – 2520, (2009)

[26] "*Instrumental measurement of bitter taste in red wine using an electronic tongue*"; Rudnitskaya A., Nieuwoudt H. H., Muller N., Legin A., du Toit M., Bauer F. F.; Analytical and Bioanalytical Chemistry, Vol. 397, Pg. 3051–3060, (2010).

[27] "*Instrumental measurement of beer taste attributes using an electronic tongue*"; Rudnitskaya A., Polshin E., Kirsanov D., Lammertyn J., Nicolai B., Saison D., Delvaux F. R., Delvaux F., Legin A.; Analytica Chimica Acta, Vol. 646, Pg. 111–118 (2009).

[28] "*Prediction of bitterness and alcoholic strength in beer using an electronic tongue*"; Arrieta Á. A., Rodríguez-Méndez M. L., de Saja J. A., Blanco C. A., Nimubonad D.; Food Chemistry, Vol. 123, Pg.642–646, (2010).

[29] "*Electronic tongue based on an array of metallic potentiometric sensors*"; Lvovaa L., Martinelli E., Mazzone E., Pede A., Paolesse R., Di Natale C., D'Amico A.; Talanta, Vol. 70, Pg. 833–839, (2006).

[30] "*Evaluation of the polyphenolic content of extra virgin olive oils using an array of voltammetric sensors*"; Rodriguez-Mendez M.L., Apetrei C., de Sajac J.A.; Electrochimica Acta, Vol. 53, Pg. 5867–5872, (2008).

[31] "*Electronic tongue based on an array of metallic potentiometric sensors*"; Lvova L., Martinelli E., Mazzone E., Pede A., Paolesse R., Di Natale C., D'Amico A.; Talanta, Vol. 70, Pg. 833–839 (2006).

[32] "*Amperometric sensors based on poly (3,4-ethylenedioxythiophene)-modified electrodes: Discrimination of white wines*"; Pigani L., Foca G., Ionescu K., Martina V., Ulrici A., Terzi F., Vignali M., Zanardi C., Seeber R.; Analytica Chimica Acta, Vol. 614, Pg. 213–222 (2008).

[33] "*Monitoring the aging of beers using a bioelectronic tongue*"; M. Ghasemi-Varnamkhasti, M. L. Rodríguez-Méndez, S. S. Mohtasebi, C. Apetrei, J. Lozano, H. Ahmadi, S. H. Razavi, J. A. de Saja; Food Control , Vol.25, Pg. 216-224 (2012).

2

Bitter taste molecular markers detection in liquid phase : RP-HPLC-MS

2.1 Bitter Taste Molecular Markers in Bakery Commodities

One of the main markets in bakery products is represented by biscuits. In the food industry the organoleptic description of foodstuff is deputed to panel groups that use several sensorial techniques, like the previous mentioned profile attribute analysis (PAA), to describe the overall taste of the final product. This approach cannot be easily used for daily quality control because it is time consuming and allows to analyze only a limited number of samples daily. The main advantage is represented by the matrix independent approach that this technique offers; it is not important if the panel group is checking a solid or a liquid sample, a sweet or a bitter compound, because each session start with an adequate training tuned on the product to be tested. On the other hand, in chemical analysis, this advantage is often absent and each analysis is strongly matrix dependent. Generally, aspect and taste are checked by the workers directly on the manufacturing site and these analyses are mainly made on the basis of the experience of the personnel and with the support of standard and photographs like in the case of the colour check.
In bakery products like biscuits the main recurrent tastes are sweetness and bitterness. Saltiness and sourness play generally a minor role and are strongly present only in few special cases. Umami taste is completely absent. The sweetness detection is generally a simple task were only sucrose is used in the recipe because it is commonly added in large quantities. Bitterness is more difficult to be evaluated because several factor can influence and modify its intensity. Before developing a dedicated method for the bitter taste molecular markers detection, it is important to know with precision what we are searching for and which concentration ranges we have to face.
Bitter tastants are a class of molecular markers that cover a wide range of functional groups and in many case there is no presence of structural affinities between the molecules. As mentioned in the previous chapter, bitter taste is mainly used by humans to detect molecules potentially harmful for our body. This task is achieved thanks to a network of more than 30 different receptors dedicated to the bitter detection on the human tongue.
Classes of molecules able to elicit this taste are:

- Inorganic salts, like iron sulphate for example;
- Alkaloids and amines, for their potential pharmacologic effect
- Polyphenols, metabolized in different pathways inside the body
- Maillard compounds
- Peptides (not all the peptides are sensed as bitter but certain sequences [1] that are originated in special cases are sensed as bitter)

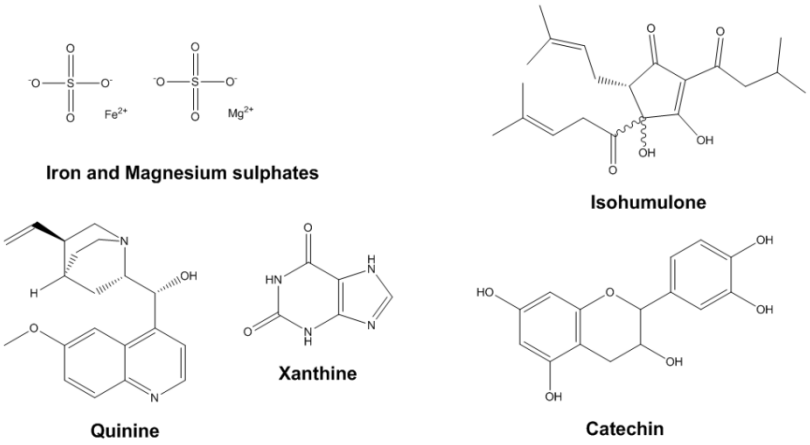

Figure 1- Examples of known bitter taste molecular markers with no structural affinities

Some of these bitter taste markers structures are summarized in figure 1. There is no structural affinity between them; this is possible because the transduction system used by the tongue to sense the bitterness is tuned to sense the largest variety possible of molecules in order to detect known and unknown xenobiotic molecules. Luckily only a limited number of bitter tastant molecules are present in biscuits. In order to identify these classes, an analysis of raw materials used in the recipe is necessary, together with the understanding of potential bitter molecules that can be produced during the thermal process.

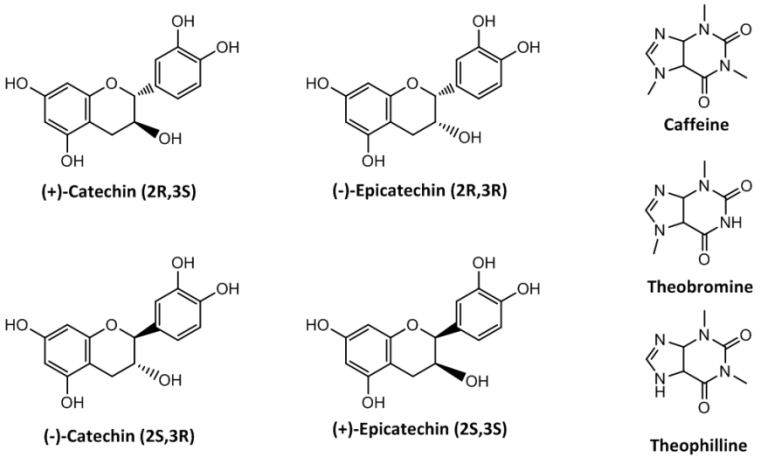

Figure 2- Main bitter taste molecular markers in biscuits

The main recurring ingredients in biscuits are cocoa (in the form of cocoa powder or chocolate), nuts and coffee. All these ingredients have in common two main classes of molecules that are known to elicit a bitter taste (figure 2):

- Xanthines (caffeine, theobromine and theophylline).
- Polyphenols ((+)/(-) epicatechin and (+)/(-)catechin), mainly.

Xanthines are present in larger amount in all these food products [2]. Xanthines are characterized by a typical purinic base structure with a pirimidinic ring directly fused with an imidazole (Figure 2). The three main xanthines taken here into account are: caffeine (1, 3, 7-trimetilxanthine), theobromine (3, 7- dimethylxanthine) and theophylline (1, 3-dimethylxanthine); their concentration in natural products is variable but the only constant is that the theophylline is the less concentrated in all natural products. All the three molecules elicit a bitter taste and they are responsible for the bitter taste of coffee and chocolate.
Polyphenols are a large class of aromatic compounds with a different amount of hydroxyl group directly attached to the aromatic ring. The most studied polyphenols have flavan-3-ol skeleton (like catechins shown in Figure 2) and in many cases they are esterified with one or more gallate units. Polyphenolic compounds represent a wide group of phytochemicals produced by plants subgroups of phenolic acids, flavonoids, natural dyes, lignans etc. . . . These natural bioactive compounds possess a variety of beneficial effects including antioxidant and anticarcinogenic activities, protection against coronary diseases as well as antimicrobial properties [3,4]. They are present in different types of food like tea leaves, coffee, cocoa and all their derivatives in large amounts. In all of these products they are responsible for the astringent taste that they elicit in the mouth even if they are present only at relatively low concentration (0.1-0.3 mg g^{-1} in cocoa powder for example) [*5*].

2.2 HPLC Methods in Quality Control

A lot of efforts were made in the last two decades to develop appropriate sensors for the taste discrimination, without using panel groups. This challenge was partially accomplished during the ’90 when many of different sensor systems called “electronic tongues” were developed. These sensors are, mainly, array of electrodes of different types (naked-, polymer or enzyme coated- electrode) that work in amperometry o voltammetry and are based on the blind analysis technique [5-10]. In most of these examples the molecular origin of the taste is lost in order to obtain a larger discrimination of the analyzed samples. Only few examples are based on the detection

of specific molecular targets [11-12] but in these cases there is no parallelism between the perceived taste (using PAA or other sensorial techniques) and the concentration of the analyte.

Other types of studies are aimed to understand, and reproduce with different methods, the molecular recognition mechanism of the human tongue [13-14]. Even if understanding the recognition of opportune molecular target remains a challenge, the real problem remains the identification of these molecular markers in complex matrices. If we want to maintain the molecular origin of the taste during the analysis we need first to know what we are searching for and in which concentration these molecules are present inside the samples.

In scientific literature there are available different examples of HPLC methods for the detection of xanthines or polyphenols in food matrices based on the use of DAD [15-17] or MS [18-19], but all of these methods are not able to detect these two classes of substances in a single chromatographic run .

For routine analysis of caffeine, theobromine and theophylline on coffee and beverages it is mostly used liquid chromatography (LC) in the reversed-phase mode C18 silica phases combined with UV-detection. For the determination in complex biological matrices the coupling of the LC system to mass spectrometry (MS) via electrospray ionization (ESI) [20-23] and fast atom bombardment (FAB) [24] are also proposed.

To have shorter analysis time we developed a new liquid chromatography method able to detect in a single run both the polyphenols and xanthines of interest.

Our attention has been focused on bakery products with a different percentage content of coffee and chocolate, like biscuits, and very different bitter taste measured by a Profile attribute analysis (PAA). The hypothesis was that cookies with very high bitter taste have also a high concentration of polyphenols and xanthines at the same time.

2.3 Experimental – LC-MS Analysis

2.3.1 Materials And Methods (Chemicals)

Methanol and acetic acid were HPLC grade solvent and supplied by Merck (Darmstadt, Germany). Ultrapure water was used throughout the experiments (MilliQ system, Millipore, Bedford, MA, USA). Glass vials with septum screw caps were supplied by Agilent. Syringe filters (0.45 µm) were made by Whatman (Maidstone, Kent, UK), glass vials with septum screw caps were supplied by Agilent Technologies (Willimgton, DE, USA). Theobromine and caffeine were purchased from Fluka. (+)-Catechin, (-)-epicatechin, (-)-epigallocatechin gallate and theophylline were obtained from Sigma Aldrich (Milan, Italy). Eleven different categories of commercial biscuit packs were

collected from the market, stored wrapped in aluminum foil at room temperature and progressively used for building the necessary calibration curves.

2.3.2 Sample preparation

Different types of commercial cookies were analyzed spreading from cream based cookies to cocoa based cookies. The sample solutions were prepared suspending 10 g in 20 mL of MeOH/H_2O 7/3 and heating at 80°C the dispersion in a Teflon sealed flask for 30 minutes. The dispersion was cooled at room temperature then filtrated on Buchner and filled up with the MeOH solution to restore the starting volume.

2.3.3 Calibration and quantification

All standard solutions were made dissolving in a 7/3 methanol / water solution using a ultrasound bath for 15 minutes obtaining solutions with a concentration ranging from 0.02 to 10 mg/kg^{-1} for all standards with the exception theobromine where the concentrations ranged from 0.25 to 10 mg/kg^{-1}. All standard solutions were filtered with a 0.45 μm syringe filter before LC-MS analysis. Quantification was based on the areas of the corresponding peaks of the ion monitored by external standard calibration modality.

2.3.4 Liquid chromatography

The pump used for reversed-phase high-performance liquid chromatography (RP-HPLC) was a Surveyor LC Pump (Thermo Finnigan, San Jose, CA, USA), a dual piston quaternary pump with a built–in vacuum degasser. The chromatography separation was performed using a Phenomenex Gemini 5U C18 110A (length : 15 cm, diameter : 2 mm) column with a flow rate of 0.4 mL/min and a gradient solvent program based on 5% acetic acid in water and methanol (see table 1). Injections (10 μL) were made using a Surveyor Autosampler (Thermo Finnigan).

Time (min)	Flux (ml/min)	H_2O (5% acetic acid)	MeOH (5% acetic acid)
0	0.2	90%	10%
3	0.2	60%	40%
21	0.2	20%	80%
25	0.2	20%	80%
27	0.2	90%	10%

Table 1 – MeOH/H_2O gradient in RP-HPLC-MS

2.3.5 Mass spectrometry

Electrospray ionization (ESI) experiments were carried out in a Ion-Trap LXQ (Thermo Scientific) mass spectrometer with a capillary temperature of 350 °C and a sheat gas flow rate set to 20 units; the spray voltage was kept at 4 kV and the capillary voltage was kept at -23 V for negative ion monitoring; instead, for positive ion monitoring, spray voltage was kept at 5 kV and capillary voltage +25 V. All parts of the equipment and data processing were performed by the computer software Xcalibur (Thermo Finnigan). In table 2 all the monitored transitions are summarized.

Analyte	Molecular weight	Ion scan mode	m/z	Normalized Collision energy
Caffeine	194.2	SRM	195±1 ; 138±1 (ESI +)	25
Theobromine	180.2	SIM	181±1 (ESI +)	/
Theophylline	180.2	SIM	181±1 (ESI +)	/
(-) Epicatechin	290.3	SRM	289±1 ; 138±1 (ESI -)	17
(+) Catechin	290.3	SRM	289±1 ; 245±1 (ESI -)	17
(-) Epigallocatechin gallate	458.4	SIM	457±1 ; 331±1 (ESI -)	13

Table 2 – ESI-MS and MS/MS parameters for Xanthines and Polyphenols.

2.4 Results and Discussion

The different samples of commercial biscuits were chosen on the base of their bitter taste. The bitterness was measured using the standard Profile Attribute Analysis (PAA) with a group of 8 panellists trained using solutions of caffeine at different concentration in a scale from 4 (no bitterness) to 12 (strong bitterness). The references used by panelists for the training sessions are summarized in table 3 .

Standard solutions	Bitter taste Index (B.I.)	Concentration of the solution (% v/v)	
Standard 1 (low bitterness)	4	0,05%	Caffeine
Standard 2 (average bitterness)	8	0,10%	Caffeine
Standard 3 (high bitterness)	12	0,20%	Caffeine

Table 3 – Solutions used by panellists during the PAA training phase

The analyzed samples span from the one made with cream, honey and cereal that don't elicit a reasonable bitter taste (bitter taste index less than 4). The addition of raw materials like chocolate or cocoa change the sensed taste enhancing the overall bitterness, so the biscuit made with chocolate and cream or made with nuts and cocoa have a higher score around 6. The only two samples made with a higher amount of chocolate and higher percentages of cocoa elicit the higher bitterness: this is the case of chocolate biscuits 2 and 3 that scored a bitter taste index of 7 and 8 respectively. It is interesting to note that biscuits considered very bitter in reality shown an index that is only in the middle point of the panel group training solutions range (table 4).

Sample	Bitter Taste Index (B.I.)
Chocolate Biscuit 3	*8*
Chocolate Biscuit 2	*7*
Nuts Biscuit	*5*
Chocolate & cream Biscuit	*5*
Chocolate Biscuit	*6*
Chocolate & cream Biscuit 2	*5*
Coffee Biscuit	*4*
Lemon Biscuit	*4*
Cereal Biscuit	*< 4*
Honey Biscuit	*< 4*
Cream Biscuit	*< 4*

Table 4 – Bitter taste index for every sample tested

These entire samples were extracted using a hot methanol water solution (ratio 7/3 v/v) as previously described and then all the standards were analyzed using ESI-LC-MS-MS, in order to determine the best detection conditions for all the analytes. All the ESI parameters were varied in real time to evaluate and provide the highest intensities for the detectable characteristic signals and to optimize operative conditions in terms of capillary potential and eluent composition.

Based on these results we chose to monitor the xanthines using positive scan mode for caffeine and negative scan mode for theobromine. Instead polyphenols were scanned in negative mode.

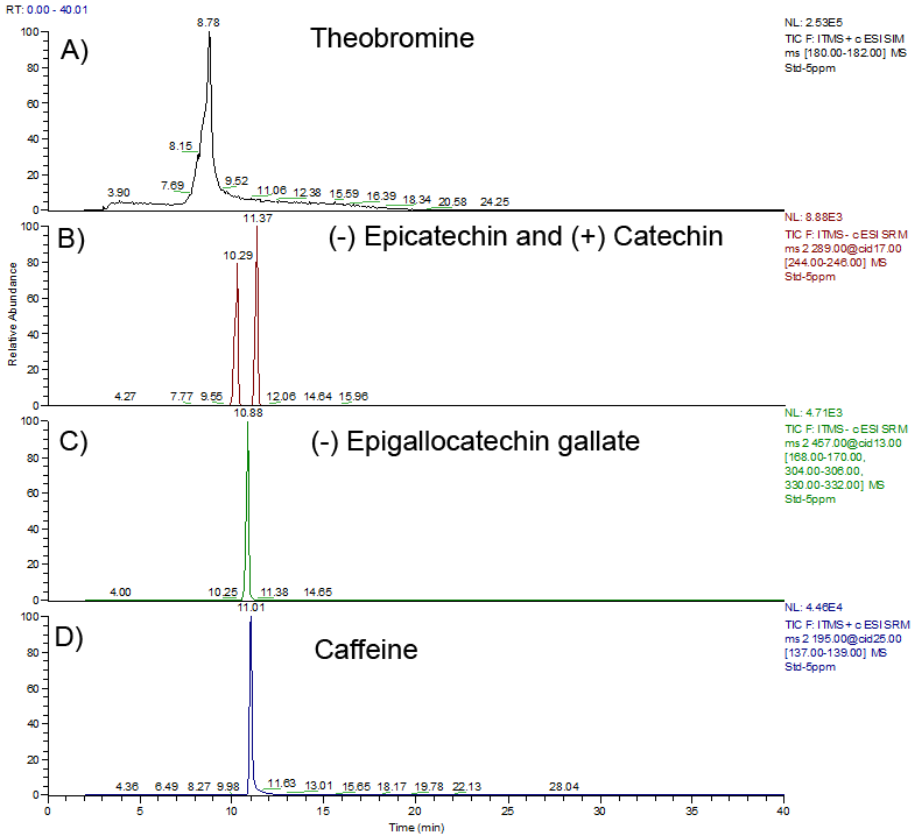

Figure 3- Typical standards chromatograms : a) Theobromine (SIM), b) (-) Epicatechin and (+) Catechin (SRM), c) (-) Epigallocatechin gallate (SRM), d) Caffeine (SRM).

To evaluate the content of xanthines a polyphenols in several bakery products extracts (as described in the sample preparation section) by HPLC-MS detection, we developed the LC method using a standard C18 column and trying to optimize the retention time of all the analytes to better separate them. Results are summarized in figure 3.

We made a calibration curve for each analyte observed using standards (made in a MeOH/H_2O 7/3 (v/v) solution) at different concentration and two replicates for each concentration level: 0.02 mg kg^{-1}, 0.05 mg kg^{-1}, 0.2 mg kg^{-1}, 1 mg kg^{-1}, 3 mg kg^{-1}, 5 mg kg^{-1}, 10 mg kg^{-1}. For the theobromine the lowest level used was 0.2 mg kg^{-1}. In figure 3 there are shown the 4 calibration curves exploited for the following quantitative analysis.

(-) Epicathechin R^2 = 0.9976

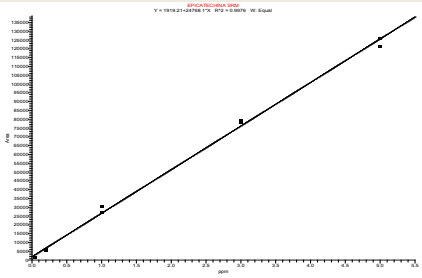

(+) Cathechin R^2 = 0.9991

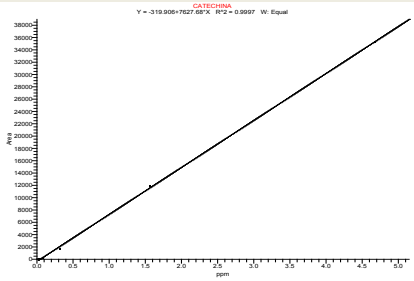

Caffeine R^2 = 0.9977

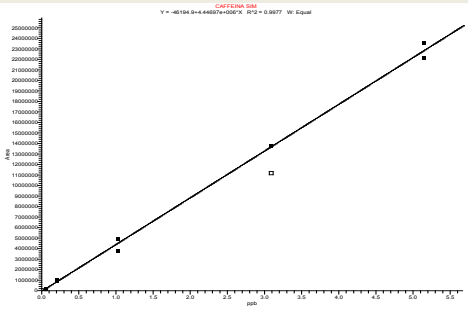

Theobromine R^2 = 0.9989

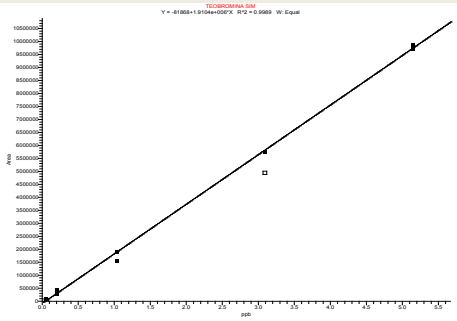

Figure 4- Examples of calibration curves

Each biscuit sample extract was analyzed using this method, giving back a chromatogram like the one shown in figure 5. The presence of theophylline and epicatechin gallate was found too low to be quantified for our purposes. For this reason these markers were not quantified. So for common analysis all the detected markers were restricted to theobromine, caffeine, (+)-catechin and (-)-epicatechin only.

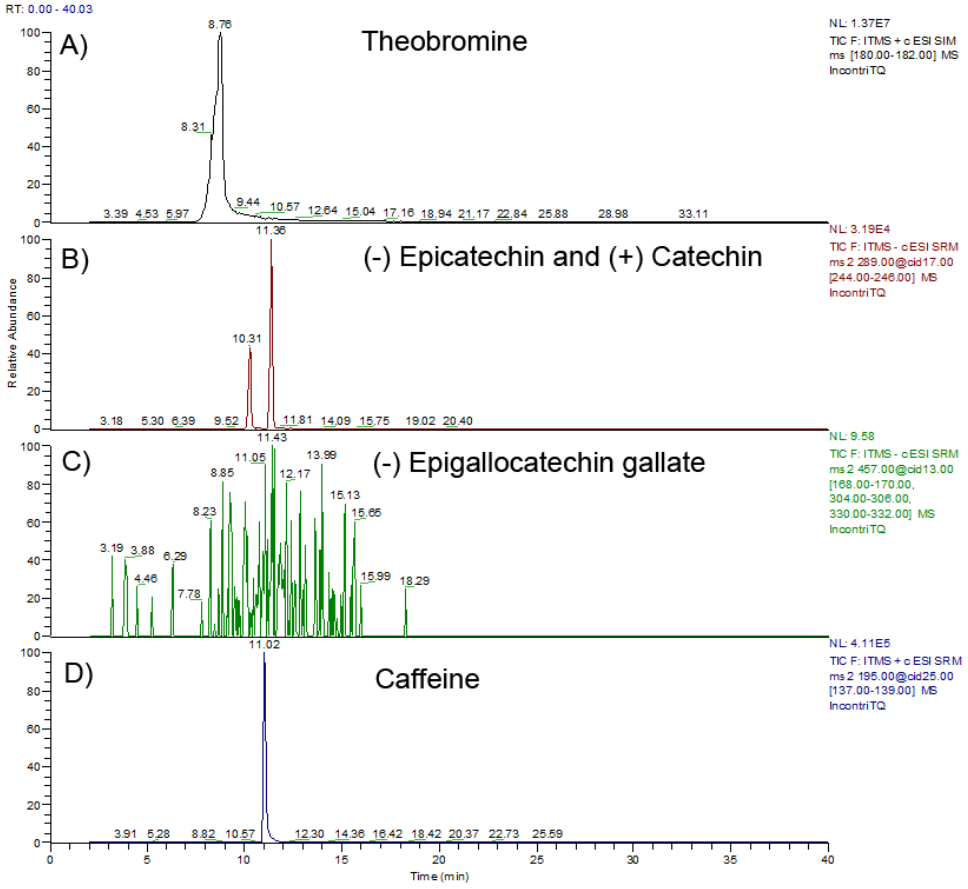

Figure 5 – Typical biscuit sample extract chromatogram related to chocolate biscuit 3 : a) Theobromine (SIM), b) (-) Epicatechin and (+) Catechin (SRM), c) (-) Epigallocatechin gallate (SRM), d) Caffeine (SRM).

2.5 Method validation

2.5.1 Limit of detection (LOD) and Limit of Quantitation (LOQ)

The detection limit (y_d) and quantification limit (y_q) were preliminarily calculated as signals based on the mean blank (y_{bm}) and the standard deviation (SD) of the blank signals as follows:

$$y_d = y_{bm} + 2TSD \qquad y_d = y_{bm} + 10TSD$$

(LOD) *(LOQ)*

Equation 1 – Definition of LOD and LOQ

Where T is a constant of the t-Student distribution (one-sided) depending on the confidence level and the degrees of freedom (v = n-1, n = number of measurements). A total of 10 blanks measurements were performed to calculate y_{bm} and *SD*. As blank we choose an extract of cream based cookie that is known to have the low content of xanthines and polyphenols among the sample tested. The results obtained with six different extracts of the same sample are reported in table 5.

Yd and y_q were converted from the signal domain to the concentration domain to estimate the limit of detection (LOD) and limit of quantification (LOQ). In this way, under the optimized LC-MS conditions and operating in SRM mode, LOD and LOQ for each analyte are summarized in table 5.

	Theobromine	Caffeine	Epicatechin	Catechin
LOD	5,2	0,7	0,5	0,1
LOQ	15,3	1,6	2,4	0,2

Table 5 – LOD and LOQ results for the method

2.6 Data obtained on real samples

Eleven types of commercial biscuits were analyzed in order to demonstrate the effective application of this method and the matching with the sensorial data. The biscuits were chosen on the base of their percentage of cocoa that we suppose being directly proportional to xanthines and polyphenols content.

The entire samples obtained from cocoa based biscuits were diluted by a 100 factor using the same extraction solution. For biscuits with no cocoa inside, any dilution was performed. Results are summarized in table 6. There is a very good matching between the PAA and the ESI-MS data for the extreme cases : the lower 4 entries show concentration both of polyphenols and xanthines under the LOQ or close to it. In these cases the PAA highlighted a bitterness taste index lower than 4; this means that these biscuits don't elicit any appreciable bitter taste. On the opposite case we can see another good matching between the two analyses for biscuits with a high concentration of cocoa: here there is a perfect parallelism between the analytes concentrations and the bitterness taste index. Also the remaining analyzed cases show a good matching between the techniques, but in this case there are several unexpected minimal mismatching. For example, comparing biscuits like chocolate and cream biscuits 1 and 2 we can see that the PAA results are the same (a score of 5) but the content of bitter taste molecular markers are not the same.

SAMPLE	BITTER TASTE INDEX (B.I.)	THEOBROMINE mg kg^{-1} on solid	CAFFEINE mg kg^{-1} on solid	TOTAL XANTINE mg kg^{-1} on solid	CATECHIN mg kg^{-1} on solid	EPICATECHIN mg kg^{-1} on solid	TOTAL POLYPHENOLS mg kg^{-1} on solid
Chocolate Biscuit 3	*8*	1428	98	1526	28.7	54.9	83.6
Chocolate Biscuit 2	*7*	851	79	930	17.2	38.5	55.7
Nuts Biscuit	*5*	833	58	891	9.6	7.2	16.8
Chocolate & cream Biscuit 1	*5*	773	71	844	16.1	37.6	53.7
Chocolate Biscuit	*6*	626	45	671	9.6	6.2	15.8
Chocolate & cream Biscuit 2	*5*	210	17	227	3.1	2.2	5.3
Coffee Biscuit	*4*	35	31	66	0.3	0.3	0.6
Lemon Biscuit	*4*	36	4	40	1.0	< 2.4	≤3.4
Cereal Biscuit	*< 4*	< 15	< 1.6	< 17	0.2	< 2.4	≤ 2.6
Honey Biscuit	*< 4*	< 15	< 1.6	< 17	< 0.2	< 2.4	≤ 2.6
Cream Biscuit	*< 4*	< 15	< 1.6	< 17	< 0.2	< 2.4	≤ 2.6

Table 6 – Results on real samples

Polyphenols are 10 times more concentrated in Chocolate and Cream biscuit 1 than in 2 and xanthines are 4 times more concentrated anyway there is apparently no difference in the taste sensed by the panel. This fact could be due principally to the dispersion of the cocoa inside the final product. These two samples are very different in formulation, in the case of the most concentrated one the cocoa is localized in spots and probably it is abundant in xanthines and polyphenols but it is surrounded by a great quantity of cream based matrix that contain the markers only at the trace level. Even if the final concentration of markers is high their effect is probably not completely sensed by the panel. On the other hand the ESI-MS analysis was made on a ground sample. Therefore the difference in matrix homogeneity probably makes possible that the bitter taste index results the same even if the absolute markers content is different.

2.7 Conclusions

A new ESI-LC-MS-MS methodology for the simultaneous quantification of main xanthines and polyphenols as bitter taste molecular markers in bakery commodities was developed. The LOQ showed by this method are 1,6 mg kg^{-1} in the case of caffeine

and 15,3 mg kg^{-1} in the case of theobromine. The LOQ related to the polyphenols are 0.2 mg kg^{-1} in the case of (+)-catechin and 2,4 mg kg^{-1} in the case of (-) - epicatechin. There is a very good correlation between the sensorial data obtained using PAA and the HPLC method. Results show that sensorial analysis in the food can be done using the data collected on particular classes of biscuits.

ESI-MS is able to detect differences at the molecular level with a great precision but it is not able to predict differences due to the matrix physical composition. Therefore it is a good starting point for a taste analysis based on the molecular origin of the taste itself, but alone it is not sufficient for a complete description of a particular taste attribute directly related to morphology and texture of the analyzed biscuit .

References

[1] "*Bitter peptides and bitter taste receptors*"; Maehashia K., Huang L.; Cellular and Molecular Life Sciences, Vol. 66, Pg. 1661–1671 (2009).

[2] "*Theobroma cacao L., the Food of the Gods: A scientific approach beyond myths and claims*"; Rusconi M., Conti A.; Pharmacological Research, Vol. 61, Pg. 5–13 (2010).

[3] "*Plant polyphenols: Structure, occurrence and bioactivity*"**;** Pietta P., Minoggio M., Bramati L.; Studies in Natural Products Chemistry, Vol. 28, Pg. 257–312 (2003).

[4] "*Anti-diabetic activity of green tea polyphenols and their role in reducing oxidative stress in experimental diabetes*"; Sabu M.C., Smitha K., Ramadasan K.; Journal of Ethnopharmacology, Vol.83, Pg. 109-/116 (2002).

[5] "*Evaluation of bitterness and astringency of polyphenolic compounds in cocoa powder*"; Serra Bonvehi J., Ventura Coll F.; Food Chemistry, Vol. 60, Nr. 3, pg. 365-370 (1997).

[6] "*Comparison of sensory and consumer results with electronic nose and tongue sensors for apple juices*"; Bleibaum R. N., Stone H., Tan T., Labreche S., Saint-Martin, E. Isz, S.; Food Quality and Preference, Vol.13, Nr.6, Pg. 409–422 (2002).

[7] "*Amperometric electronic tongue for food analysis*"; Scampicchio M., Ballabio D., Arecchi A., Cosio S. M., Mannino S.; Microchimica Acta, Vol. 163, Pg. 11–21 (2008).

[8] "*Amperometric sensors based on poly (3,4-ethylenedioxythiophene)-modifiedelectrodes : Discrimination of white wines*"; Pigani L., Foca G., Ionescu K., Martina V., Ulrici A., Terzi F., Vignali M., Zanardi C., Seeber R.; Analytica Chimica Acta, Vol.614 , Pg. 213–222 (2008).

[9] "*Nonspecific sensor arrays ("electronic tongue") for chemical analysis of liquids*"; Vlasov Y., Legin A., Rudnitskaya A., Di Natale C., D'Amico A.; Pure Applied Chemistry, Vol.77, Pg. 1965 (2005).

[10] "*Electronic tongues and their analytical application*";Vlasov Y., Legin A., Rudnitskaya A.; Analytical and Bioanalytical Chemistry; Vol. 373,Pg. 136-146 (2002).

[11] "*Determination of Bisulfites in Wines with an Electronic Tongue Based on Pulse Voltammetry*"; Labrador R.H., Olsson J., Winquist F., Martinez-Manez R., Soto J.; Electroanalysis; Vol.21, Nr. 3, Pg. 612–617 (2009).

[12] "*Electronic Tongue Integrated Sensor System Based on an Array of Ion-Selective Field-Effect Transistors for Multicomponent Analysis of Liquid Media*"; Ipatov A., Moreno L., Abramova N., Bratov A., Vlasov Y., Dominges K.; Russian Journal of Applied Chemistry, Vol. 82, No. 8, pp. 1384−1389 (2009).

[13] "*Artificial β-Barrels*"; Sakai N., Mareda J., Matile S.; Accounts Of Chemical Research, Vol. 41, Nr. 10, Pg. 1354-1365 (2008).

[14] "*Synthetic pores with reactive signal amplifiers as artificial tongues*"; Litvinchuk S., Tanaka H., Miyatake T., Pasini D., Tanaka T., Bollot G., Mareda J., Matile S.; Nature Materials, Vol. 6, Nr.8, Pg.576-580 (2007) .

[15] "*Sensory-Guided Decomposition of Roasted Cocoa Nibs (Theobroma cacao) and Structure Determination of Taste-Active Polyphenols*"; Stark T.,Bareuther S., Hofmann T.; Journal of Agricultural and Food Chemistry, Vol. 53, Pg. 5407−5418 (2005).

[16] "*Survey of Polyphenol Constituents in Grapes and Grape-Derived Products*"; Xu Y., Simon J. E., Welch C., Wightman J. D., Ferruzzi M. G., Ho L., Passinetti G. M., Wu Q.; Journal of Agricultural and Food Chemistry, Vol.*59*, Pg. 10586–10593 (2011).

[17] "*The electronic tongue and ATR–FTIR for rapid detection of sugars and acids in tomatoes*"; Beullensa K., Kirsanov D., Irudayaraj J., Rudnitskaya A., Legin A., Nicolai B. M., Lammertyna J.; Sensors and Actuators B Vol. 116, Pg. 107–115 (2006).

[18] "*Analysis of caffeine, theobromine and theophylline in coffee by near infrared spectroscopy (NIRS) compared to high-performance liquid chromatography (HPLC) coupled to mass spectrometry*"; Huck C.W., Guggenbichler W., Bonn G.K.; Analytica Chimica Acta Vol.538, Pg. 195–203 (2005).

[19] "*LC/MS characterization of phenolic constituents of mate (Ilex paraguariensis, St. Hil.) and its antioxidant activity compared to commonly consumed beverages*"; Bravo L., Goya L., Lecumberri E.; Food Research International, Vol. 40, Pg. 393–405 (2007).

[20] "*Determination of N-acetylation phenotype using caffeine as a metabolic probe and high-performance liquid chromatography with either ultraviolet detection or electrospray mass spectrometry*"; Baud-Camus F., Marquet P., Soursac M., Davrinche C., Farinotti R.; Journal of Chromatography B, Vol. 760, Pg. 55–63 (2001).

[21] "*Quantification of theobromine and caffeine in saliva, plasma and urine via liquid chromatography–tandem mass spectrometry: A single analytical protocol applicable to cocoa intervention studies*"; Ptolemy A. S., Tzioumis E., Thomke A., Rifai S., Kellogg M.; Journal of Chromatography B, Vol. 878, Pg. 409–416 (2010).

[22] "*Determination of neutral pharmaceuticals in wastewater and rivers by liquid chromatography–electrospray tandem mass spectrometry*"; Ternes T., Bonerz M., Schmidt T.; Journal of Chromatography A, Vol. 938, Pg. 175–185 (2001).

[23] "*Extractionless method for the determination of urinary caffeine metabolites using high-performance liquid chromatography coupled with tandem mass spectrometry*"; Schneider H, Ma L, Glatt H.; Journal of Chromatography B, Vol. 789, Pg. 227–237 (2003).

[24] "*Highly sensitive and rapid determination of theophylline, theobromine and caffeine in human plasma and urine by gradient capillary high-performance liquid chromatography frit- fast atom bombardment mass spectrometry*"; Hieda Y., Kashimura S., Hara K., Kageura M.; Journal of Chromatography B, 667 (1995) 241-246

Bitter taste molecular markers detection in liquid phase : alternative methods

3

3.1 Detection Of Bitter Taste Molecular Markers In Liquid-Phase

In the previous chapter we introduced an HPLC method to detect bitter taste molecular markers in solid samples with a good precision, directly correlated to the PAA sensorial procedure. In spite of this consideration a large amount of time is needed in order to obtain a biscuit extract and perform the HPLC chromatographic run. This technique can be used for the analysis of new matrices but it cannot be used for daily quality control because it is too time consuming and it needs trained personal and expensive instruments to be performed. Alternative approaches are needed to detect the same markers in a simple and faster way.

One approach for the detection of bitter taste molecular markers can be afforded by the use of supramolecular complexes in solution. Different examples are reported in literature about the complexation of markers, like caffeine, in solution [1-8]. Such a kind of approach is not particularly fast because all the known methods work only in solution and an extraction is still needed even avoiding the chromatographic run time. Furthermore, the two classes of bitter taste molecular markers cannot be analyzed using a single complexing agent.

3.2 Detection Of Polyphenols – Folin Ciocalteu Method

One of the most simple way to quantify polyphenols in a solution is represented by the Folin-Ciocalteu method. This technique is based on the oxidation of the polyphenols dissolved in water with a solution of phosphotungstic acid ($H_3PW_{12}O_{40}$) and phosphomolybdic acid ($H_3PMo_{12}O_{40}$) known as the Folin Ciocalteu reagent. These two substances are reduced by polyphenols in watery solutions with the rapid formation a blue product called “Molybdenum Blue” that can be quantified recording its absorbance at 765 nm. With this technique it is possible only to quantify the total polyphenols content and it is impossible to make a distinction by among Cathechin, Epicatechins or Procyanidines (polymeric polyphenols made by 3 or 4 catechin sub unit). The quantification of the antioxidant present in solution can be done building a calibration curve with appropriate standards of Gallic acid as described in ISO procedure [9]. Five different standards at different concentrations were made as summarized in table 1 and the spectra obtained after the application of the Folin-Ciocalteu method are showed in figure 1. The regression curve made with the absorbance measured at 765 nm shows a good linearity with the value of intercept (0.0333) and R^2 coefficient (0.9985) comparable to the one described in the guideline of the ISO. Then an extract of a biscuit with a high content of polyphenols was chosen (Chocolate biscuit 3) in order to evaluate the best dilution ratio to be used in the analysis and the accuracy of the analysis itself.

Standard Name	Standard's concentration (mg Kg^{-1})
A	10
B	20
C	30
D	40
E	100

Table 1 – Gallic acid standards used for calibration curve in Folin-Ciocalteu approach

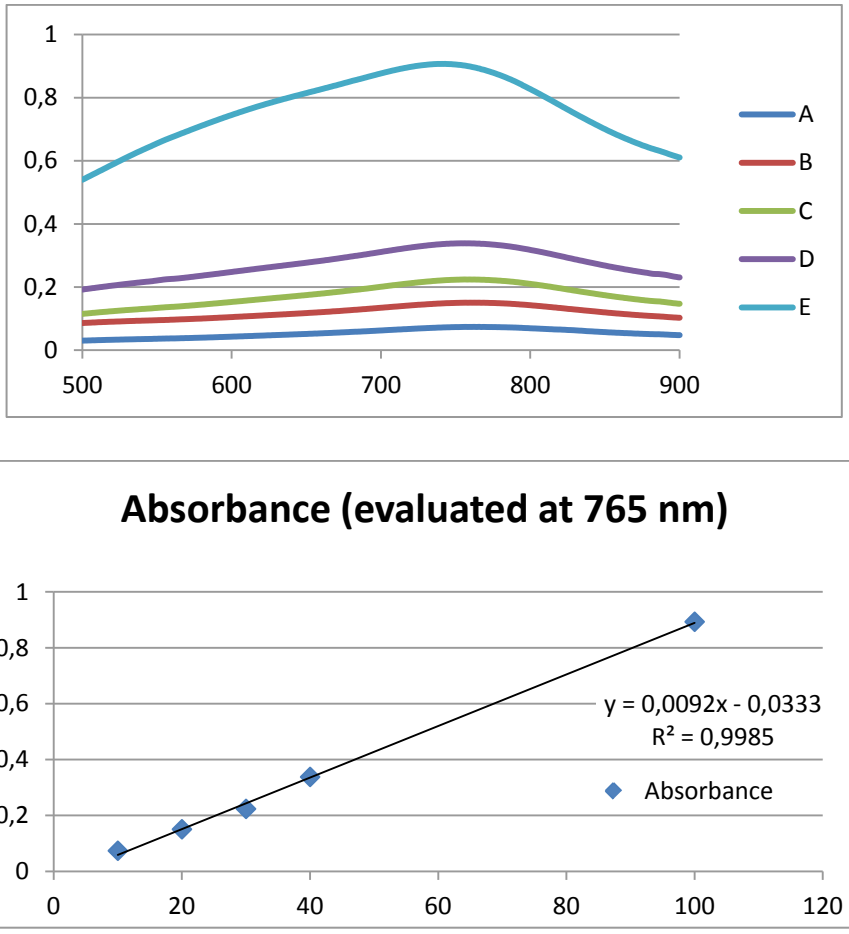

Figure 1 – Standards UV-Vis Spectra and calibration curve (Folin-Ciocalteu Method)

Three different samples were made extracting 10 g of sample in 20 mL of distilled water at 80°C for 30 minutes. The suspension was filtered with a Buchner and then were diluted with three ratios:

- One sample was not diluted.
- One sample was diluted 10 times.
- One sample was diluted 100 times.

In order to calculate the concentration of polyphenols inside the extract equation 2 was applied following the ISO guidelines.

$$w_T = \frac{\left(D_{sample} - D_{intercept}\right) * V_{sample} * d * 100}{S_{standard} * m_{sample} * 10000 * w_{DM,sample}}$$

Equation 2– Total phenolic content on dry matter basis.

Where:

D_{sample} is the absorbance of the tested sample;

$D_{intercept}$ is the intercept at the y axis;

S_{std} is the angular coefficient of the straight line;

m_{sample} is the mass (in grams) of the solid used for the extraction;

V_{sample} is the volume of the sample analyzed;

d is the dilution factor

$w_{DM,sample}$ is the mass (in grams) of the dry solid used for the extraction

w_T is the total phenolic content referred on a dry basis and expressed as % w/w

In order to obtain a readable absorbance a value comprised between 0.2 and 1 is needed. In table 2 there the results for the three different dilutions of the same extract are summarized.

Sample	Absorbance (765 nm)	Equivalent mg kg^{-1} of gallic acid	w_T (% w/w)
Chocolate biscuit 3 Extract	2.72382	300 (*)	0.64 %
Chocolate biscuit 3 Extract (diluted 10 times)	0.45167	53	1.3 %
Chocolate biscuit 3 Extract (diluted 100 times)	0.07097	11	2.44 %

Table 2 – Folin-Ciocalteu results for the three extract; (*) means that the absorbance is out of the calibration range and the results are extrapolated.

The best dilution factor is 10 (table 2) because it makes possible to read an absorbance of 0.4 on an extract of sample rich in polyphenols. It is important to note that the test did not give back the same results in all the three analyzed cases. For the not diluted sample this is not a real problem because this output was expected due to extrapolated concentration; but for the other two samples mismatch between the results is too high. There is also a great difference between the data obtained with Folin-Ciocalteu method and the HPLC results. Folin method gives back a higher result because it is an aspecific test that measure all the oxidizable molecules present in the aqueous solution, also the ones with a non-phenolic structure. On the other hand RP-HPLC-MS method is able to detect with high precision the chosen specific molecular markers of the bitter taste. Probably in this second type of analysis some data about polyphenols with a concentration under few mg kg^{-1} are lost but the specificity toward well known bitter molecules like (+) catechin and (-) epicatechin is maintained.
In conclusion Folin-Ciocalteu method analyses the total phenolic content in biscuits, but the associated error is too high due to the interferent molecules co extracted with the phenols. Therefore, considering all the analytical advantages and drawbacks, the HPLC approach remains the best option.

3.3 Detection of Polyphenols – Adsorptive stripping voltammetry with PEDOT electrodes

All flavonoids are electroactive, easily subjected to either anodic or cathodic reaction; hence, they can be spontaneously determined by electrochemical methods. Unfortunately, flavonoids present a strong tendency to give adsorption on the electrode surfaces, often fouling them, even in the absence of any applied potential, which makes their quantitative determination problematic. It is however known that in some specific cases the adsorption phenomena can be exploited to a quantitative scope, namely in the so-called adsorptive stripping voltammetry (AdSV). In this case the analyte undergoes a pre-concentration step on the electrode surface, thanks to adsorption under well-defined mass transport conditions, and then it is determined, by oxidation or reduction, in a potential scan to more positive or more negative potentials, respectively. The pre-concentration step allows one to reach high sensitivity levels; on the other hand, the stripping potential value contributes to selectivity. AdSV has been used in the determination of some flavonoids, among which rutine and quercitine [10-15]. However, the use of conventional electrode materials (C; Pt; Au) is sometimes not always satisfactory, due to the fouling character of the adsorption, so that alternative materials, such as carbon nanotubes, have been proposed. One option at our disposal to exploit the electrochemical determination of polyphenols is the use of a conducting polymer modified electrode for the analysis of epicatechin. Poly(3,4-ethylenedioxythiophene) (PEDOT) films have attracted special interest thanks to their high conductivity and electrochemical stability.

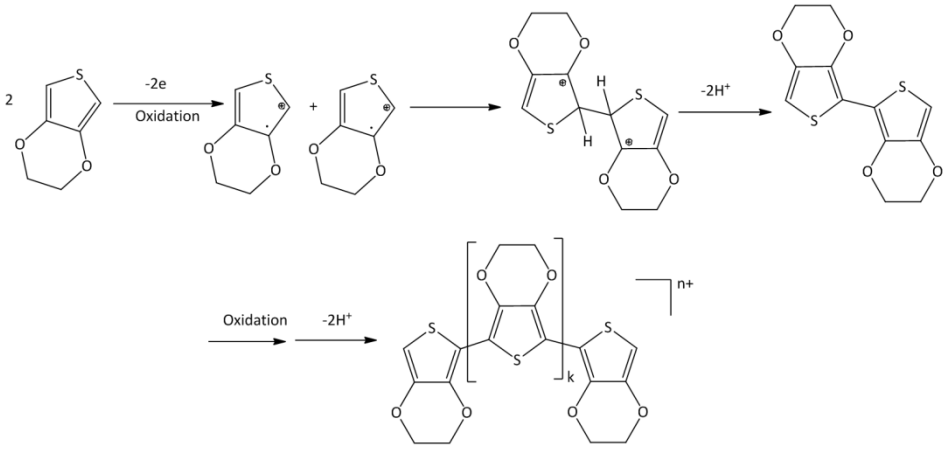

Figure 2 – PEDOT electrochemical mechanism of formation.

PEDOT also works properly in aqueous media, which renders it attractive for analyses of food matrices extract; also it can be electrochemically polymerized from a solution of 3,4-ethylenedioxythiophene (EDOT) with the mechanism proposed in figure 2 [16]. Finally, the used monomer, EDOT, is a commercial product, which constitutes a notable advantage when proposing simple realisation and consequent diffusion of sensors based on this material. PEDOT, in fact, can be easily prepared by electrochemical polymerization which produces a stable deposit on the electrode surface. A method based on AdSV at PEDOT modified electrodes has been developed for the quantitative determination of epicatechin. The anodic oxidation mechanisms of catechin has been already deeply studied, but only few scientific papers report regard the electroanalytical determination of flavonoids with flavan-3-ol structure. In particular, the adsorption conditions of epicatechin have been investigated by us in order to reach good repeatability and reproducibility of the electrochemical signal, which is a fundamental requirement for direct quantitative determination. The final goal is performing the same measurements directly on extraction solutions of commercial products.

3.3.1 Electroanalytical Apparatus and Procedures

The electrochemical experiments were carried out with an Autolab PGSTAT12 electrochemical instrument (Ecochemie, Utrecht, The Netherlands), using a single compartment, three-electrode cell. A 3 mm diameter Pt disk electrode (Metrohm) was used as the working electrode. An Ag/AgCl electrode (3 M KCl, Metrohm) and a glassy carbon rod (Metrohm) were the reference and the auxiliary electrode, respectively. Before each electrochemical test the surface of the working electrode was polished with 0.5 µm alumina powder to a mirror finish, dipped into an ultrasonic bath for 10 minutes, and then rinsed with doubly distilled water. The polymer electrode coating was prepared by direct electrochemical polymerization-deposition, carried out in a solution containing 10 mM EDOT and 0.1 M $LiClO_4$ supporting electrolyte, CH_3CN de-aerated solvent. Electropolymerization was performed using the potentiostatic method. A potential of +1.20 V was applied until a charge of 3 mC was spent; the procedure was then terminated by holding the potential at -0.80 V for 30 seconds. The growing potentials were chosen at the onset of the EDOT oxidation peak. After electrochemical deposition, the status of the polymer film was stabilized through ten subsequent cyclic voltammetric (CV) scans in the potential range -0.50 ÷ +0.50 V at a rate of 0.05 V s^{-1} in a monomer free, 0.1 M Phosphate Buffer (PB) solution. The electrochemical measurements in the epicatechin PB solutions have been performed by Differential Pulse Voltammetry (DPV) technique. The DPV scans (10 mV potential impulse, 4 mV potential step, 0.15 s impulse time and 0.6 s time interval between two

subsequent potential pulses) were performed in the potential range -0.20 ÷ +0.60 V. Before each scan, the electrode was kept at -0.50 V for 60 seconds.

3.3.2 Samples

Three different typologies of cocoa biscuits were considered in preliminary analyses. The biscuits with different cocoa percentages were named as sample A and B, respectively. A third sample, named sample C, did not contain cocoa. The extraction solutions for analysis were prepared as follow: a suitable quantity of biscuit, ranging from 5 to 10 g, was finely crumbled and after the addition of 25 mL of PB solution, posed under stirring for 1 hour. After filtration on Buchner, the solution was directly used for analysis or diluted before electroanalytical tests.

3.3.3 Results and discussion

Different electrode materials were considered in the analysis of a PB solution, pH=7, of epicatechin. Neutral pH was chosen since it is reported that flavonoids in general, and catechin in particular, present most reversible voltammetric curves and highest current values [17]. Preliminary tests evidenced that the electrochemical signal relative to epicatechin oxidation, recorded on bare metal electrodes such as Pt and Au are of no interest. More interesting results were obtained when considering glassy carbon (GC) and PEDOT modified electrodes. GC is reported to be effective in the study of the oxidation mechanism of catechin [17] and of other flavonoids, giving well defined electrochemical responses. The first voltammetric scans recorded on a GC and on a PEDOT modified electrode in the same epicatechin solution; the two electrode materials do not evidence any particularly different electrocatalytic properties, since the position of the epicatechin oxidation peak does not change significantly at varying the nature of the material. On the opposite, in the same figure the collection of higher current in the case of the PEDOT modified electrode is well visible: only this electrode material was employed in further studies.

According to the literature, voltammetric curves on epicatechin solutions present two oxidation peaks, the more anodic one being irreversible in character, resulting of less interest from an analytical point of view. Repeated scans over the potential range in which only the first oxidation occurs, evidence good repeatability of the relevant electrochemical signal, as shown in Figure 3. The peak potentials of the first anodic-cathodic peak system are located at +0.19 V and +0.16 V, respectively. The small difference between the two peak potentials suggests the occurrence of adsorptions at the electrode surface.

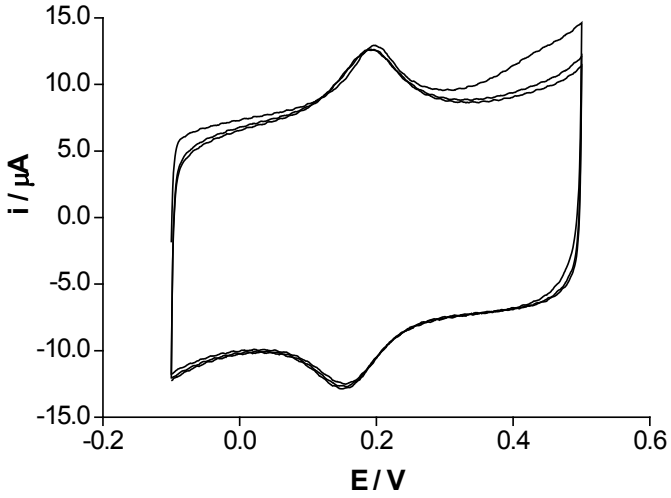

Figure 3 – CV scans recorded in a 6 ppm epicatechin PB solution on a PEDOT modified electrode. 50 mV s^{-1} scan rate.

As it is well known from the literature, flavonoids usually do adsorb on the electrode surface even at open circuit potential [17], and the adsorption is commonly irreversible. Such a behaviour was verified also for epicatechin on PEDOT modified electrodes, since the immersion of the electrode for just one minute in a solution containing the analyte, followed by a voltammetric scan to the positive potentials in a solution only containing PB, leads to record the typical peak of epicatechin anodic oxidation. In view of a possible quantitative determination, further analyses have been carried out by DPV. In particular, on the basis of the previous considerations, the possibility of establishing a relationship between the height of the DPV anodic stripping signal of the adsorbed species and the concentration of the epicatechin present in solution was verified.

The signals recorded by this technique in epicatechin solutions using PEDOT modified electrodes show well defined peaks, centred at +0.18 V, as reported in Figure 8. The influence of the accumulation time of epicatechin on the voltammetric response was also investigated. It was found that the current response increases with the accumulation time. In order to identify the time at which the equilibrium for the adsorption was reached, and hence to make the measurements under steady state conditions, we recorded DPV signals at constant interval times and compared the obtained results.

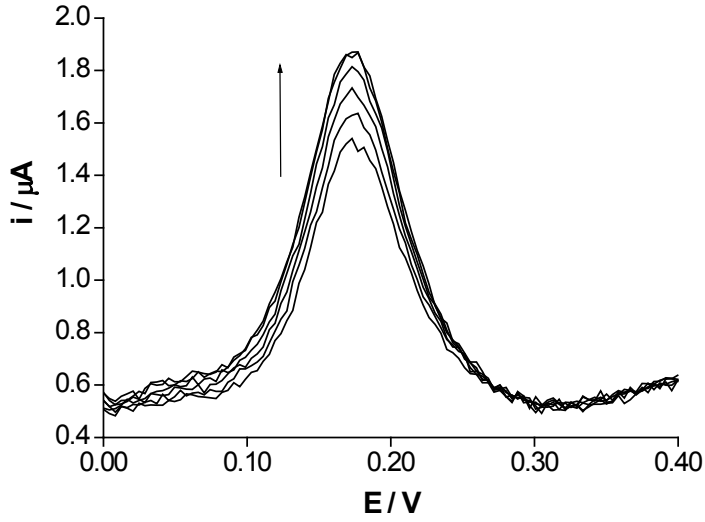

Figure 4 – DPV scans on a PEDOT modified electrode recorded in a ca. 0.6 ppm epicatechin, PB solution, at intervals of 5 minutes.

In figure 4 DPV scans recorded at intervals of 5 minutes are reported. It is clear that the height of the DPV signal increases up to reaching an almost constant value at ca. 25 minutes. Such an accumulation time was hence selected for the following experiments. The effect of stirring during the accumulation stage was also considered, leading however to poorly reproducible results.

The possibility to build a calibration plot exploiting AdSV was explored: in figure 5 the DPV curves recorded once the signal has stabilised after each addition of epicatechin are reported, showing a linear dependence of the peak current on epicatechin concentration. The reproducibility of the calibration curves obtained by subsequent additions of the analyte was evaluated over as many as 6 different PEDOT coatings. The peak currents were obtained by exploring a concentration range from 0.2 to 2.5 ppm, which was identified as the upper limit of linearity of the responses. When working at higher concentrations of epicatechin, changes in the concentration do not cause a significant change of the current, suggesting that saturation of the electrodic surface with respect to epicatechin adsorption has been reached. The electrode systems are fairly reproducible, as deduced by the lack of significant differences between the slopes of the 6 different calibrations obtained with 6 different electrodes, assessed by t-tests (P= 0.05) performed on the calibration data leading to highest and lowest slopes, respectively.

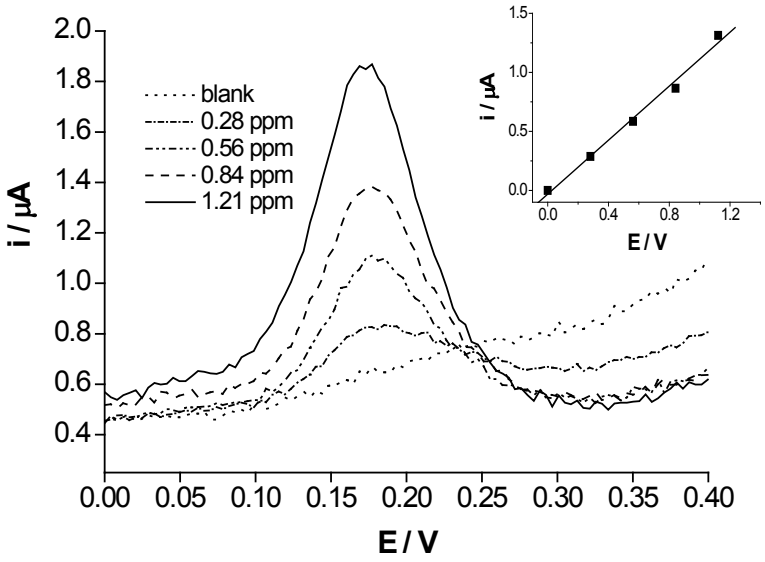

Figure 5 – DPV scans recorded on a PEDOT modified electrode in a PB solution before and after the addition of a standard solution of epicatechin in 0.1 M PB solution. Inset: relevant calibration curve.

The regression line obtained considering all the points relative to the different calibration plots shows a slope equal to 1.487 ± 0.002 mg kg^{-1} (28 points overall, 95 % confidence level), which quantifies the sensitivity of the modified electrode. The very low value of the standard deviation that includes both the repeatability of the response and reproducibility of the device, indicates very satisfactory performances with this respect. The limit of detection results of 0.002 mg kg^{-1} (LOD = 3.3 mg kg^{-1}). It is evident that a lower value would be obtained by using a single regression line, obtained by a single electrode.

On the basis of the encorauging results obtained with standard solutions, we checked if the proposed system could contribute to determine the epicatechin content directly in products of industrial interest. In particular, we tested whether the electrode could give quantitative information about the epicatechin content in different cocoa biscuits when working in the relevant PB extraction solutions (the extraction procedure is reported in the experimental part). Sample analyzed are chocolate biscuit 3, nut biscuit and cream based biscuit. All the solution analyzed refer to PB extraction solutions of biscuits with high, medium, and zero cocoa content, respectively. As it is evident from figure 6, the voltammetric responses are well defined, the pincipal peak being ascribed to the oxidation of epicatechin, on the basis of the peak potential value and of the increment of the current by addition of pure analyte. As expected, the height of the

voltammetric peaks decreases correspondingly to the decrement of cocoa content in the biscuits and, vice versa.

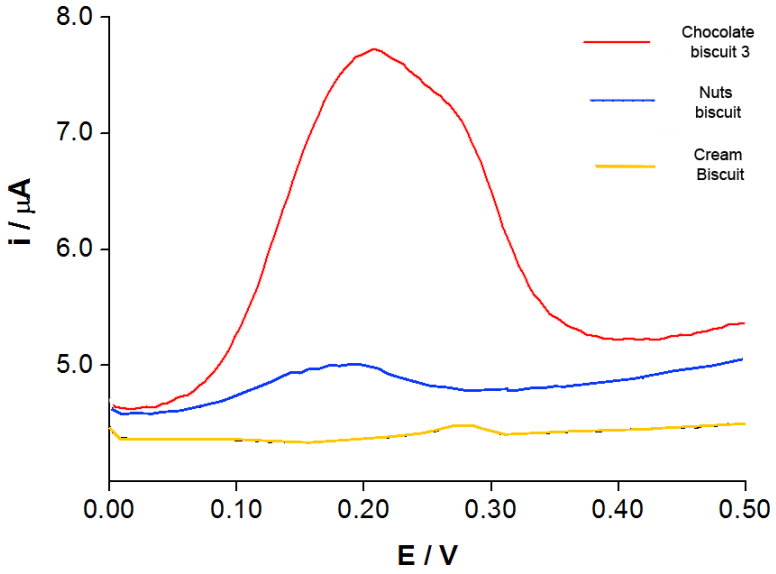

Figure 6 – DPV scans recorded on PEDOT modified electrode in extraction solutions of different biscuits samples.

The DPV trace relative to sample cream based biscuit shows the presence of a shoulder to the main peak, due to the presence of a further oxidasable species present in the extraction solution, probably another flavonoid substance, also detectable in the DPV trace relative to chocolate biscuit 3. The respective amount of polyphenols present in the three samples is summarized in table 3 (HPLC measured).

	CATECHIN	*EPICATECHIN*
SAMPLE	*mg kg^{-1} on solid*	*mg kg^{-1} on solid*
Chocolate biscuit 3	28.7	54.9
Nuts biscuit	9.6	7.2
Cream biscuit	< 0.2	< 0.1

Table 3 – *Catechin and Epicatechin content measured with LC-MS on biscuit samples*

In order to achieve a quantitative estimation of the amount of epicatechin present in samples the method of standard additions to the solution resulting from the extraction was applied, in order to take into consideration eventual matrix effects. The extraction of the biscuits solutions were suitably diluted with PB in order make the epicatechin concentration fall within the linearity interval previously defined. Following the procedure developed for the construction of the calibration plots in pure PB solutions, DPV signals were recorded both before and after each standard addition of analyte. The calibration plots relative to sample A and B are reported in figure 7.

Matrix effects are present, even working in diluted extraction solution of biscuits. However, the slopes obtained from different calibration plots for sample A and B are sufficiently similar to each other to suggest good reproducibility of the procedure as a whole.

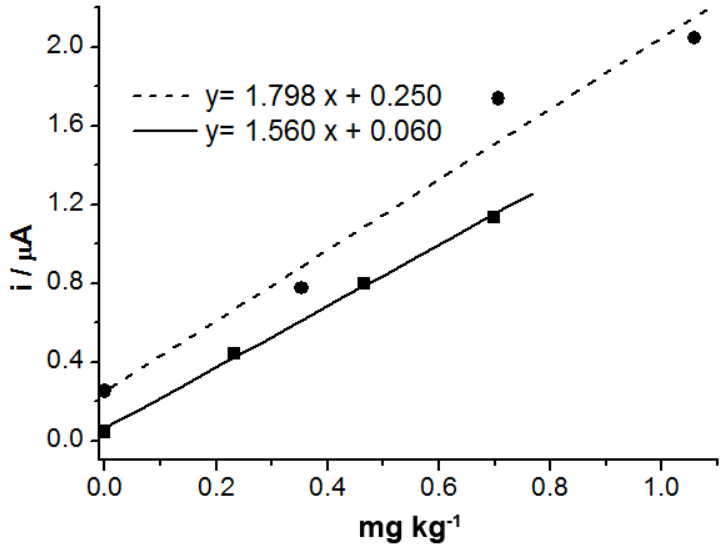

Figure 7 – DPV scans recorded on PEDOT modified electrode in extraction solutions of different biscuits samples.

Table 4 summarizes the measures on three different samples of chocolate biscuit 3 compared with the relative concentration detected with LC-MS method. In all the three cases taken into exam the PEDOT overestimate the overall polyphenols concentration by tenths of mg kg^{-1}. This behavior can be attributed to the presence of other oxidizable species that originates a peak centered at 0.25 V. It is plausible that this molecule (or class of molecules) has a similar structure to the epicatechin one;

probably there are more polyphenols not taken into account that are present in concentration comparable to the one of epicatechin. The presence of this peak shoulder modify the height of the epicatechin maximum resulting in an overestimated polyphenols concentration.

Chocolate Biscuit 3	Polyphenols in mg kg^{-1} (LC-MS)	Polyphenols in mg kg^{-1} (PEDOT)	Δ in mg kg^{-1}
A	114,4 ± 0,2	200,5	+ 86,1
B	114,4 ± 0,2	173,8	+ 59,8
C	114,4 ± 0,2	148,5	+ 34,1

Table 4 – Comparison of polyphenols detection between LC-MS and PEDOT methods.

3.3.4 Conclusions

PEDOT modified electrodes have been succesfully employed for the determination of a flavanol of particular interest in food analysis, i.e. epicatechin, exploiting AdSV technique. Moreover, the possibility to measure directly in extraction solutions of cocoa biscuits, as an alternative to more complex chromatographic procedures, was tested.

Moreover the DPV signals complemented by suitable chemometric treatment could be used as fast pre-screening methods for the evaluation of different parameters of interest in biscuits production, allowing to perform tasks such as assessment of sensory characteristics and process monitoring.

References

[1] "*Supramolecular Approach for Sensing Caffeine by Fluorescence*"; Siering C.; Beermann B.; Waldvogel, S. R.; Supramolecular Chemistry, Vol. 18, Nr. 1, Pg. 23-27 (2006).

[2] "*Spectroscopic Study of Porphyrin-Caffeine Interactions*"; Makarska-Bialokoz M.; Journal of Fluorescence, Vol. 22, Pg. 1521–1530 (2012).

[3] "*Stereochemical Structure and Intermolecular Interaction of Complexes of(_)-Gallocatechin-3-O-gallate and Caffeine*"; Tsutsumi H., Sato T., Ishizu T.; *Chemical Pharmaceutical Bullettin, Vol.* 59, Nr.1, Pg. 100—105 (2011).

[4] "*Theophylline detection using an aptamer and DNA–gold nanoparticle conjugates*"; Chávez J. L., Lyon W., Kelley-Loughnane N., Stone M. O.; Biosensors and Bioelectronics,Vol.26, Pg. 23–28 (2010).

[5] "*Recognition of Caffeine in Aqueous Solutions*"; Fiammengo R., Crego-Calama M., Timmerman P., Reinhoudt D. N.; Chemistry European Journal, Vol. 9, No. 3, Pg.784-792 (2003).

[6] "*First artificial receptor for caffeine – A new concept for the complexation of alkylated oxopurine*"; Waldvogel S. R., Frohlich R., Schalley C. A.; Angewandte Chemie International Edition, Vol. 39, Nr. 14, Pg. 2472-2475 (2000).

[7] "*Study on Mimetic Peroxidase and Molecular Recognition of Phenols With Inclusion Complex of Ironporphyrin Immobilized by/3-CD Polymer*"; Lu-yuan M., Hong Y., Ru-xiu C., Han-xi S., Min Z., Liu-zhan L.; Journal of Natural Sciences; Vol. 5, Nr. 1, Pg. 101-105 (2000).

[8] "*β-Cyclodextrin and Caffeine Complexes with Natural Polyphenols from Olive and Olive Oils: NMR, Thermodynamic, and Molecular Modeling Studies*"; Antonio Rescifina, Ugo Chiacchio, Daniela Iannazzo, Anna Piperno, Giovanni Romeo; Journal of Agricultural and Food Chemistry, Vol. 58, Nr. 22, Pg. 11876–11882(2010).

[9] "*Determination of substances characteristic of green and black tea*"; International Standard ISO 14502-1 (2005).

[10] "*Preconcentration at a carbon-paste electrode and determination by adsorptive-stripping voltammetry of rutin and other flavonoids* "; Zoulis N.E., Efstathiou C.E., Analitica Chimica Acta, Vol. 320, Pg. 255-261 (1996).

[11] "*Adsorptive Stripping Voltammetric Detection of Tea Polyphenols at Multiwalled Carbon Nanotubes-Chitosan Composite Electrode*"; Guo D., Zheng D., Mo G., Ye J., Electroanalysis, Vol. 21, Pg. 762-766 (2009).

[12] "*The redox thermodynamics and kinetics of flavonoid rutin adsorbed at glassy carbon electrodes by stripping square wave voltammetry*";Catunda F.E.A., de Araujo M.F., Granero A.M., Arevalo F.J., de Carvalho M.G., Zon M.A., Fernandez H., Electrochimica Acta, Vol. 56, Pg. 9707-9713 (2011).

[13] "*Novel Application of Square-Wave Adsorptive-Stripping Voltammetry for the Determination of Xanthohumol in Spent Hops*"; Moreira M.M., Carvalho A.M., Valente I.M., Goncalves L.M., Rodrigues J.A., Barros A.A., Guido L.F., Journal of Agricultural and Food Chemistry, Vol. 59, Pg. 7654-7658 (2011).

[14] "*Electrochemical behavior and adsorptive stripping voltammetric determination of quercetin at multi-wall carbon nanotubes-modified paraffin-impregnated graphite disk electrode*"; Jin G.P., He J.B., Rui Z.B., Meng F.S., Electrochimica Acta, Vol. 51, Pg.4341 (2006).

[15] "*Determination of Rutin in Pharmaceutical Compounds and Tea Using Cathodic Adsorptive Stripping Voltammetry*"; Ensafi A.A., Hajian R., Electroanalysis, Vol. 18, Pg. 579 (2006).

[16] "*Electrochemistry of Conducting Polymers - Persistent Models and New Concepts*"; Heinze J., Frontana-Uribe B. A., Ludwigs S.; Chemical Review, Vol.110, Pg. 4724–4771 (2010).

[17] "*Catechin electrochemical oxidation mechanisms*"; Janeiro P., Oliveira Brett A. M.; Analytica Chimica Acta, Vol. 518, Pg.109–115 (2004).

FT-NIRS method, sensory and confirmatory analytical procedures:

4

Xanthines and polyphenols detection in Bakery Products

The content of this chapter has been published :

"Rapid and simultaneous analysis of xanthines and polyphenols as bitter taste markers in bakery products by FT-NIR spectroscopy"; Bedini A., Zanolli V., Zanardi S., Bersellini U., Dalcanale E., Suman M., Food and Analytical Methods, Vol. 6, Nr. 1, Pg. 17-27 (2013)

Different approaches for the bitter taste molecular markers detection are taken into account in the previous chapters; but no one of them is able to provide a response in short time. In order to develop a rapid method implementable in daily quality control assurance shorter analysis time are needed. The HPLC-MS method demonstrated that several different markers are present inside the analyzed bakery products. Furthermore there is a direct correlation between their presence and the perceived bitter taste scored by the panel group. The method is accurate (LOD and LOQ see chapter 2) and reproducible but it is expensive and the total amount of time needed to perform an analysis is too high for quality control purposes. This is due to the long time of extraction needed in order to obtain a single sample and the length of the chromatographic run. So a method that works directly on solids is desirable to reduce the analysis time and human handling of the samples. In order to develop a rapid method usable for daily quality control purposes different, requirements are needed:

- Fast method, to screen all the production batch made by the industrial line;
- Method that work directly on the solid phase, to avoid extractions with solvents;
- Simplicity of the method, amenable to be used by non specialized operators;
- Repeatability, the same sample must give back the same analysis results over time;
- Interlaboratory repeatability, i.e. the method can be applied by different quality control laboratories giving back comparable results

Precision must be partially sacrificed if we want a fast method; furthermore considering the need to work directly on the solids to avoid pretreatments the solution of the adequate analytical strategy toward infrared spectroscopy fulfill the possibility to work directly on grinded solid, allows measurements with simple pretreatment, a typical cause of errors [1].

4.1 FT-NIR Spectroscopy

The wavelengths that compose the infrared region of the electromagnetic spectrum can be subdivided into three distinct groups:

- Near Infrared (NIR, 14000-4000 cm^{-1});
- Medium Infrared (MIR, 4000-400 cm^{-1});
- Far infrared (400-10 cm^{-1});

Different spectroscopic techniques are based on infrared light and are used to obtain identify and study molecules on the basis of their vibrational behavior when exposed

to infrared light. These three different regions can be analyzed using instruments based on Michelson interferometer but the information that can be obtained are different from region to region: (i) The NIR wavelengths provide information about overtones and combination of vibrations; (ii) in MIR wavelengths falls fundamental vibrations; (iii) far infrared is used instead for rotational spectroscopy. Consequently a large part of the infrared spectrum can be used to provide information about the structure of molecules due to the vibrations of the bonds that compose the analyzed molecule.

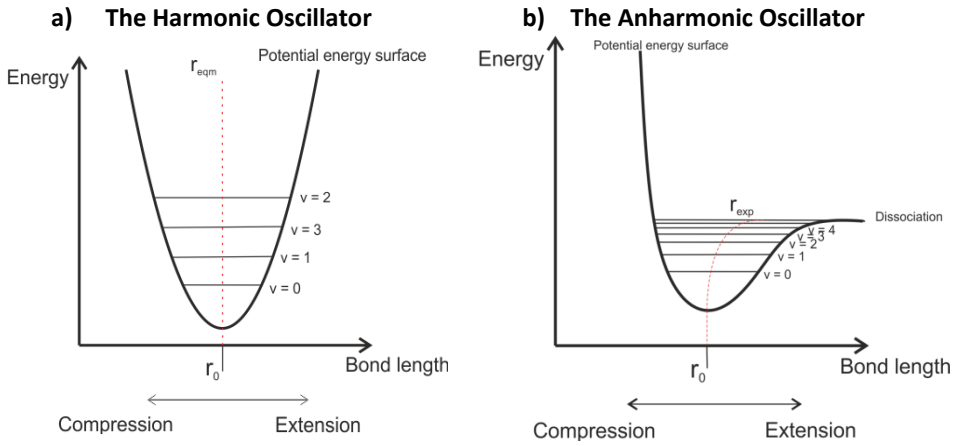

Figure 1 – Differences in the energy levels spacing for: a) Harmonic Oscillator; b) Anharmonic oscillator models.

Infrared light is able to interact with molecules modifying the energy of their vibrational state. This interaction is commonly described starting from the analysis of the interaction with a single bond, using the so called "diatomic oscillator model" (figure 1). In this model the single bond is treated like a spring that follows the Hooke's law. If we imagine a single bond in a molecule, ignoring the rest of the molecule, we can describe the vibrational potential energy (V) as a function of the bond strength (k) and the relative position of the atoms in respect to the equilibrium position ($r\text{-}r_e$) (equation 1.1).

$$V = \frac{1}{2}k(r - r_e)^2 = \frac{1}{2}kx^2$$

Equation 1.1 – Potential energy for a single bond.

This mathematical treatment of the problem gives back the equation 1.2 that correlates the frequency of the absorbed infrared radiation (ν) with a force constant typical of the stimulated bond (k) and with the reduced mass (μ).

$$\nu = \frac{1}{2\pi}\sqrt{\frac{k}{\mu}} \qquad\qquad \mu = \frac{Mm}{M+m}$$

Equation 1.2 – Harmonic oscillator main equation, M and m are the mass of the two atoms involved in the vibration.

As depicted in figure 1a, this model is a great approximation of the real behavior of a bond because all the contributes of the neighboring functional groups are not taken into consideration. A quantomechanical treatment of this model shows us that vibrations are arranged with energy levels equally spaced, as shown in equation 1.3

$$E_{vib} = h\nu\left(n + \frac{1}{2}\right)$$

Equation 1.3 – Harmonic oscillator energy levels (where ν is the previously described frequency and n is the vibrational quantum number).

In order to have an infrared absorption band it is needed a variation of dipole moment during the bond vibration and a jump of vibrational quantum number of 1 (equation 1.4).

$$\left(\frac{d\varepsilon}{dx}\right) \neq 0 \qquad\qquad \Delta n = 1$$

Equation 1.4 – Harmonic oscillator selection rules.

The vibrational frequencies that rise from this model are commonly used for the structural elucidation of the investigated compound in the region of MIR (4000-400 cm^{-1}). Even if the model is approximated there is a good matching between theoretical and real absorption frequencies. But if we want to describe also the bands observable in the NIR region (12500-4000 cm^{-1}), a more accurate model is needed. The harmonic oscillator model isn't able to describe the vibration with Δn greater than 1.
Introducing anharmonicity (equation 1.5) in the potential energy, we obtain the second curve shown in figure 1 that is able to describe also the presence of this other type of bands.

$$V = \frac{1}{2}kx^2 + k'x^3 + \cdots \qquad\qquad k' \ll k$$

Equation 1.5 – Potential energy in an anharmonic oscillator model.

Introducing this new expression of the potential energy in the Schrödinger equation we can finally calculate a new form for the energy of the vibrational levels (equation 1.6).

$$E_{vib} = h\left(\bar{\nu}\left(n+\frac{1}{2}\right) - X\left(n+\frac{1}{2}\right)^2\right)$$

Equation 1.5 – Vibrational energy in an anharmonic oscillator model (where $X=x_e\bar{\nu}$ and x_e is the anharmonicity factor) .

From this new equation it is possible to see that energy levels are no longer equally spaced (figure 1b). From a quantomechanical point of view the variation of the dipole moment is still needed but the vibrations with a Δn greater than 1 are now allowed. These bands are very important because they fall in the NIR region and they are the one used for FT-NIR analysis. Two main types of bands are observable in NIR:

- Combination bands, originated by the absorption of two quantum of infrared lights corresponding to two absorption with Δn = 1. The frequency of this absorption is the sum of the two single frequencies of the involved vibrations.

- Overtone bands, originated by a jump of Δn greater than 1. When Δn = 2 this is called "first overtone", when Δn = 3 this is called "second overtone". Third overtones are rare because the intensity of these bands decrease with the increasing of Δn; so bands with $\Delta n \geq 4$ are no more observable.

In MIR spectroscopy a typical spectra is composed by different, well defined, peaks each one attributable to a specific vibration with no difficulties. This techniques is in fact commonly use for the characterization of pure unknown compounds.
Differently, the NIR spectra, are composed by broad large overlapped bands that make difficult, or even impossible, a direct interpretation. To overcome these problems the analysis of material is commonly executed with the assistance of chemometric dedicated software able to use multivariate statistical methods to retrieve the chemical information hidden inside the NIR spectra. These different approaches to the problem make possible to investigate both pure and complex samples allowing us to use NIR technique for the analysis of complicate matrices like foodstuffs.
Various liquid or solid samples can be investigated with FT-NIR. The exact nature of the matrix can vary from slurry to powder samples and even solids samples (like seeds) can be directly analyzed. This is due to the high penetration level that NIR light owns. It has

the advantage that samples can be prepared easily and rapidly; in addition the sample is not destroyed and remains therefore available for further analysis. FT-NIR instruments generally work with two types of operative modes (figure 2):

- Reflectance, measuring the light reflected by the sample
- Transmittance, measuring the light transmitted through the sample
- Transflectance, measuring the light reflected by a mirror positioned behind the sample an transmitted a second time through the sample

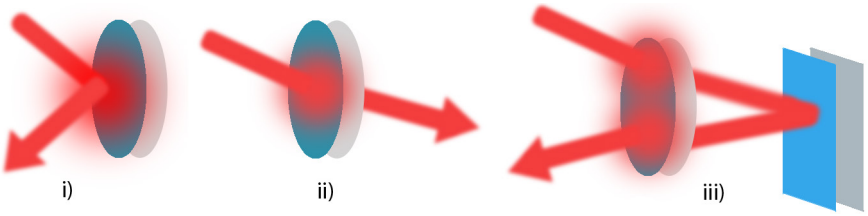

Figure 2 – The three commonly detection modes for FT-NIR : i) Reflectance; ii)Transmittance; iii) Transflectance.

The most widely used method for recording FT-NIR spectra is the reflectance modality, because the reflected light is more intense than in the other two cases and this allows the instrument to record a readable spectrum with a lower number of scans and correspondent shorter recording time. FT-NIR can be used both for qualitative recognition and quantitative analysis. In both cases a calibration is needed prior to make the routine measures. The number of samples needed to obtain a calibration curve can vary by multiple causes like:

- Concentration of the investigated analyte
- Type of matrix
- Possible presence of interfering molecules (like water, e.g. the level of moisture in the product)

In general at least 80 samples are needed to calculate a reliable calibration curve with a PCA (Principal Component Analysis) method like PCR (Principal Component Regression) or PLS (Partial Least Square). The general approach to develop a calibration curve is to identify the main regions where the bonds of the molecular target fall and then record a sufficient number of representative samples with known concentration of the target. Then the curve is made more robust adding spectra of the same matrix with concentration levels previously unexplored inside the desired detection range to improve correlation coefficient (R^2) and standard error of

calibration and prediction (SEC and SEP). The standard deviation of the FT-NIR calibration curve is directly related to the one of the reference method used to analyze reference samples. In general the relation between FT-NIR method and the reference method is the one showed in equation 1.6 [2-3].

$$s(\hat{y} - y) = \left[(1 + h_i)SEC^2 - S^2{}_{ref}\right]^{1/2}$$

Equation 1.6 – Relation between standard deviation of FT-NIR and reference method .

From the previous equation the difference between the measured value and the mean value is directly correlated to the reference method standard error. It depends from the SEC (standard error of calibration) of the FT-NIR method but also from the square of the reference method ($S^2{}_{ref}$) and h_i (the leverage of the calibration set, the distance between a value and the center of the calibration training set). All these terms are elevated to the ½ and this means that the argument must be positive and this is possible only if the product $(1 + h_i)SEC^2$ is bigger than$S^2{}_{ref}$.

We choose to use this technique to determine the content of bitter taste molecular markers despite the significant uncertainty that could be related to the measurements because FT-NIR allows the possibility to exploit a measure in few minutes with only a finely grinded powder samples. In this research our attention is focused on bakery products like commercial biscuits, there are so many formulation and final form of these products that is impossible to analyze them without grinding; we opted for this homogenization technique because it is simple and rapid as the analysis itself and this is an advantage in food quality control.

4.2 Material and methods

4.2.1 Materials and reagents

Methanol and acetic acid were HPLC grade solvent and supplied by Merck (Darmstadt, Germany). Ultrapure water was used throughout the experiments (MilliQ system, Millipore, Bedford, MA, USA). Glass vials with septum screw caps were supplied by Agilent. Syringe filters (0.45 µm) were made by Whatman (Maidstone,Kent, UK). Theobromine and caffeine were purchased from Fluka. (+) Catechin, (-) epicatechin and (-) epigallocatechin gallate and theophylline were obtained from Sigma Aldrich (Milan, Italy). Eleven different categories of commercial biscuit packs were collected from the market, stored wrapped in aluminum foil at room temperature and progressively used for building the necessary calibration curves.

4.2.2 Panel test – Profile Attribute Analysis

These eleven types of different biscuits were chosen on the base of the ingredients used for making their original dough: in all the selected biscuit categories, flour is the principal ingredient, followed by fats and sugars; then there are other minor ingredients such as cocoa, cream, coffee, etc.
Three types were chosen on the base of a significant content of cocoa and chocolate, four present a mixture of cocoa and cream, the other ones were characterized by the presence of cream, honey and cereals.
The bitter taste of all these samples was checked using a Profile Attribute Analysis (PAA) [4] and the correspondent precise values are summarized in table 2.
PAA is an objective method of sensorial analysis undertaken by an expert panel to describe an overall experience in terms of quantity, using profile attributes. These attributes are depicted using a limited range of characteristics which, if appropriately selected and defined, will provide a complete sample description, with minimum loss of descriptive information.
Limiting the number of attributes that the panellist measure means five samples can be assessed per session. It uses the expertise of trained panels to identify and define appropriately the range of critical attributes for each specific project.
A group of eight panellists produces sufficiently standardized results for reaching significant classification of samples after two or three repetitions.
To identify specific attributes necessary for a PAA study and to develop their definition, the panel will initially hold guidance sessions. The panel is presented with a wide variety of products covering the entire range of different sensorial experiences that will be included in the specific study.
The panellists define the sensorial properties in these products by a descriptive analysis; the profile attributes required for a complete description of the range of products will then be selected among these definitions. Once the profile attributes have been selected, the scoring is then defined for the actual attributes. The panellists will be trained to use the profile attributes and reference standards. All attributes are defined on a so-called “Bitter Taste Index” (BTI) scale from 1 to 12, where each unit represents a difference that the panellist can identify easily in repeated analyses.
In the PAA evaluation session, after the panel leader has clearly explained the objectives of the test, each panellist performs her/his own tasting and the assessment of intensity of the attributes listed. The panel leader then takes note of results and subsequently coordinates a discussion of the notes; if it is necessary, the intensity will be revalued with the help of references. In this specific case the reference water solutions used for the bitter sensation are: (i) 0,05% w/v caffeine (BTI 4, low bitter taste); (ii) 0,10% w/v caffeine (BTI 8, medium bitter taste); (iii) 0,20% w/v caffeine (BTI

12, high bitter taste). The main bitter taste molecular markers present inside these products are summarized in figure 3.

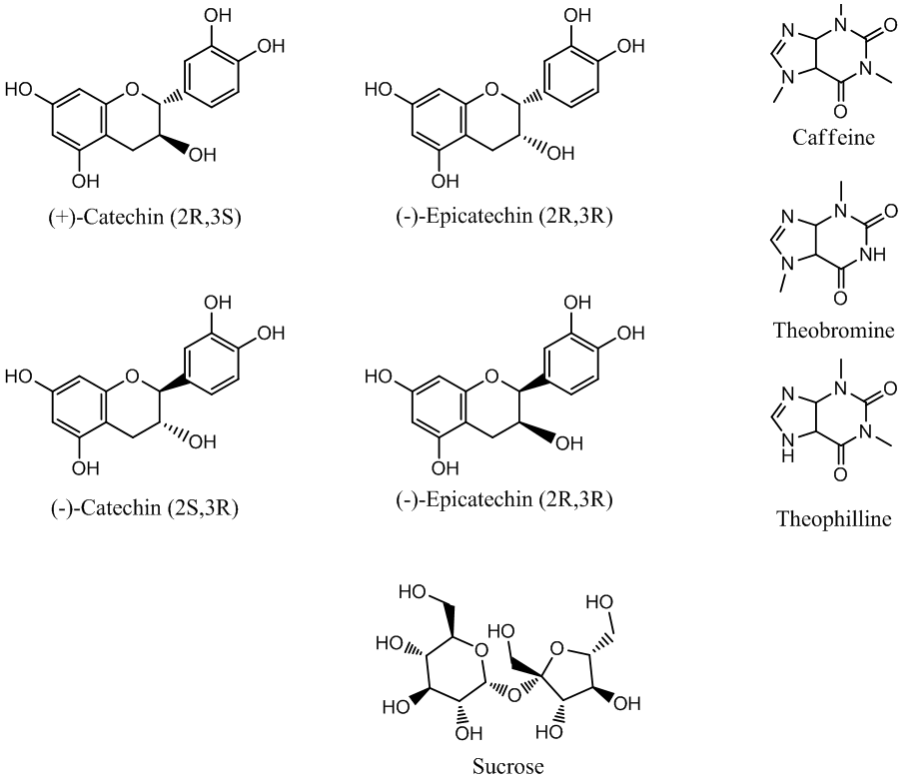

Figure 3 - Polyphenols (Catechins and Epicatechins), Xanthines (Caffeine, Theobromine and Theophylline) and Sucrose structures.

4.2.3 LC-ESI-MS-MS measurements

According to an ESI-LC-MS/MS analytical procedures based on available scientific literature [33-35] together with further modifications and improvements introduced in our laboratory (see chapter 2), all the biscuits and their chosen mixtures dedicated to the following generation of the FT-NIR calibration database, were ground and 10 g were extracted with 20 mL of MeOH:H_2O 70:30 for 40 minutes at 70 °C in a teflon sealed tube. Then the extracts were allowed to cool at room temperature and filtered using a Buchner funnel with filtration paper. Fresh MeOH: H_2O 70:30 solution was used to restore the starting volume (20 mL) and these final extracts were analyzed by the LC-MS method indicated above. Standard solutions were obtained by dissolving opportune amounts of selected Xanthines and polyphenols in MeOH: H_2O 70:30,

applying an ultrasound bath for 15 minutes: the concentration ranges of the calibration curves vary from 0.02 to 10 mg kg^{-1}. All samples and standard solutions were filtered with a 0.45 µm syringe filter before LC-MS analysis. Quantification was based on the areas of the corresponding peaks of the ion monitored with an external standard calibration approach. The pump used for liquid chromatography was a Surveyor LC Pump (Thermo Finnigan, San Jose, CA, USA). The chromatographic separation was performed using a Gemini C18 5 µm 15x2.0 mm (Phenomenex, Torrance, CA, USA) column with a flow rate of 0.2 mL/min. Injections (injection volume: 10 µL) were made using a Surveyor Autosampler (Thermo Finnigan). A linear binary gradient was within a total run time of 27 minutes. Eluent A was water and eluent B was methanol, both containing 0.5% acetic acid. A gradient elution was performed by changing the mobile phase composition as follows: the proportion of eluent B was linearly increased from 10% to 40% in 3 min, then increased to 80% in other 18 min, and kept constant for 4 min. The column was finally re-equilibrated to 10% eluent B in 2 min.

The electrospray ionization (ESI) experiments were carried out in a Linear-Ion-Trap LXQ (Thermo Scientific) mass spectrometer in positive and negative scan mode. The capillary temperature was set to 350 ºC; the sheath gas set to 20 units; the spray voltage was kept at 4 kV and the capillary voltage was kept at -23 V for negative ion monitoring; instead, for positive ion monitoring, spray voltage was kept at 5 kV and capillary voltage +25 V. Multiple Reaction Monitoring (MRM) experiments were performed according to parameters reported in chapter 2. All parts of the equipment and data processing were performed by the computer software Xcalibur (Thermo Scientific).

4.2.4 FT-NIR measurements

All the biscuits were finely ground prior to use. FT-NIR spectra were recorded exploiting a NIRFlex N500 (BUCHI Labortechnik, Flawil, Switzerland) instrument, operating in the wave numbers between 10,000 and 4000 cm^{-1} with a resolution of 8 cm^{-1}. The spectra were measured by keeping 40 g of sample in a quartz Petri plate; for each sample, three spectra were recorded at three different points by rotating the sample plate by 120°. Reference spectra of Xanthines and polyphenols as pure solid samples, were firstly recorded for the detection of the typical IR overtone bands and their corresponding attribution to the different functional groups in the products.

Different samples were used for the FT-NIR calibrations. One set of pure biscuit samples was used to cover the maximum and minimum concentrations of the calibration curve. Then, for a full coverage of the detection range within these levels, different mixtures of the biscuit samples (in defined opportune ratios) were also

prepared and measured. In total, 255 different spectra of 85 samples were recorded in reflectance mode; each spectrum was the average of 16 scans to reduce noise due to inhomogeneity.

Partial Least Square (PLS) algorithm was applied for the quantification to establish a correlation between the concentration of markers previously measured with the confirmatory LC-MS analysis and the NIR spectra. All the calibration curves were calculated allowing the software to choose the optimal number of primary components automatically. Then the calibration curves were evaluated in terms of SEC (standard error of calibration), SEP (standard error of prediction) and R^2 (coefficient of determination).

The standard error of calibration is described as shown in equation 1.7.

$$SEC = \sqrt{\frac{\sum(y_i - \hat{y}_i)^2}{n-p-1}}$$

Equation 1.7- Standard error of calibration.

where y_{es} is the predicted value and $\hat{y}_i$ the true value, *n* is the number of samples used in calibration and *p* is the rank. This value describes the error between the true and the predicted value and it is directly correlated to the residue. Lower values indicates a good agreement between the values used in calibration and the calibration curve itself.

Standard error of prediction is described as shown in equation 1.8.

$$SEP = \sqrt{\frac{\sum(y_i - \hat{y}_i)^2}{n}}$$

Equation 1.8 –Standard error of Prediction.

In this case low value of SEP represents good agreement between the predicted value and the calculated one on unknown samples used in validation.

Using NIRCal v5.4 software (BUCHI Labortechnik) for PLS analysis 70 % of the spectra were used for calibration curve and the remaining 30 % were used for validation curve. The optimum number of factors used for the individual prediction was determined by cross-validation and the best calibrations were chosen as the ones with the lowest SEC (the standard deviation of the differences between LC–ESI–MS and NIR-results in the calibration set) and SEP values (the counterpart of SEC for the test-set samples), with the ratio SEC/SEP and the R^2 coefficient more closed to 1.0 [5].

4.3 Results and discussion

4.3.1 LC-MS results

LC-MS experiments showed that the biscuits with the highest concentration of Xanthines and polyphenols are the ones made using cocoa or chocolate (an example of an extracted ion chromatogram is reported in Figure 4): the main compounds present being theobromine, caffeine, catechin and epicatechin.

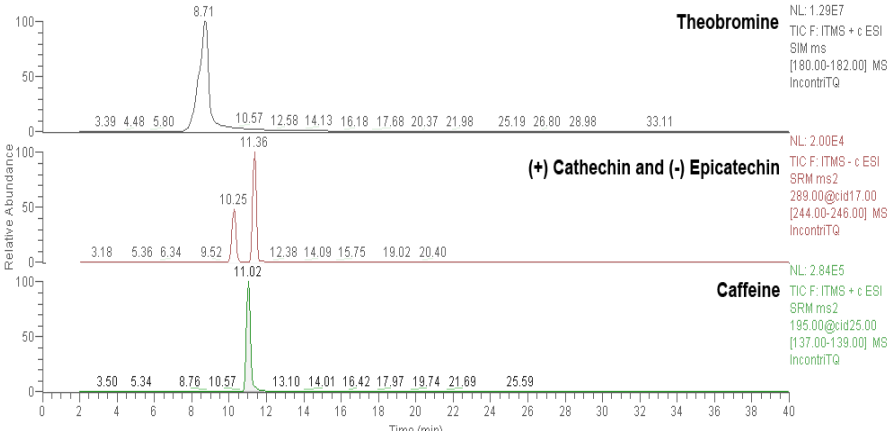

Figure 4 - Example of LC-MS extracted ion chromatogram of a cocoa based biscuit.

The concentration of theophylline and epigallocatechin gallate were found to be lower than 2 and 0.3 mg kg^{-1}, respectively, and consequently neglected. Analysis showed that biscuits with high content of cocoa have concentrations of xanthines in the order of hundreds of mg kg^{-1} (Table 1).

In particular, in the case of Chocolate Biscuit 3, the concentration is more than one thousand of mg kg^{-1} and also Profile Attribute Analysis (PAA) indicated that this is the most bitter-tasting biscuit of the analyzed series. On the contrary, the biscuits containing in the recipe coffee (little percentage) or lemon achieved levels of tens of mg kg^{-1} and, finally, biscuits containing cream, cereals and honey didn't show any remarkable amount of xanthines. The analysis made on polyphenols showed almost the same trend and this is probably due to their cocoa origin in this context: biscuits made with relevant amount of this ingredient reported concentrations in the order of tens of mg kg^{-1}. Again, in the case of biscuits made with cream, cereal and honey a negligible amount of polyphenols was found.

SAMPLE	BITTER TASTE INDEX	THEOBROMINE mg kg^{-1} on solid	CAFFEINE mg kg^{-1} on solid	TOTAL XANTINE mg kg^{-1} on solid	CATECHIN mg kg^{-1} on solid	EPICATECHIN mg kg^{-1} on solid	TOTAL POLYPHENOLS mg kg^{-1} on solid
Chocolate Biscuit 3	*8*	1428	98	1526	28.7	54.9	83.6
Chocolate Biscuit 2	*7*	851	79	930	17.2	38.5	55.7
Nuts Biscuit	*5*	833	58	891	9.6	7.2	16.8
Chocolate & cream Biscuit 1	*5*	773	71	844	16.1	37.6	53.7
Chocolate Biscuit	*6*	626	45	671	9.6	6.2	15.8
Chocolate & cream Biscuit 2	*5*	210	17	227	3.1	2.2	5.3
Coffee Biscuit	*4*	35	31	66	0.3	0.3	0.6
Lemon Biscuit	*4*	36	4	40	1.0	< 2.4	≤ 3.4
Cereal Biscuit	*< 4*	< 15	< 1.6	< 17	0.2	< 2.4	≤ 2.6
Honey Biscuit	*< 4*	< 15	< 1.6	< 17	< 0.2	< 2.4	≤ 2.6
Cream Biscuit	*< 4*	< 15	< 1.6	< 17	< 0.2	< 2.4	≤ 2.6

Table 1 - Bitter Taste Index and LC-MS data recorded on the different biscuit categories.

The comparison between panel test and LC-MS data demonstrated that there is a correlation between the concentration of xanthines and polyphenols and the biscuits bitterness, confirming the hypothesis that these two classes of molecules are included within the main compounds responsible of this taste.

4.3.2 FT-NIR Partial least square regression (PLS) – Xanthines

All recorded spectra were normalized (i.e. ordinate-values are stretched between zero and one) and transformed to their first derivative before calculating the linear PLS.
In order to obtain the best results from PLS calculation and avoid artifacts, spectra of pure Theobromine were recorded (Figure 5): the main peaks related to CH, amide and carbonyl groups were identified and then used for calibration to enhance the final performance of the correspondent developed predictive model.
Four different regions can be detected: from 4000 to 5000 cm^{-1} it is possible to see different overlapped signals related to CH_3 and CONH combination bands and also the C=C stretching band. Moving between 5000 and 6000 cm^{-1} it is possible to see the region with the signal of the first overtone of amide group hydrogen bonded, the first

overtone of the methyl group and the signal of the carbonyl group (5130 cm^{-1}). Around 7000 cm^{-1} falls the same amide overtone but here this is related to the free amide; also water can absorb in this region. Then, in the last region between 8000 and 9000 cm^{-1} there is the possibility to see the second overtone of the methyl group.

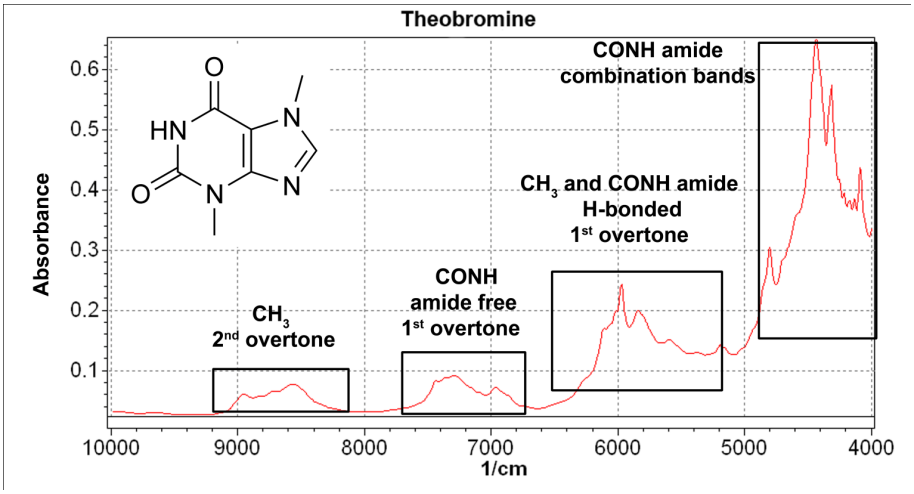

Figure 5 - FT-NIRS spectra of pure Theobromine.

A spiking experiment was done adding progressive amounts of theobromine in a xanthines-free reference biscuit matrix: to be more precise, 0.04 mg, 0.4 mg and 4 mg of Theobromine were added to 40 g of matrix in order to reach the concentration of 1 mg kg^{-1}, 10 mg kg^{-1} and 100 mg kg^{-1}, respectively. The theobromine was first dissolved in 1 mL of CH_2Cl_2 and then added to the biscuits matrix homogeneously through the use of a micropipette to obtain the best dispersion possible; these samples were left to gently air dry for 3 hours to completely remove any residual trace of solvent. The correspondent spectra were recorded using NIR spectrophotometer: from the stacked spectra shown in Figure 6 it is evident a rising of typical xanthines peaks as the concentration of Theobromine increases, supporting the possibility to establish a real correlation between xanthines concentration and NIR absorption using these spectral regions.

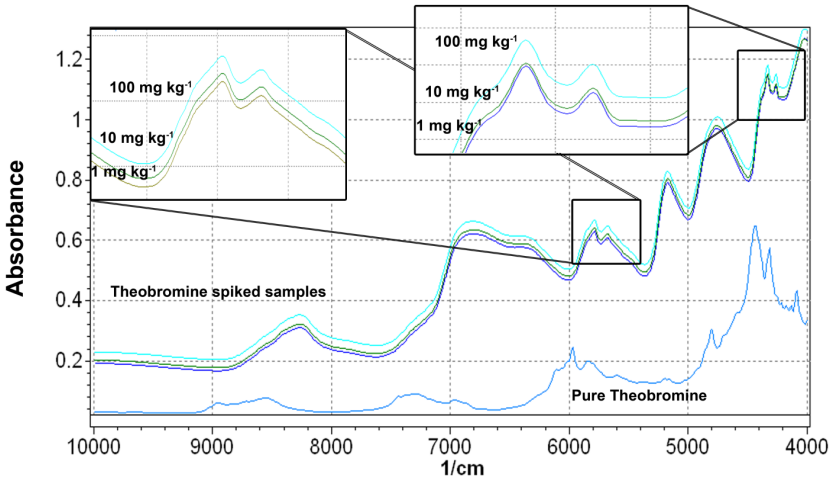

Figure 6 - Spiking\FT-NIRS experiment on xanthines free biscuit matrix.

The use of the 1st derivative pre-treatment enhances the difference and the signal increments between the spectra (Figure 7) in this way a calibration curve with a final R^2 coefficient of 0.97 (as shown in Table 3, Figure 8) was obtained.

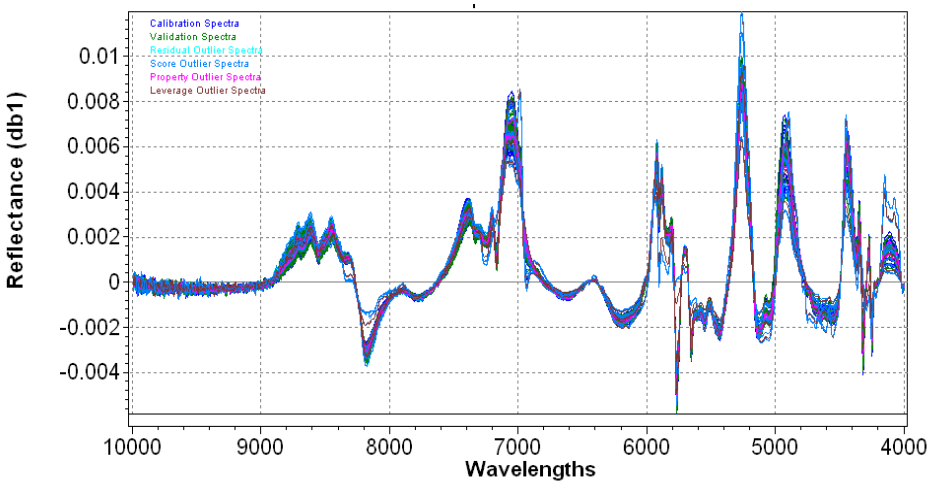

Figure 7 - FT-NIRS stacked spectra of 85 different samples (biscuits and their relative mixes) pretreated with 1st derivative.

This good degree of correlation is almost the same as the validation curve (R^2=0.96). The consistency of this model is close to 1 (SEC/SEP ratio) and the error of prediction can be estimated to be lower than 10 % with respect to the mean values recorded for the eleven categories of biscuits.

The method repeatability was evaluated through ten subsequent determinations performed by the same analyst in the same operative conditions on a Chocolate Biscuit 3 matrix: a mean value of 1524 mg kg^{-1} with a standard deviation of 30 mg kg^{-1} was recorded (Relative Standard Deviation equal to 2%).

Compound	*Set*	*N° of Samples*	*Range*	R^2	*SEC-SEP*
Xanthines	**C-SET**	**164**	**1-1600 mg kg^{-1}**	**0.97**	**77 mg kg^{-1}**
[mg kg^{-1}]	**V-SET**	**79**	**1-1600 mg kg^{-1}**	**0.96**	**77 mg kg^{-1}**

Table 2 - Statistical parameters of FT-NIR calibration curve for xanthines.

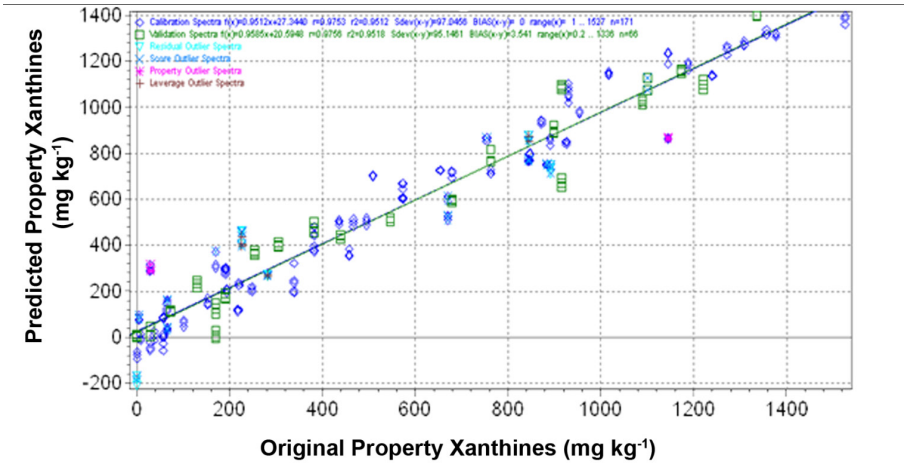

Figure 8 - FT-NIR xanthines calibration and validation curves. ◊ Calibration spectra, □ Validation spectra, ▽ Property Outlier spectra, ✳Residual Outlier spectra, X Score Outlier spectra,+ Leverage Outlier spectra.

4.3.3 FT-NIRS Partial least square regression (PLS) – Polyphenols

In this second case, the spectra of pure catechin samples were recorded as described above for theobromine. The main peaks related to CH, OH (both aromatic and aliphatic) and ether groups were therefore identified and they are summarized in Figure 9.

For the polyphenols three different spectral regions can be detected. From 4000 to 5000 cm^{-1} it is possible to see two different signals related to CH_3 and CH_2 combination bands (4400 cm^{-1} and 4300 cm^{-1} respectively). There are also the overlapped signal of OH combination band (2000-4850 cm^{-1}) and OH bending 2nd overtone (4200 cm^{-1}). Between 6000 and 7000 cm^{-1} it is possible to see the region with the signal of the first

overtone of alcoholic group with intermolecular and intramolecular hydrogen bond. Then, the last region is between 8000 and 9000 cm^{-1} and here the second overtone of the methyl group and the signals related to aromatic CH can be recognized.

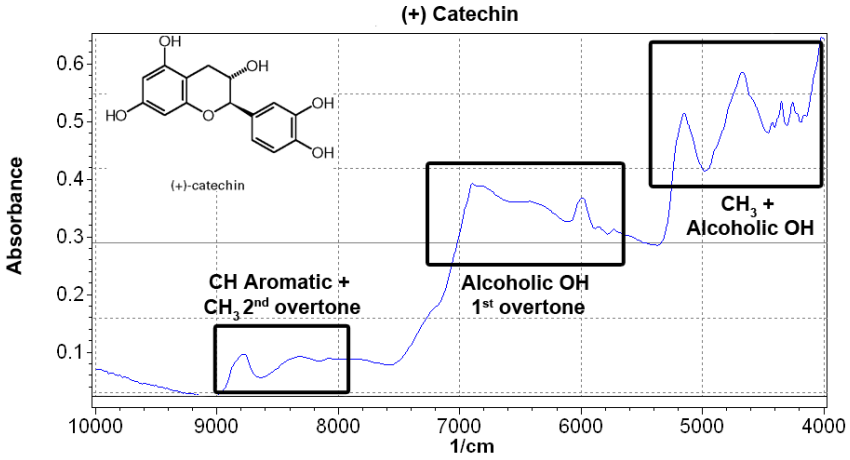

Figure 9 - FT-NIRS pretreated spectra of pure Catechin.

In this case, the concentration range actually present in the selected biscuit categories and also used for the correspondent calibration is much lower than the one used for xanthines: from hundreds of mg kg^{-1} to tens of mg kg^{-1}. This last concentration level is close to the detection limit typical for an FT-NIR instrument in these kinds of applications: larger deviations in measurements can occur frequently.

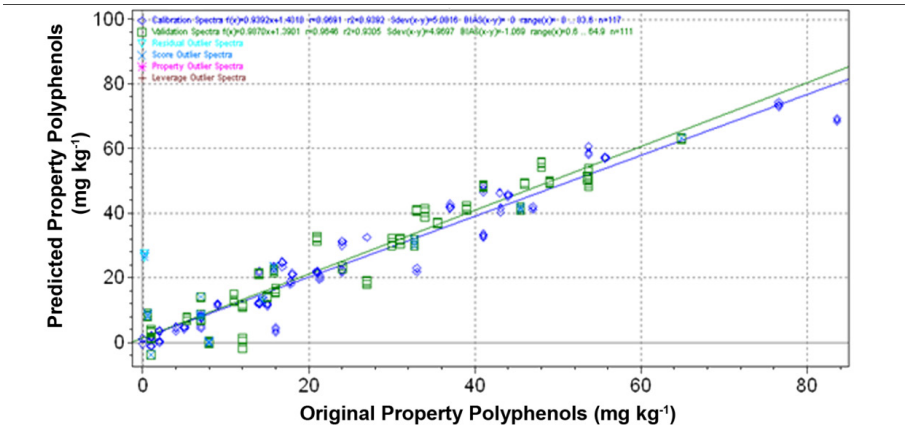

Figure 10 - FT-NIR polyphenols calibration and validation curves. ◊ Calibration spectra, □ Validation spectra, ▽ Property Outlier spectra, ✳Residual Outlier spectra, X Score Outlier spectra,+ Leverage Outlier spectra.

The same spectra of the xanthines calibration curve were exploited for building the polyphenols calibration curve (Figure 10) but in this case the spectra were used without any further mathematical pretreatment (Figure 11), because they showed better statistical results with respect to the application of the 1st derivatives. R^2 coefficient is 0.96 for calibration and 0.96 for validation curve, with a SEC and a SEP which still remain below the 10 % threshold (Table 3).
The method repeatability was evaluated, as in the previous case for xanthines, through ten subsequent determinations performed by the same analyst in the same operative conditions on a Chocolate Biscuit 3 matrix: a mean value of 52 mg kg^{-1} with a standard deviation of 6 mg kg^{-1} was recorded (Relative Standard Deviation equal to 11%).

Compound	*Set*	*N° of Samples*	*Range*	*R^2*	*SEC-SEP*
Polyphenols	**C-SET**	**156**	**0-83 mg kg^{-1}**	**0.96**	**3 mg kg^{-1}**
[mg kg^{-1}]	**V-SET**	**78**	**0-83 mg kg^{-1}**	**0.96**	**3 mg kg^{-1}**

Table 3 - Statistical parameters of FT-NIR calibration curve for polyphenols.

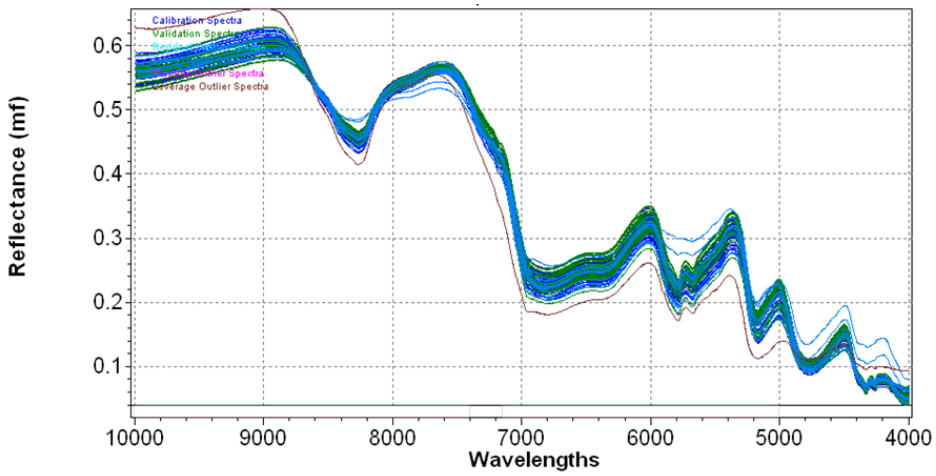

Figure 11 - FT-NIRS stacked spectra of 85 different samples (biscuits and their relative mixes) pretreated only with SNV mathematical treatment.

4.3.4 FT-NIRS Partial least square regression (PLS) – Sucrose

The third and last molecular marker analyzed is sucrose. The total compute of the bitter taste in bakery products like biscuits cannot be exploited without knowing the concentration of sugar inside the final product. Bitter and sweet tastes are able to interact each one with the other in a negative way suppressing their respective

intensities. Sucrose is present in large quantities inside the final products in a range that can vary from 14 % up to 47 % in the previously analyzed products as shown in table 5.

All the sample where analyzed with a method internally developed by Barilla. All the biscuits were ground and a quantity such as to have a concentration of sugars between 0.5 and 10 mg/mL of each sugar is picked up. Then 25 mL of ACN/H_2O 6/4 was added and the suspension was stirred in a ultrasound bath for 60 minutes. Then an aliquot was drawn and filtered with a 0.45 µm filter before LC-MS analysis. Quantification were based on the areas of the corresponding peaks measured with a refractive index detector maintained at 35°C. The pump used for liquid chromatography was a Surveyor LC Pump (Thermo Finnigan, San Jose, CA, USA). The chromatographic separation was performed using Pelliguard column LC-NH2 as precolumn and a Aminopropyl (NH2) LC-NH2, 5 µm, 25 cm x 4.6 mm ID column with a flow rate of 1.2 mL/min of ACN/H_2O 75/25 isocratic gradient. The calibration curve were made dissolving each sugar in the extraction solution at the concentrations of 0.5, 1 , 2.5 e 5 mg/ml.

Sample	*% in weight of total carbohydrates*	*% Sucrose*	*% Fructose*	*% Glucose*	*% Maltose*
Chocolate cookie 2	28.50	28.5	0	0	0
Chocolate and Cream cookie 2	23.2	23.2	0	0	0
Cream cookie	16.7	16.7	0	0	0
Lemon cookie	24.1	21.4	2.7	0	0
Chocolate cookie 2	22.3	22.3	0	0	0
Honey cookie	28.3	28.3	0	0	0
Coffee cookie	47.23	46.95	0.28	0	0
Chocolate cookie	23.8	23.09	0	0.31	0.44
Nuts cookie	23.33	23.33	0	0	0
Cereal cookie	14.28	14.28	0	0	0
Chocolate and Cream cookie	22.22	22.22	0	0	0

Table 4 - Carbohydrates concentration inside biscuits.

The spectrum of pure sucrose was recorded to identify the main peaks associable to the CH, OH, CO and COC bonds and they are summarized in figure 12.

Three different regions can be identified for sucrose. As seen in the previous case from 4000 to 5000 cm^{-1} it is possible to see two different signals related to CH_3 and CH_2

combination bands (4400 cm^{-1} and 4300 cm^{-1} respectively). Between 5000 and 7000 cm^{-1} there is a series of overlapped bands of aliphatic alcoholic groups present in the molecule, both free and intramolecular bound. Around 8000 cm^{-1} a large band is generated by the presence of several methylene groups inside the sucrose molecule. The last observable band is near 10000 cm^{-1} and it is due to the second overtone of the intramolecular hydrogen bonds of the carbohydrate molecule. In this case the concentration present inside the final products is far higher than the one seen in the two previous cases: the range of concentration is in the order of tens of percentage points as summarized in table 4.

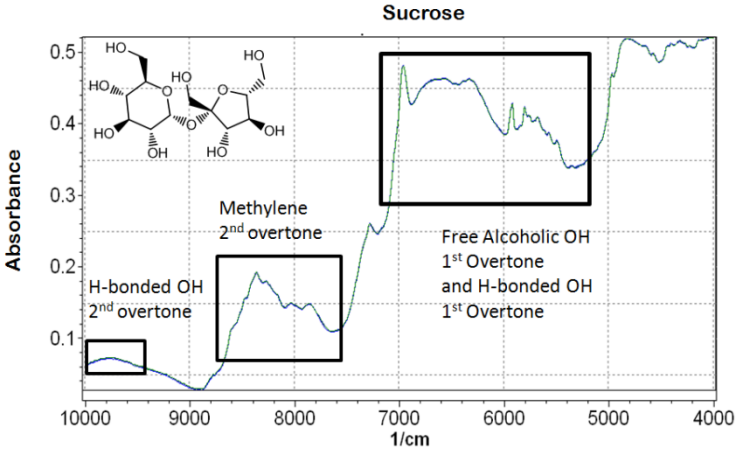

Figure 12 - FT-NIRS pretreated spectra of pure sucrose.

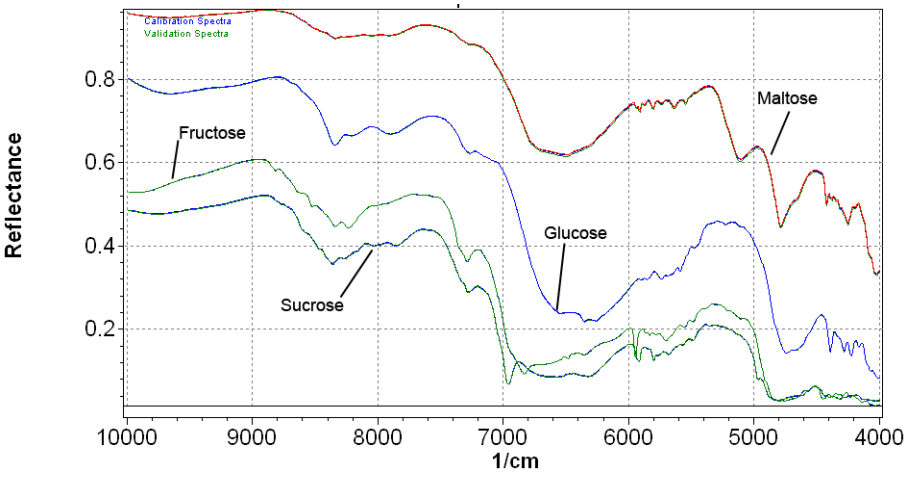

Figure 13 - FT-NIRS overlapped spectra of the four sugars.

There are also other sugars used in some biscuits: glucose, fructose and maltose. These carbohydrates do not interfere with the total sugars content evaluation executed

through the FT-NIR measurements : this is because their main absorption bands fell all together in the same spectral regions (figure 13).
Spectra of the different carbohydrates show a very similar absorption in the same regions. Sucrose is the most used sugar in all the analyzed receipt of biscuits (table 5) and therefore for the detection we decided to set the calibration curve generically on the sucrose. Only four cases show the use of sugars different form sucrose in low concentration and in all of them a larger quantity of sucrose is still present (figure 13).

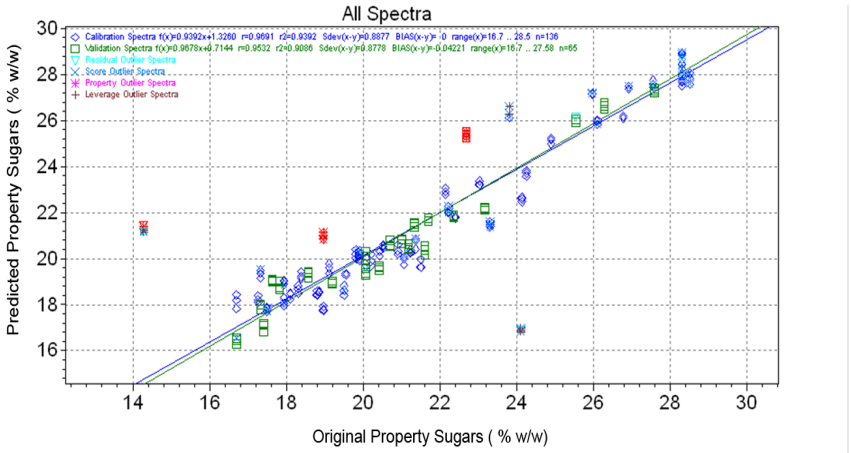

Figure 14 - FT-NIR Total sugars calibration and validation curves. ◊ Calibration spectra, ☐ Validation spectra, ▽ Property Outlier spectra, ✳Residual Outlier spectra, X Score Outlier spectra,+ Leverage Outlier spectra.

All the previous recorded spectra were used for the calculation of the calibration curve. The spectra were normalized using standard normal variance (SNV) algorithm before performing PCA analysis (figure 15). Calibration shows an R^2 coefficient of 0.93 both for calibration validation; SEC and SEP are far below the 10 % threshold (table 5).
The method repeatability was evaluated, as in the previous cases, through ten subsequent determinations performed by the same analyst in the same operative conditions on a Chocolate Biscuit 3 matrix: a mean value of 22.28 % (w/w) with a standard deviation of 0.75 % (w/w) was recorded (Relative Standard Deviation equal to 3 %).

Compound	*Set*	*N° of Samples*	*Range*	*R^2*	*SEC-SEP*
Total Sugars	**C-SET**	**136**	**14.28-47.23 %**	**0.93**	**0.88**
[% w/w]	**V-SET**	**65**	**14.28-47.23 %**	**0.93**	**0.87**

Table 5 - Statistical parameters of FT-NIR calibration curve for sugars.

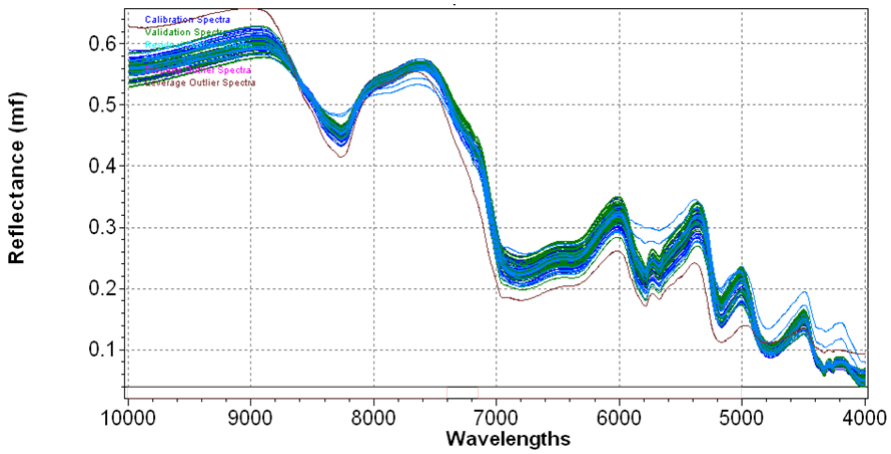

Figure 15 - FT-NIRS stacked spectra of 85 different samples (biscuits and their relative mixes) pretreated only with SNV mathematical treatment.

4.3.5 Interference of water in FT-NIRS : is this a real problem in standardized industrial biscuits production ?

Interference in FT-NIR spectroscopy can be relevant due to the of water presence in large quantities (intended in terms of moisture inside the analyzed sample). The presence of different intense water adsorption bands is able to modify dramatically the transmittance spectra. In order to measure if this phenomenon is interfering with the xanthines and the polyphenols measurements inside the analyzed samples, a series of water spiked samples was tested. A nuts based cookie with an average concentration of bitter taste markers was chosen as reference biscuit for this test. First of all the native moisture concentration was measured. Using a oven at 70°C with a pressure of 100 mbar for one night; the weight of the sample was measured before and after the heating procedure and the total moisture is calculated as the difference between the two weights. The cream based cookie contains 1.7 % of water (on a weight basis) with a tolerance of 0.5 %. Ten samples were created ad hoc and were analyzed in double (1 standard samples and 4 samples with raising and controlled moisture). In table 6 all the data about these samples are summarized.

	Matrix Weight	H_2O added (mL)	Theoretical Moisture (% w/w)
S1	-	-	1.7
S2	-	-	1.7
A1	20.1427	0.2	2.7
A2	20.1538	0.2	2.7
B1	20.069	0.3	3.1
B2	20.0672	0.3	3.1
C1	20.2432	0.4	3.6
C2	20.0727	0.4	3.6
D1	20.6138	0.5	4.0
D2	20.4575	0.5	4.0

Table 6 – Theoretic moisture inside the 10 samples.

All these samples were analyzed using FT-NIR in order to evaluate the Xanthines and polyphenols concentration. The results are summarized in table 7. The S entries refer to the standard reference cookie without the addition of water. The A, B, C and D samples are the spiked ones.

	Sucrose (% w/w)	Xanthines (mg/kg)	Polyphenols (mg/kg)
S1	22.72	987.21	26.95
S2	22.52	1077.65	26.64
A1	23.65	873.33	31.7
A2	23.73	858.57	27.9
B1	24.94	875.62	37.6
B2	24.82	866.79	30.3
C1	24.82	793.83	41.9
C2	25.03	878.21	40.2
D1	25.75	789.95	35.2
D2	25.29	861.3	33.4

Table 7 – FT-NIR results for spiked samples.

	H_2O Wavelength (cm^{-1})	Aliphatic Alcohol Wavelength (cm^{-1})	Aromatic Alcohol Wavelength (cm^{-1})
Combination	518-5150 7270-7220	-	-
1st overtone	6900-6850	6970-6270	6970-6270
2nd overtone	10260-10250	10200-10100, 9960-9570	10200-10100, 9960-9570
3rd overtone	13510-13330	-	-

Table 8 – Absorption bands in NIR region for water, aliphatic alcohols and aromatic alcohols.

These results show a remarkable interference effect due to the presence of water inside the samples. This effect is relevant for sucrose and polyphenols because these two categories of gustative markers have NIR absorption bands almost identical. Hydroxyl groups in carbohydrates are aliphatic and in polyphenols are both aliphatic and aromatic. In table 8 the main absorption bands of water, aliphatic alcohols and aromatic alcohols are summarized. The first and the second overtone bands of these three categories of markers are overlapped and this means that the water can interfere dramatically on the quantification of sucrose and polyphenols because the interferometer is not able to sense the water as different with respect to these two molecular marker categories. The effect is pronounced in the case of sucrose because both sucrose and water are in the concentration level of percentage points. The polyphenols, even with their lower concentration level (mg kg^{-1}), are less influenced by the water because the moisture level of the analyzed biscuits is only few percentage points to the utmost. In conclusion water is a big interferent for bitter taste molecular markers analysis made with FT-NIR, anyway its presence can be easily controlled inside the final product by other quality control analysis directly at the manufacturing site : the biscuits with moisture levels out of the standard specifications are therefore eliminated already before any possible FT-NIR measurement of bitterness evaluation

4.3.6 FT-NIRS prediction performances on real samples

In order to test the reliability of the developed FT-NIRS protocol we tried to apply it for predicting the concentration of pure biscuit samples working within the same categories used for calibration. In figure 16 it is illustrated the prediction ability for polyphenols: the error is in general relatively high due to the low concentrations involved, except for chocolate biscuit categories. In particular, it can be seen that chocolate- based biscuits, having the higher concentration of polyphenols, reveal the

best achievable performance; biscuits made with a limited percentage of cocoa (like nut biscuits and chocolate & cream biscuits) show an increased error of prediction.

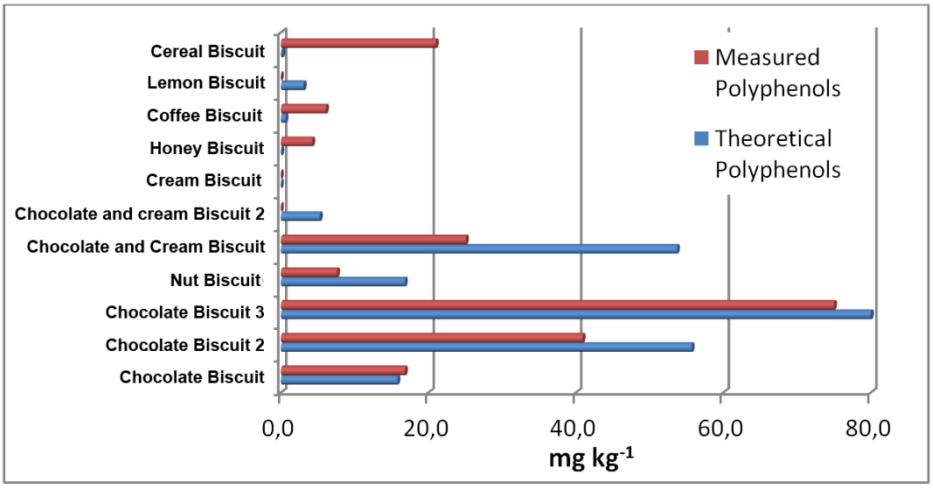

Figure 16 - FT-NIRS validation experiment for polyphenols.

On the other hand, in the case of xanthines (Figure 17), the concentration range explored being 1-2 orders of magnitude higher than in polyphenols, the percentage error in the measurements is significantly lower and the agreement between FT-NIRS and LC-MS reference method is very good, in particular for chocolate-based biscuits but not for cereal, lemon and coffee biscuits were the matrices are less homogeneus.

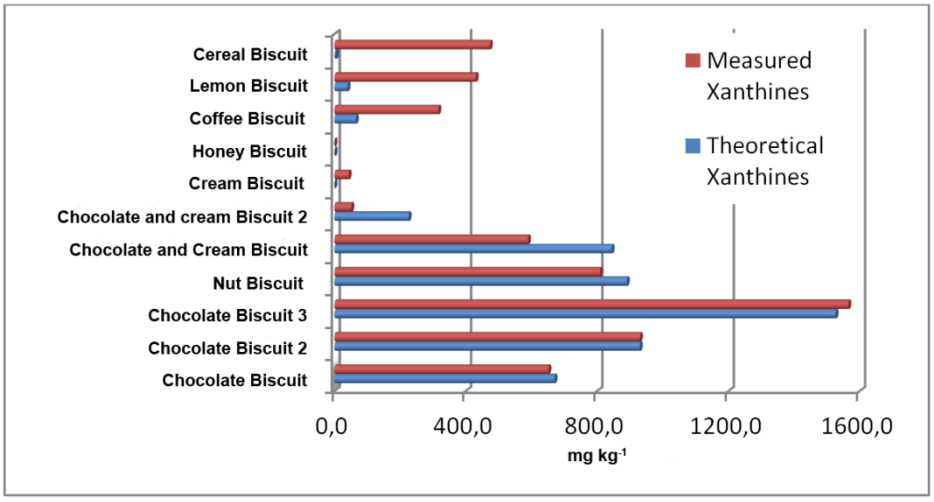

Figure 17 - FT-NIRS validation experiment for xanthines.

In order to facilitate the use of this strategy for routine analysis, it could be useful to introduce a specific BIAS correction (that consider the variation of recipe in terms of different ingredients, corresponding to changes of the spectra), which must be calculated for each type of biscuit category, adapting correspondently the calibration curve intercept.

In the case of sugars there is a better agreement between the two techniques due to the higher concentration involved in the samples analyzed. Less sweet sugar has a content of about 15 % on a weight basis that is far higher than the previously discussed concentrations. So there is also a better agreement between the HPLC-MS and the NIR data. In this case the best agreement is reached on the biscuits with the more homogeneous phases because concentration of the analyte is no more a problem. Sample like the cereal cookie is at the same time the one with the lesser concentration of sugars and with a heterogeneous phase difficult to be finely grinded. These two aspects are responsible of the discrepancy between NIR and reference technique. On the other hand also the sample with the higher concentration of sugars shows a relevant difference between the two techniques. The grinded solids seem like a fine powder and posses a different aspect in comparison to the other sample used to build up the calibration curve. This difference in the matrix composition is responsible of the big error made in quantification of sweeteners inside the coffee based cookie.

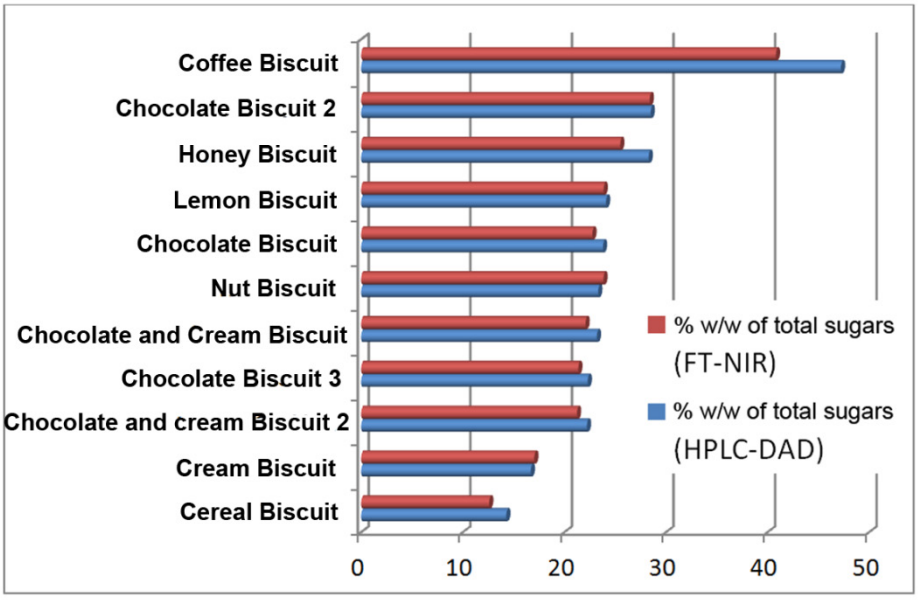

Figure 18 - FT-NIRS validation experiment for sugars.

4.3.7 Interlaboratory validation

In the manufactory of biscuits the taste of the final product is directly checked on-site by the personnel on the basis of their experience. For the everyday production, no PAA is performed in order to check the taste of the product and there is no possibility to archive taste analysis performed on each single batch. FT-NIR can be used to fill this lack in quality control helping the personnel with a standardized method able to detect molecular markers directly correlated with the overall bitter taste sensation. The production of nuts-based biscuits was checked for twelve production turns by two different laboratories. Control charts were developed in order to monitor if the bitterness is constant among the productive batches (Figure 19).

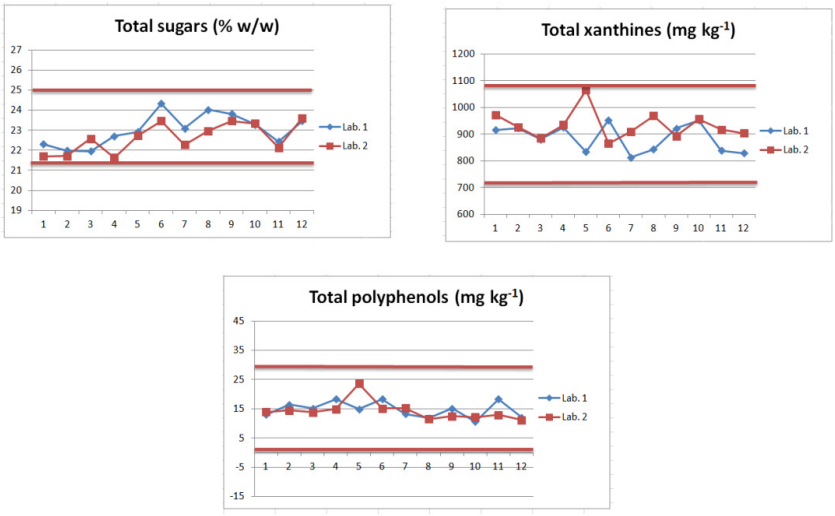

Figure 19. Bitter taste molecular markers control chart for Laboratory 1 and 2.

Results showed by Laboratory 1 and 2 were performed on the same samples and agree for all the three categories of taste molecular markers. It is possible to see that the 12 analyzed samples exhibits all the three categories of markers inside the acceptance limits imposed for the nuts based biscuits. This demonstrate the possibility to apply the FT-NIR methods on different quality control laboratories obtaining similar results.

4.4 Concluding Remarks

A rapid and simple FT-NIR spectroscopy procedure, coupled with an appropriate multivariate calibration method was developed to estimate bitter taste molecular markers in bakery commodities [6]: the overall results demonstrate that major Xanthines and polyphenols content can be directly determined on ground solid biscuits in few minutes.

This FT-NIR strategy was successfully validated by performance comparison with a reference LC-MS method, working with eleven selected biscuit categories differentiated for their characterizing ingredients. Chocolate-based biscuits, having the higher concentration of polyphenols, reveal the best achievable predictability for this class of compounds. In the case of Xanthines, the concentration range explored being 1-2 orders of magnitude higher than in polyphenols, the percentage error in the measurements is significantly lower and the agreement between FT-NIR and LC-MS is particularly satisfying.

A further comparison between sensory panel test data demonstrated that there is a correlation between the concentration of these compounds and the perceived bitter taste on the biscuits.

This technique has been shown to be fast, nondestructive and versatile, that is adaptable to different class of molecules and can be used in future to improve quality control directly on the production site for routine analysis.

4.5 Acknowledgements

The authors would like to thank Giovanni Campolongo (Büchi Labortechnik, Switzerland), Dante Catellani and Gilda Re (Barilla SpA, Italy), for help and fruitful discussions.

References

[1] "*Near Infrared Spectroscopy Principles, Instruments, Application*" ; Siesler H. W., Ozaki Y., Kawata S., Heise H. M.; Wiley-VCH, ISBN 3-527-30149-6.

[2] "*Standard error of prediction for multiway PLS 1. Background and a simulation study*"; Faber N.M., Bro R., Chemometrics and Intelligent Laboratory Systems, Vol. 61, Pg. 133–149 (2002).

[3] "*Estimation of partial least squares regression prediction uncertainty when the reference values carry a sizeable measurement error*"; Fernandez P. et alter, Chemometrics and Intelligent Laboratory Systems, Vol. 65, Pg. 281-291 (2003).

[4] "*Applied Sensory Analysis of Food. Vol.1*"; Neilson A.J., Moskowitz H., Ed. CRC Press, Inc., Boca Raton, FL, Chapter 2 (1988).

[5] "*Handbook of the NIR-spectrometer System"*; A.G. Buchi ; Uzwil, Switzerland (1993).

[6] "*Rapid and simultaneous analysis of xanthines and polyphenols as bitter taste markers in bakery products by FT-NIR spectroscopy*"; Bedini A., Zanolli V., Zanardi S., Bersellini U., Dalcanale E., Suman M., Food and Analytical Methods, Vol. 6, Nr. 1, Pg. 17-27 (2013).

Design of Experiment

5

5.1 What is Design of Experiment ?

Design of Experiment (DoE) involves making a set of experiments representative with regards to a given question. The way to do this is dependent from the problem taken into account and in function of that the complexity of the statistical experimental design may vary considerably [1]. DoE can be used with different purposes in regard to the same problem, it can be used to optimize a process or an analytical technique or to check the robustness for example. Another important problem that can be solved with DoE is the identification and the screening of important factors; this means that DoE is able to show interaction between variables that are not directly observable.

The design of experiments (DoE) method provides guidelines for the design of all information-gathering exercises where variation is present, whether this variation under the full control of the analysis or not. Design of experiments is a series of tests in which purposeful changes are made to the input variables of a system or process and the effects on response variables are measured: the analyst is interested in investigating phenomena and studying the synergistic effects of some interventions (the 'treatments') to optimise the final process. Experimental design is an effective tool for maximizing the amount of information gained from a study while minimizing the amount of data to be collected; factorial experimental designs are geometrically constructed to investigate the effects of many different factors by varying them simultaneously and orthogonally, instead of changing only one factor at a time. Factorial designs collect data at the vertices of a cube in p-dimensions (p is the number of factors being studied). If data are collected from all of the vertices, the design is a full factorial, requiring 2^p runs. Since the total number of combinations increases exponentially with the number of factors studied, fractions of the full factorial design can be constructed. Fractional factorial designs collect data from a specific subset of all possible vertices and require 2^{p-q} runs, with 2^{-q} being the fractional size of the design [2]. In our case the selected DoE approach makes possible to realize the minimum number of biscuits, in a pilot plant, in order to clarify the connection between bitterness, ingredients, molecular markers concentration and baking parameters. Using a statistical software package (in our case Modde 9.0, Umetrics, Umeä, Sweden), it is possible to calculate the minimum number of experiment that can be done in order to characterize completely the model with the analytical techniques at our disposal.

5.2 Maillard compounds, colorimetric and fluorescence detection

The realization of a DoE on bakery products necessitate the introduction of new analytical techniques aimed to detect the presence of bitter taste compounds

originated during the baking process. This class of markers is composed by the Maillard compounds (figure 1). Their formation starts with a reaction between a reducing sugar and a compound that posses a free amino group (like an amino acid or a peptide amino terminal). The resulting condensation product is able to rearrange in the form of the Amadori compounds [3-4]. Depending on the pH these class of molecules are able to became furfural (pentose sugar and pH<7) or hydroxymethylfurfural (hexose sugar and pH<7). At basic pH a large variety of compounds able to go under further reaction are generated and in the final stages they originate the melanoidine [5] brown polymers and oligomers (type I and type II shown in figure 1).

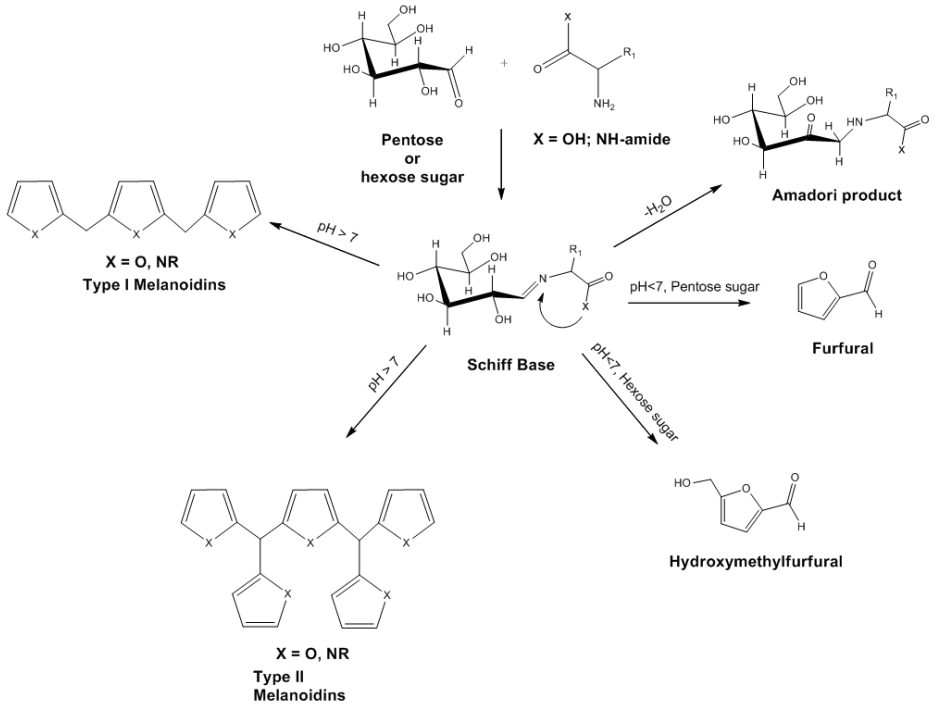

Figure 1 – Maillard reaction, possible pathways.

Generally Maillard compounds are attributed to be responsible of two important characteristics of the final products [6] :

- **The "cooked" aroma**, due to the presence of volatile compounds like furfurals.

- **The brown color**, due to the presence of melanoidins (brown polymers rich of nitrogen).

The large quantity of products with no strong structural analogies that compose Maillard compounds make their detection a difficult task. This problem can be overcome focusing only on the coloured molecules that rise in the late part of the reaction, like the melanoidins. A practical solution can be the measure of changing of colours in the surface of the sample. This can be done measuring the intensity and the colour itself with a colorimeter in an appropriate colour space coordinates.

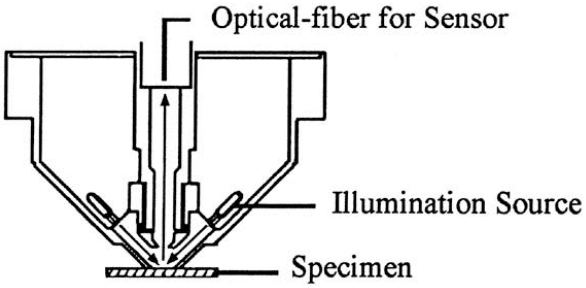

Figure 2 – Colorimeter scheme

The colorimeter (figure 2) is able to detect with precision the colour of the sample only in a precise spot and the overall colour cannot be measured in a single time. In order to do that we need to measure different spots on the sample surface and express the overall measure as a mean value. In our case we choose to measure 10 spot on the biscuits surface. For these analysis the colour space chosen is the 1976 CIELab* (because it is independent from the instrument used for the colorimetric measures). These coordinates permit to define a specific colour in terms of :

- **L***, indicates the luminance of the sample where 0 is the black and 100 is the white.
- **a***, define the red/green tonality. A negative value indicate the green instead a positive value indicate the red.
- **b***, define the yellow/blue tonality. A negative value indicate the blue instead a positive value indicate the yellow.

It is possible to identify univocally a single colour using a tern of these coordinates[1]. A second analysis of Maillard compound was performed using the fluorescence generally possessed by this class of molecules [7-8]. The differences between Maillard compounds can be attributed to the peptides involved in the first step of the reaction. This lead to different compounds with similar structures but with a large variety of substituents. The structural affinities lead to a common response toward the fluorescence. Most of them can be excited, in water solution, with 370 nm UV light and can be detected reading the fluorescence at 440 nm. Colorimetry and fluorescence lead to complementary information about Maillard compounds because with the first one it is possible to spot the Melanoidins at high molecular weight and with fluorescence all the water soluble Maillard compounds can be practically detected[2]. All the data regarding colorimetric and fluorimetric measurements are summarized in table 3 in the following paragraph.

5.3 DoE on bitter taste molecular markers

The aim of the present design of experiment is to prove and quantify the correlation between the different bitter taste molecular markers investigated with different techniques (FT-NIR, RP-HPLC-MS, fluorimetry and colorimetry) and the overall bitterness sensation measured by a panel group (PAA). Few reports are found in the literature in relation to the combination of several techniques to be used together to analyze food [9]. The present DoE consists in the preparation of different samples ad hoc with different ingredients, with a known content of xanthines and polyphenols, cooked with an opportune time/temperature combination chosen in a technological range commonly used for technological commercial biscuits production.

The factors that we decided to change can be divided into two categories :

- ingredients;

[1] All measures were made with a Konica-Minolta CR-400 and the overall colour described by the coordinates L*, a* and b* was calculated as the mean value of ten different measures on the biscuits upper surface.

[2] 30 g of a selected biscuit were finely grinded and 9.5 g of them were taken and extracted with 20 mL of water at 60 °C for 1 hour. The suspension was filtered first on a Buckner funnel and then with a 0.45 µm filter (it is important that the final extract is clean without any impurity). The eluate was rinsed with fresh water in order to restore the starting volume. A polyethylene cuvette was filled with 1 mL of the solution and the fluorescence in arbitrary units (FSU) was recorded for the DoE analysis (λ exc= 370 nm; λ em =440 nm).

- process parameters;

The chosen ingredients are :

1. **Cranberries juice (Cro%)**, added to modulate the concentration of polyphenols inside the biscuits. The cranberries juice is added in concentration of 2%, 4% and 6% (w/w).
2. **Cocoa in powder (Coc%)**, added to modulate the concentration of xanthines inside the biscuits. In this case the concentration chosen are 2%, 6% and 10% (w/w) (levels commonly retrieved in commercial biscuits).
3. **Sucrose (Sug%),** added to modulate the sweet taste and also to mask the bitter taste of the other compounds. The chosen concentration are 12%, 20% and 28% (w/w).

The process parameters are :

1. **Baking time (Bak_t),** in order to give time to the mixture to form a biscuit with an opportune consistency : both for panel test and FT-NIR analysis the time condition chosen are 6, 8 and 10 minutes.
2. **Baking temperature (BakT),** chosen with the same criteria of the previous process parameter between 160°C, 180°C and 200°C.

The present study is based on a fractional factorial Screening Design of Experiments (SDoE) in which the experiments varied five process parameters for biscuits. Each selected treatment was varied over a defined range and replicates of the central point were performed to estimate the experimental error. The experimental data were then analysed using a multivariate analysis approach based on the partial least-squares technique included in a dedicated statistical package (MODDE software, vers. 9.0, Umetrics; Umea, Sweden). In order to calculate the minimum number of experiment needed for the DoE different measurable variable must be chosen. The selected responses are summarized in table 1.

Name	Label	Unit of measurements
Total Xanthines (LC-MS)	X-LC	mg kg^{-1}
Total Xanthines (FT-NIR)	X-FT	mg kg^{-1}
Total Polyphenols (LC-MS)	P-LC	mg kg^{-1}
Total Polyphenols (FT-NIR)	P-FT	mg kg^{-1}
Total Sugar (FT-NIR)	S-FT	% (w/w)
Bitterness Index (PAA)	BI	B.I.
Total Maillard Compounds (Fluorescence)	MaiF	FSU
Maillard Compound L parameter (CIELab)	HeaL	L
Maillard Compound a parameter	HeaA	a

(CIELab)		
Sweet Index (PAA)	SI	S.I.
Astringency index (PAA)	AI	A.I.

Table 1 – Recorded responses for DoE

All the responses were previously discussed. In this case the sensorial analysis (PAA) refers not only to the bitter taste but also to sweet and astringent taste. Astringency is not a real taste because there is no interaction between receptors on the tongue and astringent molecules. This sensation is due to the precipitation of glicoproteins that act as tensioactive in the saliva induced by the presence of flavonoids like polyphenols or procyanidin [10].

The necessary experiments for the realization of the DoE were evaluated using the Modde software package on the basis of the factors and measurable variables chosen. Table 2 summarizes all the needed experiments and the value of each factor used. Each experiment refers to a biscuit baked with an opportune time/temperature combination and with a determined amount of ingredients.

Exp N°	Exp Name	Run Order	Cocoa percentage in recipe (%w/w)	Cranberries juice percentage in recipe (%w/w)	Baking Temperature (°C)	Baking time (minutes)	Sugar percentage in recipe (%w/w)
1	N1	2	2	6	160	6	12
2	N2	5	10	2	200	6	12
3	N3	11	10	2	160	10	12
4	N4	10	2	2	200	10	12
5	N5	7	10	6	200	10	12
6	N6	4	2	2	160	6	28
7	N7	3	10	6	160	6	28
8	N8	6	2	6	200	6	28
9	N9	1	2	6	160	10	28
10	N10	12	10	2	200	10	28
11	N11	8	10	6	200	10	28
12	N12	13	10	6	200	10	28
13	N13	9	10	6	200	10	28

Table 2 – Experiment for DoE

All the experiments were conducted changing several factors at the same time; on the contrary the experiments labeled from N11 to N13 posses the same recipe in terms of baking time, temperature and composition in order to use them as control experiments for the developed model. In table 3 there are summarized all the results obtained applying the previously described analytical techniques to the 13 samples baked for the DoE.

Exp N°	Exp Name	Run Order	Xanthines tot LCMS	Xanthines tot FTNIR	Polyphenols tot LCMS	Polyphenols tot FTNIR	Sugar tot FTNIR
1	N1	2	979	658	120	19	17
2	N2	5	1945	1596	124	70	17
3	N3	11	1227	1664	78	49	15
4	N4	10	333	482	30	19	18
5	N5	7	1767	1459	107	27	13
6	N6	4	386	315	41	18	30
7	N7	3	2109	1411	177	64	26
8	N8	6	471	406	54	7	25
9	N9	1	351	441	44	< LOQ	25
10	N10	12	1668	1251	124	2	23
11	N11	8	2242	1213	131	2	22
12	N12	13	2069	1149	106	< LOQ	24
13	N13	9	2159	1205	113	< LOQ	23

Exp N°	Exp Name	Bitterness Index	Maillard compounds through fluorescence response	Over/under-heating through CIELab coordinate L	Over/under-heating through CIELab coordinate a	Sweet Index	Astringency Index
1	N1	5	58202	47	17	5	8
2	N2	8	9999	33	12	5	8
3	N3	8	8261	33	12	5	9
4	N4	3	45036	49	12	6	6
5	N5	10	1592	31	12	4	9
6	N6	2	50489	49	11	9	5
7	N7	7	36414	23	13	8	9
8	N8	4	52955	40	15	4	9
9	N9	5	44354	39	15	5	9
10	N10	7	2122	30	11	6	6
11	N11	8	1612	28	12	5	9
12	N12	8	1713	27	11	4	8
13	N13	8	1795	28	12	4	9

Table 3 – Experiments for DoE : responses.

On the basis of these data various statistical tests were performed in order to evaluate the correlation between the previously identified taste markers and the bitterness elicited by the biscuits:

1. Distance between the replicates
2. Model fitting
3. Correlation between variables

4. Residuals
5. ANOVA
6. Variable importance plot
7. Scaled and centered coefficients
8. Contour Plot

5.3.1 Distance between the replicates

Distances between replicates can be used for an overall description of the model in order to look if each analytical technique used is able to discriminate the samples. For each table the first important result, about the reproducibility of the method, can be read about the 3 replicate experiments (in our case N11-N13). In a ideal model there will be no difference between these 3 samples, in an acceptable model the distances are minimal. Figure 3 shows a comparison between the results obtained for xanthines detection with LC-MS and FT-NIR. In both cases the N11-N13 prove the reproducibility of the two techniques because the distances between the repeated samples are reasonably low compared with the N1-N10 samples (where conditions, recipe, etc... were varied).

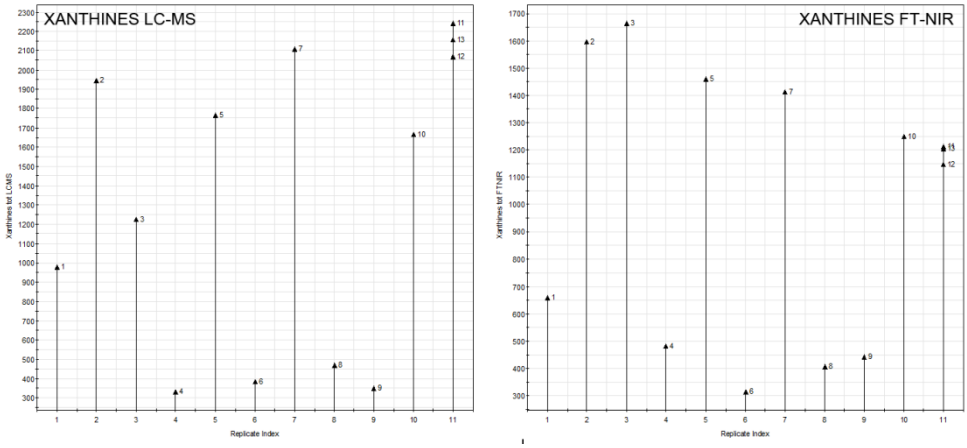

Figure 3 – Replicate index for the total xanthines concentration in samples using LC-MS (left) and FT-NIR (right)

A similar conclusion can be done for the polyphenols detection using both LC-MS and FT-NIR (figure 4). Also in this case experiments N11-N13 show that there is a good reproducibility in both the analytical techniques.

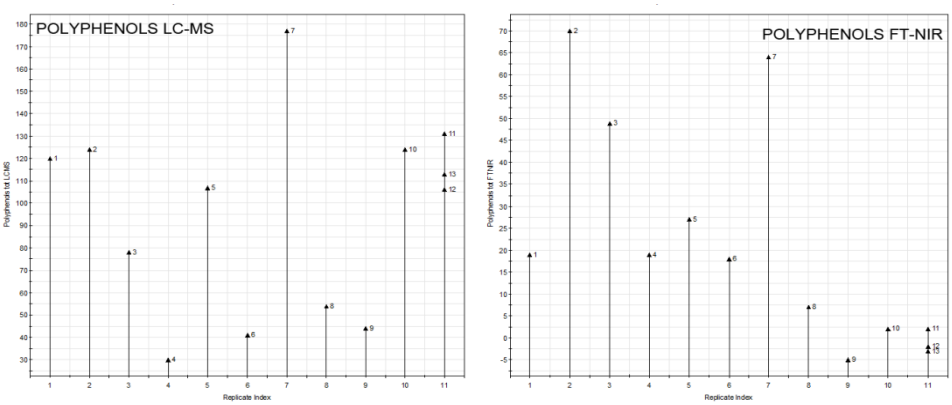

Figure 4 – Replicate index for the total polyphenols concentration in samples using LC-MS (left) and FT-NIR (right)

There is a disagreement between the absolute values recorded with LC-MS and FT-NIR for the same sample. This is due to the fact that FT-NIR calibration curve were calculated using a different set of biscuits and, in the DoE, the new matrix variables (like the presence of the cranberries juice) disturb the analysis. Nevertheless we decided to skip the dedicated calibration curve for xanthine and polyphenols for the DoE samples because in this case the main information about the taste markers can be learned by the relative values of their concentration.

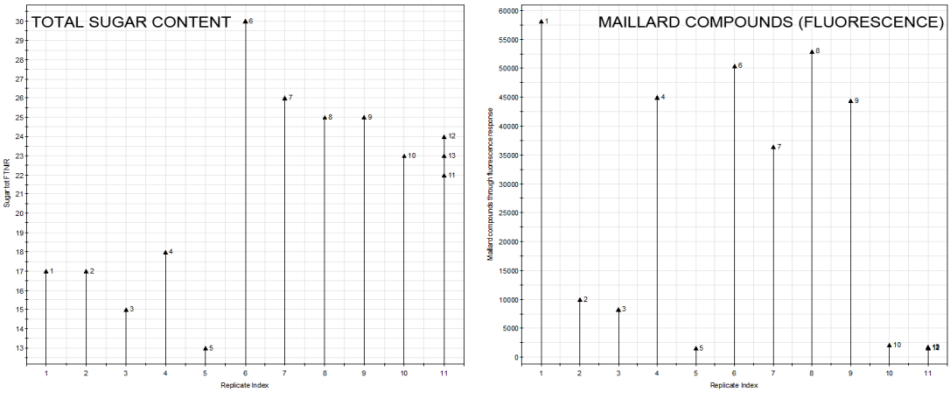

Figure 5 – Replicate index for the total sugar concentration in samples using FT-NIR (left) and Maillard compounds using fluorescence method (right).

Figure 5 represents the data concerning sugar detection (by FT-NIR) and fluorescence detection: this second one shows a particularly good reproducibility proving its potentiality in the in investigation of Maillard compounds.

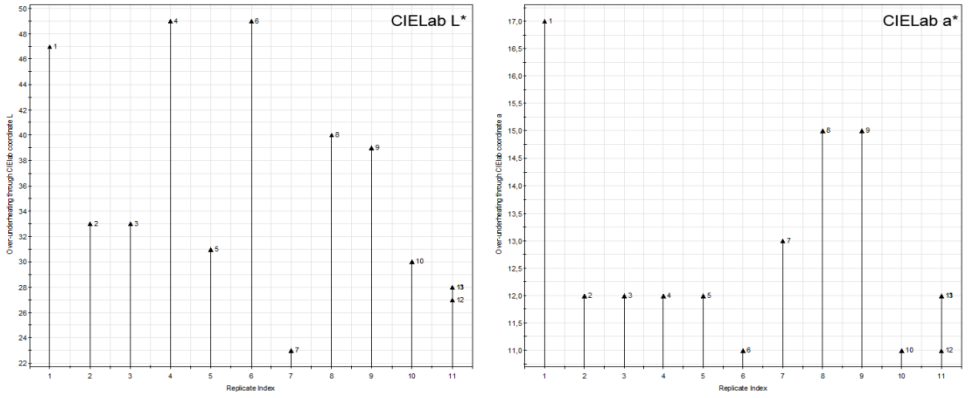

Figure 6 – Replicate index for the total sugar concentration in samples using CIELab L* (left) and CIELab L* (right).

Instead the melanoidins detection is performed using colorimetry and in particular focusing our attention on the L* and a* colour coordinates. Also colorimetry prove to be sufficiently reproducible in order to be used for the model development (Figure 6). In the last figure (7) all the three sensorial analysis performed using a trained panel group are summarized. Three different tastes aspects were detected and for all of them (especially for bitterness) a very high reproducibility can be observed.

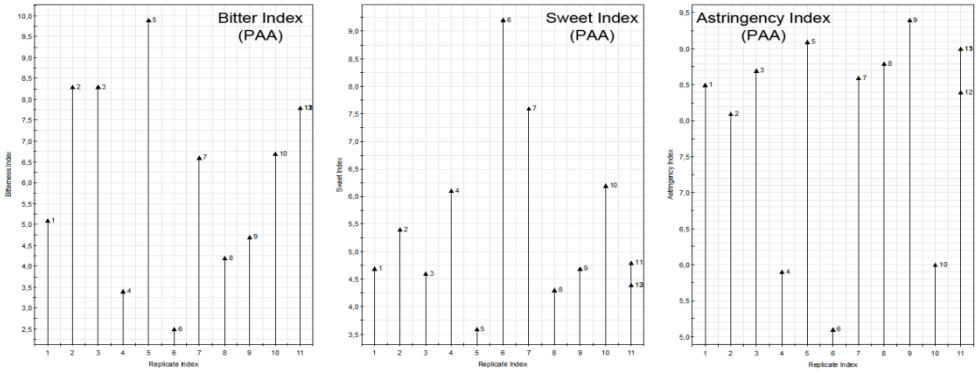

Figure 7 – Replicate index for the PAA responses.

5.3.2 Model fitting

Four different values are used for the model fitting description:

- **R^2 (green bar)** is the linearity of the model and in order to be explanatory of the model it must be superior to 0.80;

- **Q^2 (blue bar)** is explicative when the value is superior to 0.50; it describes the reliability to predict a specific variable;
- **Model validity (yellow bar)** it needs to be at least 0.20 in order to have a measure considered valid for the model;
- **Reproducibility (light blue bar)** a value close to 1.00 indicates a good reproducibility of the measurements.

The first case taken into account is the one of xanthines (figure 8). Both the LC-MS analyses and FT-NIR analyses exhibit linearity in the response, reproducibility and capability of prediction.

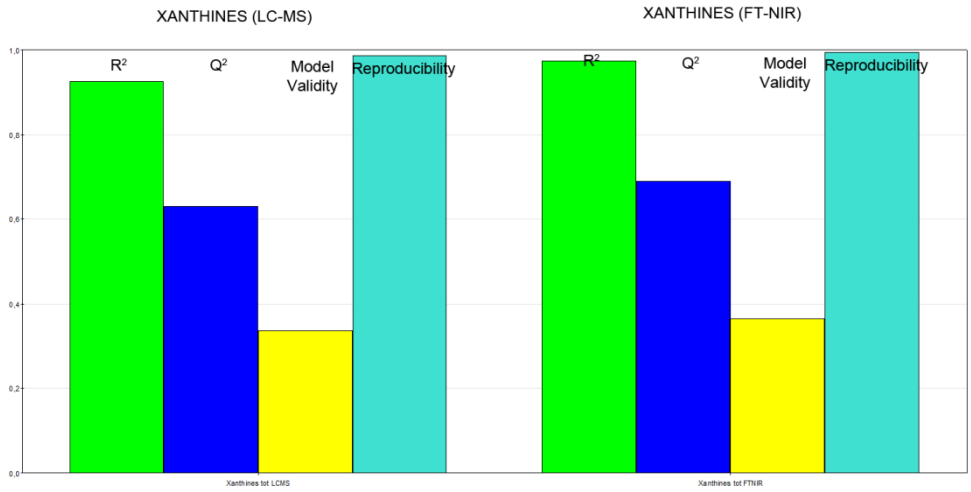

Figure 8 – Model fitting for Xanthines.

A similar consideration can be made for the polyphenols (figure 9). In this case the LC measure satisfy all the requirements for the model validity. FT-NIR shows instead a lack in the capability of prediction of the polyphenols content : the reasons for that were previously discussed.

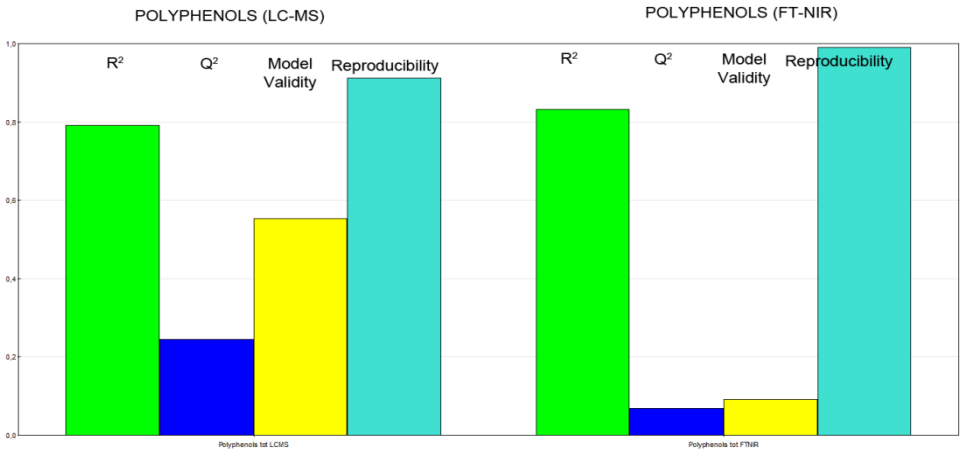

Figure 9 – Model fitting for polyphenols.

FT-NIR shows a very good capability of describing the sugar content inside the samples as demonstrated in figure 10. Fluorescence Maillard compounds detection shows a negative model validity; this means that the average error is higher than the one of single measures (lack of fit). Despite of its high reproducibility this type of measure is less reliable than the other ones described until now.

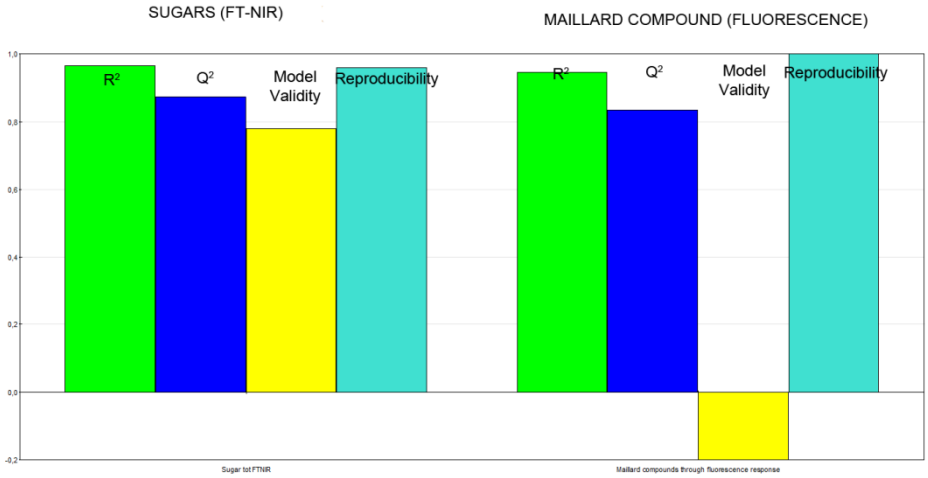

Figure 10 – Model fitting for sugars and Maillard compounds detected by fluorescence.

Instead, colorimetry manifests a better behavior in the description of Maillard compounds (mainly melanoidins) in the experimental samples (figure 11).

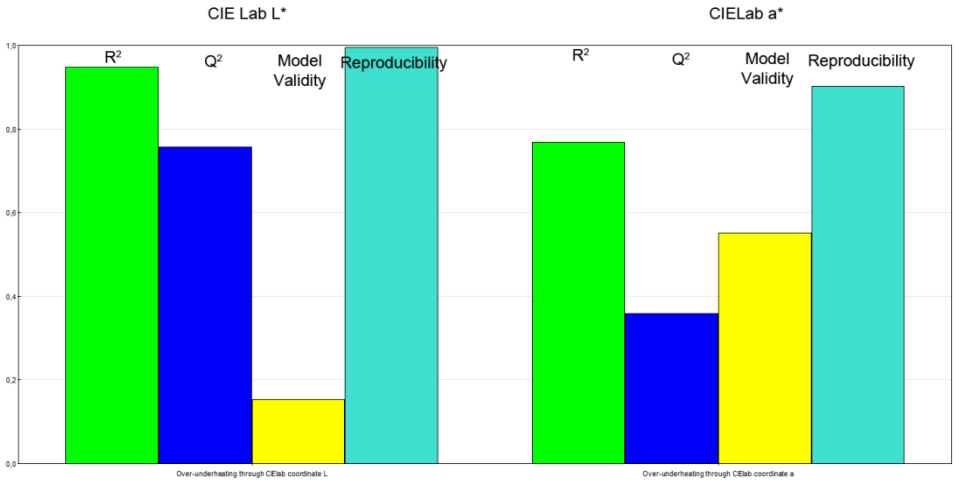

Figure 11 – Model fitting for Maillard compounds detected with colorimetry.

L* coordinate shows a better fitting with respect to a* but a lower validity due to a high mean error associated to the measure. For the colorimetric description of Maillard compounds the a* shows great capability for the detection of melanoidins on the surface of the analyzed samples. In fact melanoidins are responsible for the browning of biscuits during the baking process and the brown color is described principally by the a* coordinate.

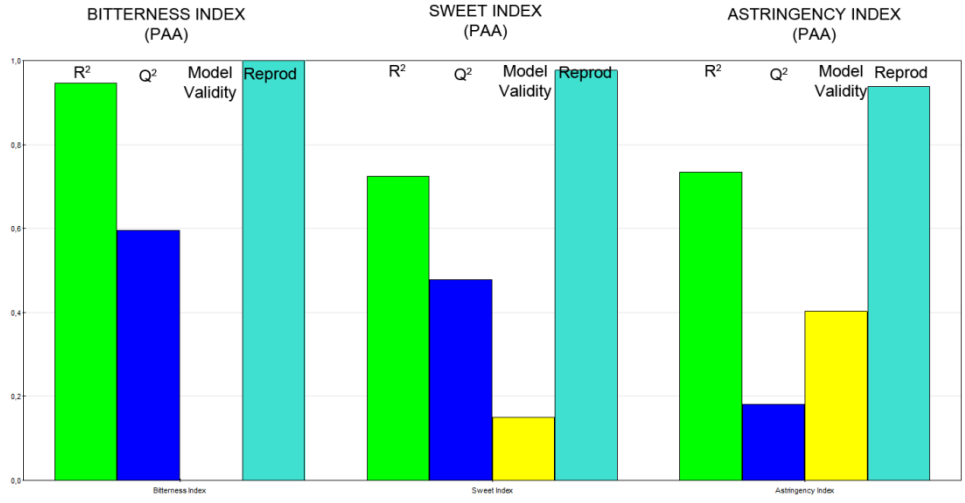

Figure 12 – Model fitting for sensorial data obtained with PAA.

The last discussed model fitting is the one related to the PAA sensorial analysis (figure 12). Both bitterness and sweetness can be detected with a good predictability and the model shows a good fitting with the proposed data. Q^2 values is good for bitterness and acceptable for the sweet taste, only the case of astringency detection, the model shows a low level of predictability.

In conclusion, the measures with the higher explicative and predictive capacity are the ones related to xanthines (both LC-MS and FT-NIR), to sugar (FT-NIR), the sensorial data of sweet and bitter taste (PAA) and the colorimetric value CIELab a*. The remaining two measures, related to the detection of Maillard compounds, are less explicative. In particular the fluorescence measure shows a value of model validity negative, too low to take into account this measure in the general model.

5.3.3 Correlation between variables

In this paragraph the important variables are summarized. Measures and factors were analyzed in pairs in order to see which measures are more correlated to each other. A positive value that tend to 1 means a direct correlation between variables, instead a negative value means an inverse correlation between variables.

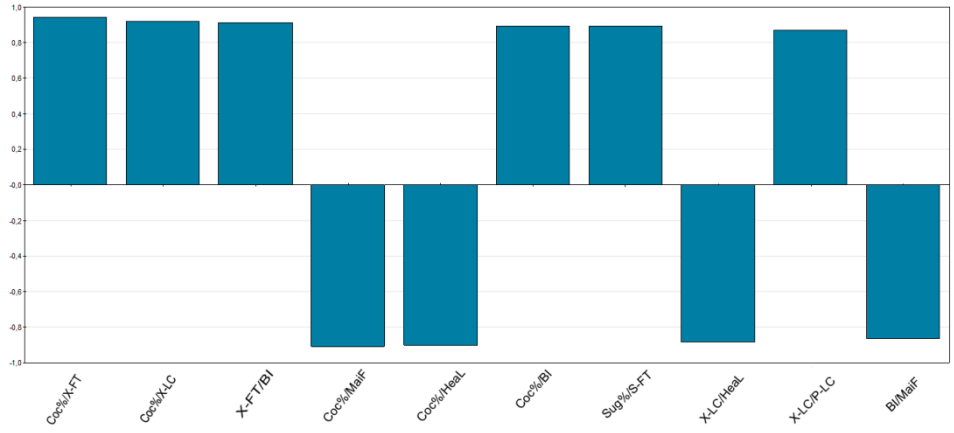

Figure 13 – Correlation between the main variables of DoE.

The chart in figure 13 summarizes the 10 most important correlation in the proposed model. Xanthine detection shows a good direct correlation with the cocoa added and the bitter taste verifying our starting hypothesis of a direct correlation between this class of bitter taste markers and the taste itself. There is also a reverse correlation between the cocoa percentage in the receipt and the Maillard detection measures

(CIELab L* and fluorescence). The cocoa is able to make the sample darker at the increasing of its concentration lowering the measured luminance (CIELab L*).

It is important to note that the bitter taste sensed with PAA and the Maillard fluorescence measure has a inverse proportionality probably due to the formation of high molecular weight compound that cannot be sensed by the tongue receptor as bitter due to their low solubility. There is obviously a direct correlation between the amount of cocoa added and the bitterness sensed by the panel group. Also the sugar shows to be detected with a very high accuracy because the proportionality between the sucrose added and the detected one posses a fitting coefficient close to 1.

In figure 14 all the correlation evidenced by the model are summarized: the most interesting are about the direct correlation between polyphenols and astringency (A). Also the choice of cranberries juice to modulate the concentration of polyphenols is correct and verified by the DoE. Another important confirmation that rise from this type of analysis is the masking effect of sugar toward bitter taste compounds (B), verified both with PAA and FT-NIR. The last effect taken into account is the one related to the Maillard compounds (C). Our starting hypothesis, based on literature, was that Maillard compound enhance the bitter taste in food products. This is generally accepted for beverages like beer [11] or solid food like cheeses [12]. In our case the DoE shows that there is a reverse correlation between the bitter taste noticed with PAA and the Maillard compounds detected with the colorimetric and fluorimetric measures. This can be attributed mainly to the polymeric nature of the compounds formed during the baking process. In order to be sensed by the tongue receptor a tastant need first to be water soluble (see chapter 1). Polymers, like the melanoidins formed during Maillard reaction, modify the taste of the final product subtracting low molecular weight Maillard compounds during the baking process. The measures used for DoE are probably able to detect only this type of compounds resulting in an inverse proportionality between the sensed bitter taste and the Maillard compounds concentration.

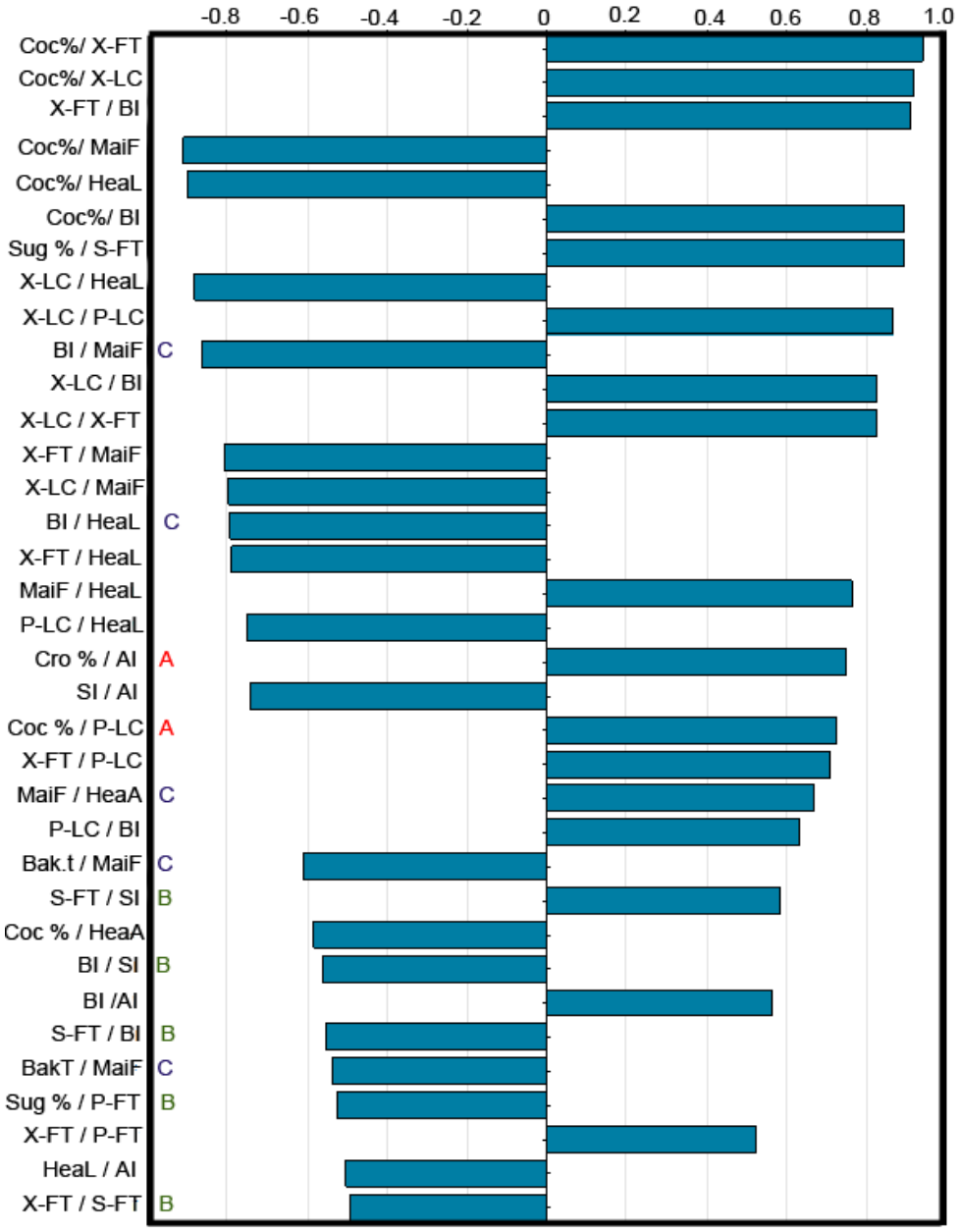

Figure 14 – All correlation between all the variables of DoE (for the etiquette meaning refer to table 1).

5.3.4 Residuals

Figure 15 show the standardized residuals for each measure taken into account.

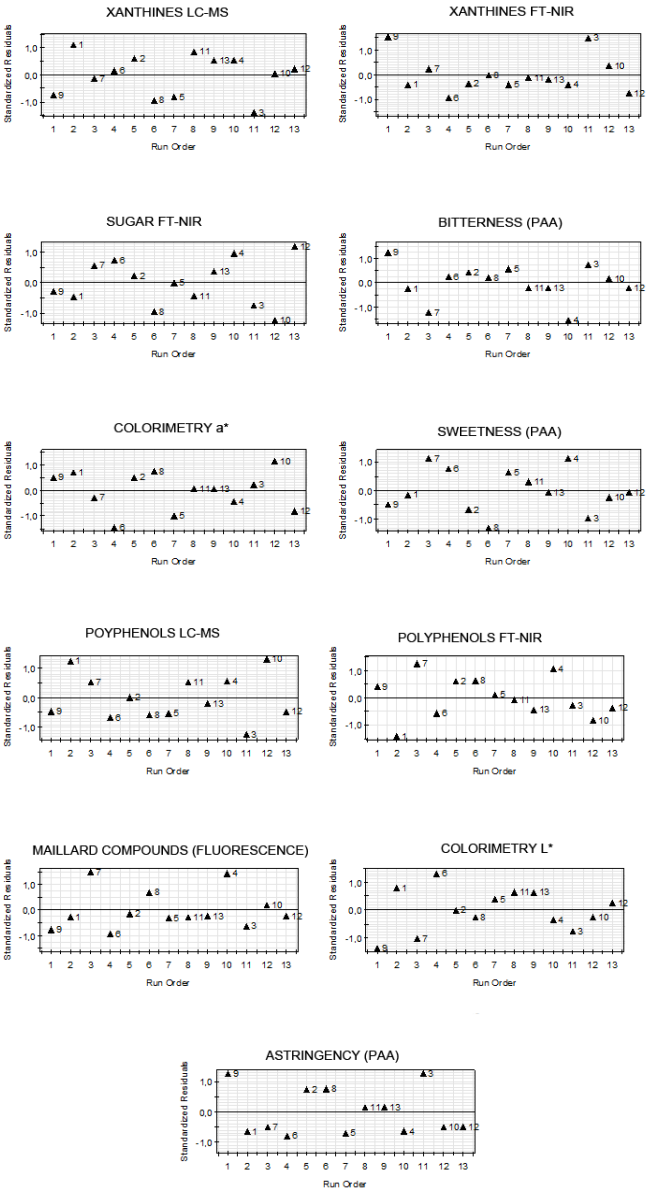

Figure 15 – Standard residual for all the variables of DoE.

In each graph the residuals for all the 13 samples realized are reported. All the tests exhibit a random distribution with respect to the order of execution of the analysis demonstrating the absence of a trend in all the observed variables, that means no presence of any significant systematic error.

5.3.5 ANOVA

The graphs presented in this paragraph are relative to the Analysis Of Variance (ANOVA) of the presented model. Three different types of values are shown:

- **SD-regression**, indicate the standard deviation of the proposed regression. This value represents the variability of the model.
- **RSD**, indicate the variance of the responses unexplained by the model. A low value means that the measure describe almost all the searched
- **F**, shows RSD (second bar) multiplied by a square root of the critical F value. This is the value of a F-distribution over which the SD regression is statistically at the 95% confidence level.

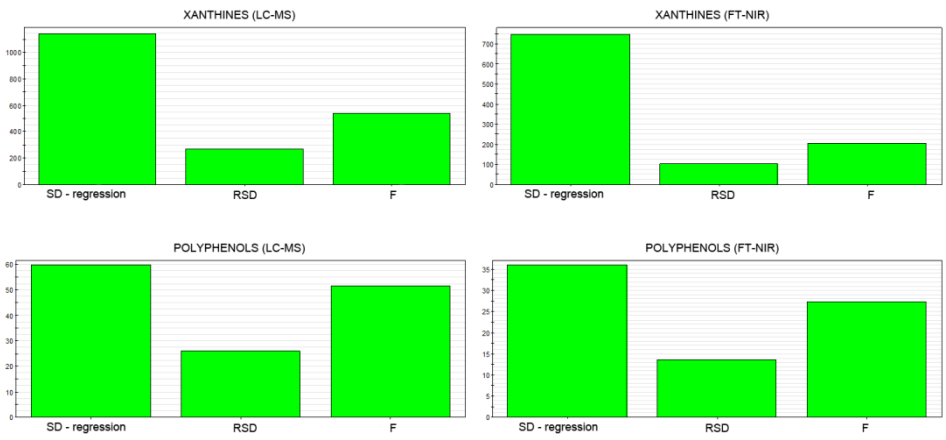

Figure 16 – ANOVA for xanthines and polyphenols measurements.

Figure 16 shows the LC-MS and FT-NIR results for xanthine and polyphenols detection. Both of them results significant for the DoE. The F-test for polyphenols gives back a value of F high and so there is a higher possibility to commit error in polyphenols measures for the proposed samples.

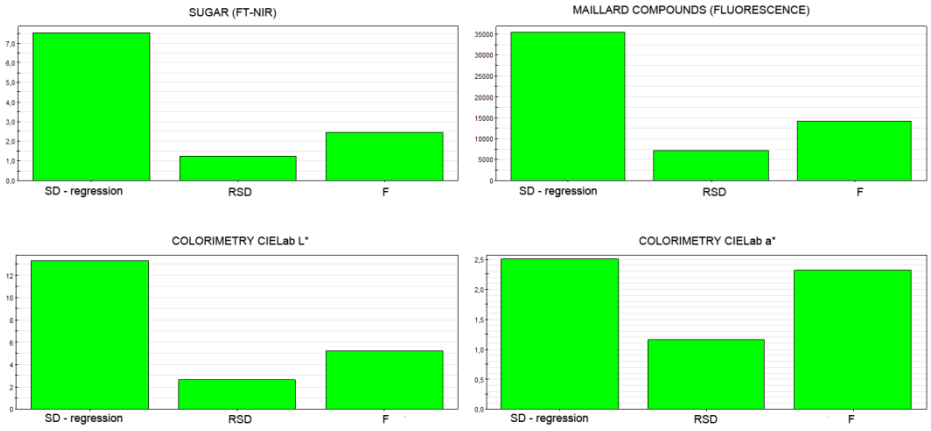

Figure 17 – ANOVA for sugar and Maillard measurements

The remaining chemical analysis related to the sugar content and to the Maillard compounds are analyzed in figure 17. FT-NIR, fluorescence and colorimetric L* measures are significant with a low F-test. The variability in CIELab a* coordinate is higher and this lower the reliability of this measure.

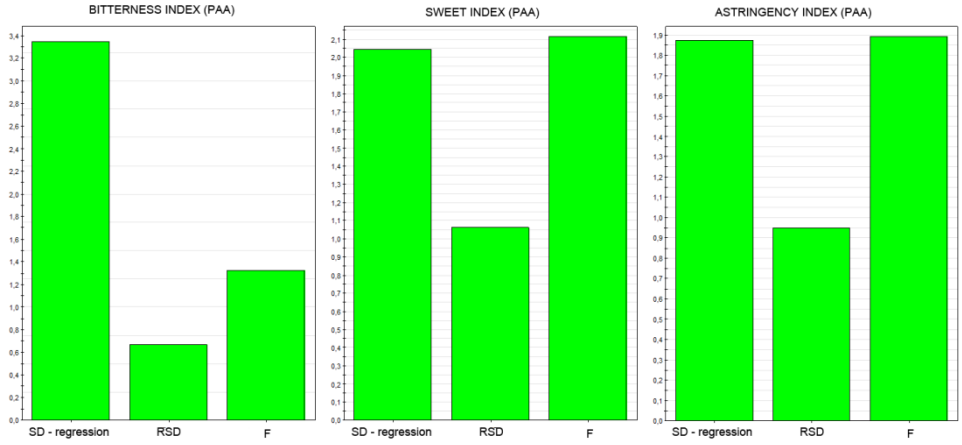

Figure 18 – ANOVA for PAA sensorial analysis.

All the PAA values are analyzed for last. Bitterness can be measured with great accuracy but the same cannot be said for sweet and astringent tastes were the F value is almost equal to the standard deviation exhibited by the 13 samples.

5.3.6 Variable importance plot

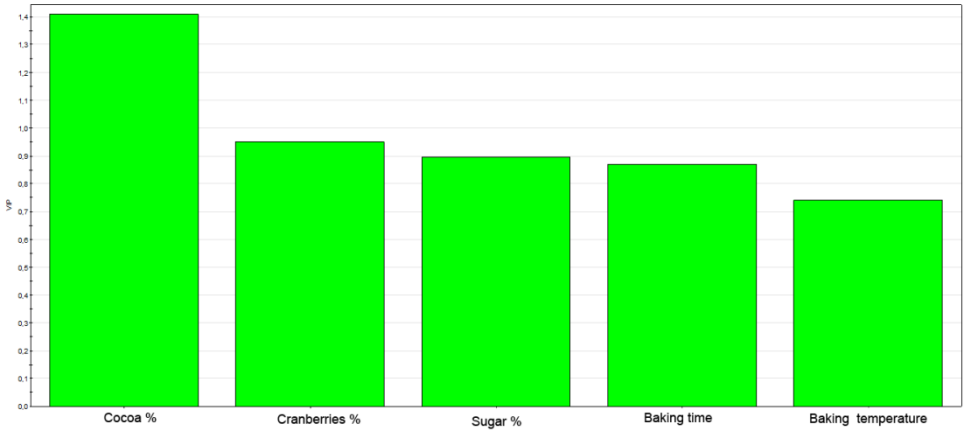

Figure 19 – Variable importance plot for the DoE.

Partial least-squares (PLS) based on two components was chosen as the statistical regression treatment. The Variable Importance Plot (VIP) illustrates the importance of a variable to the measurements of a process/phenomenon. It can also generates information regarding the most important interactions and represents the most condensed way of expressing the PLS model's output as a weighted summary of all loadings across all responses.

All the factors selected for biscuit production were classified on the basis of their importance in the final taste (figure 19). Cocoa and cranberries have the more deep impact in modifying the taste in the biscuit. Then sucrose and baking time has almost the same effect. Sucrose is able to mask the bitter taste but its fluctuation in concentration in the selected range for DoE doesn't change dramatically the overall bitter taste. Baking time has an impact on the final product by influencing the Maillard reaction. Longer times favor the formation of Melanoidins and lower the concentration of bitter Maillard compounds. The less influent variable is temperature because all the selected ones for the DoE were chosen in order to obtain always a eatable biscuit, not too far from the commercial ones.

5.3.7 Scaled and centered coefficients

The scaled and centered coefficients were used to investigate the influences of each factor in a specific measure. In figure 20 the measures for xanthines and polyphenols are shown. The LC measure depends from the cocoa added and in a minor part from

the cranberries that modify the pH of the extracting solution. Baking time and temperature are irrelevant because xanthines are thermally stable during the baking. Also the presence of sugar doesn't affect the measure. FT-NIR has a different behavior, the xanthines are influenced only by the cocoa. In this case also sugar play a minor role as interferent because some sucrose absorption bands fall near the one used for xanthines detection.

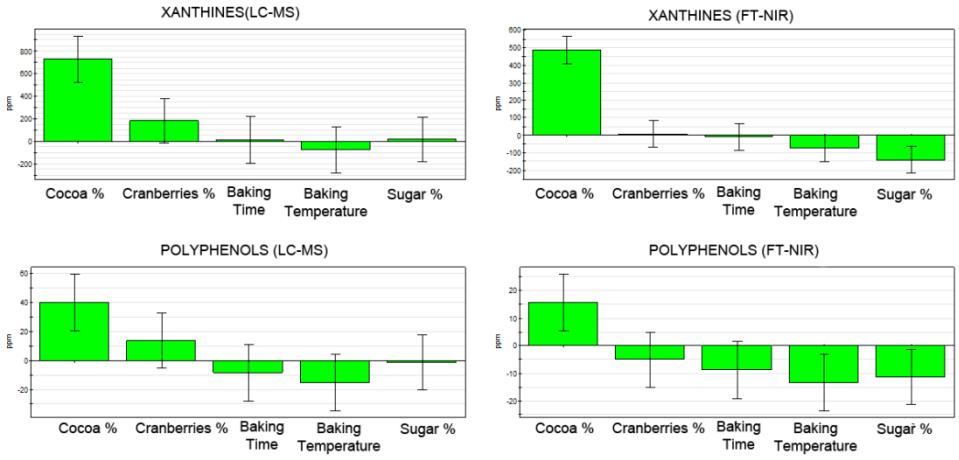

Figure 20 – Scaled coefficients for xanthines and polyphenols measures (LC-MS and FT-NIR).

The polyphenols are influenced mainly by the cocoa percentage and in fact by the cranberries presence. Baking parameters have the capability of lowering the concentration of catechins due to their thermal instability (this behavior affect mainly FT-NIR measures). Sugar is irrelevant for the LC measure but play the role of the interferent in the case of the FT-NIR measure because share most of its absorption bands with the polyphenols.

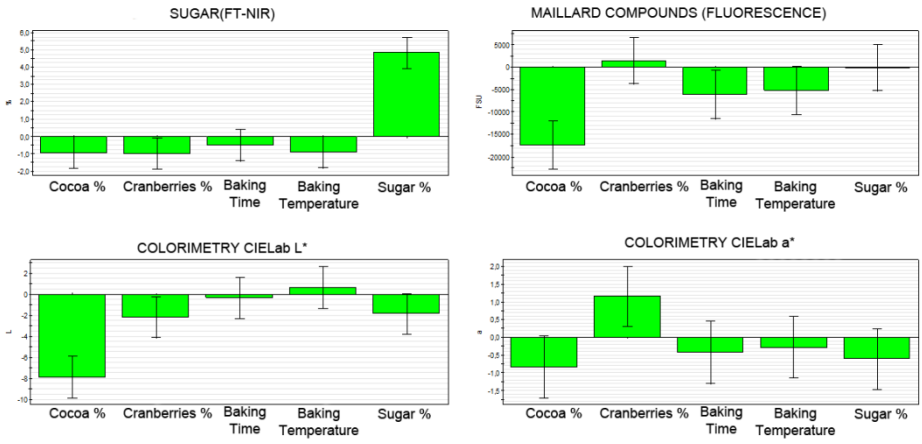

Figure 21 – Scaled coefficients for sugar and Maillard compounds measured.

In figure 21 the scaled coefficients for sugar detection show that this measure is obviously influenced obviously by the sucrose added in the recipe; baking parameters lower the sugar concentration but not in a significant way. Fluorescence of Maillard compound is lowered by the presence of cocoa that colour with an intense brown the extract making difficult the analysis. The L* coordinate is lowered by the presence of cocoa due again to its brownish colour and a similar effect is present for the a* coordinate.

The PAA scaled coefficient is proposed in figure 22. Bitterness index is influenced positively by the cocoa and in minor part by the cranberries. Also the masking effect of sugar is evident instead the baking parameters influence it is irrelevant (for the chosen time/temperature combinations). Sweetness depends mainly by the sucrose added to the receipt and in part it is lowered by the baking process (due to Maillard reaction and caramelisation). Cranberries juice lower the sweetness of the final biscuit probably because there is a negative interaction between sucrose and sour tastants present in the juice. Astringency is influenced mainly by the cranberries. A negative interaction can be noticed with the sugar, probably because polyphenols are able to interact with the sucrose, as they do in the saliva with the glycoproteins.

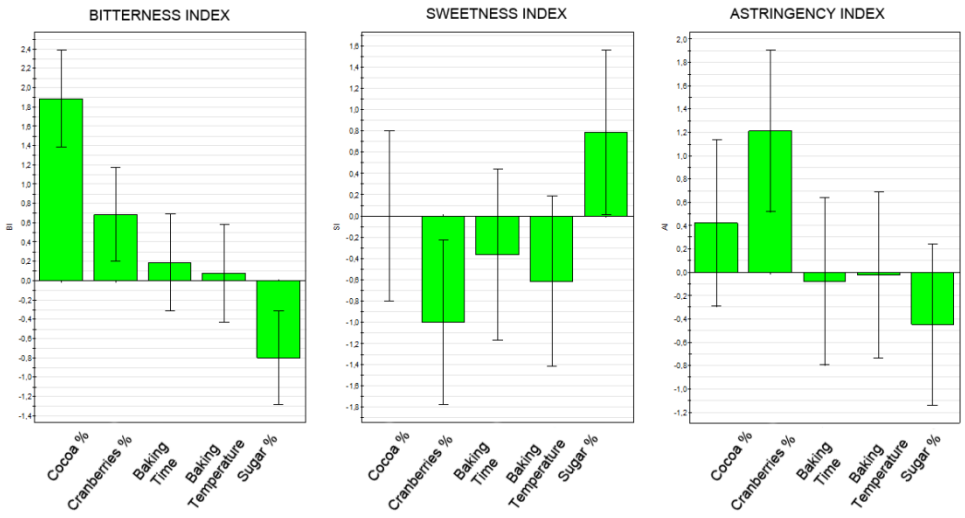

Figure 22 – Scaled coefficients for PAA sensorial analysis.

5.3.8 Contour plot

The contours plot shows the variation of a variable in function of two chosen factor. On each line of the contour plot there is a value of a specific measured variable and on the x and y axis there are the two factors of interest. A line parallel to one ax means that the factor on this ax does not influence the measure along the all explored range. This type of graphical representation is helpful in the understanding of the origin of the interactions between factors and measures in the DoE. The following contour plot are subdivided in two groups:

- **Recipe**, where variables are plotted against the cocoa and the cranberries juice concentration ;
- **Baking condition**, where variables are plotted against the baking conditions.

Recipe contour plot

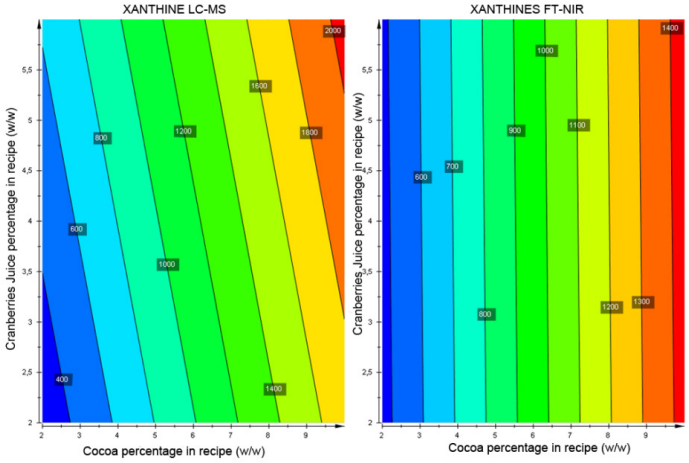

Figure 23 – Contour plot of Xanthine measures (LC-MS and FT-NIR) against cranberries juice and cocoa added to receipt.

Figure 23 shows the dependence of xanthine concentration from the cocoa and the crowberries juice added to the receipt. As was to be expected in both the cases there is a strong dependency from the cocoa and a lower dependency from the cranberries juice that disappear completely in the case of the FT-NIR measure.

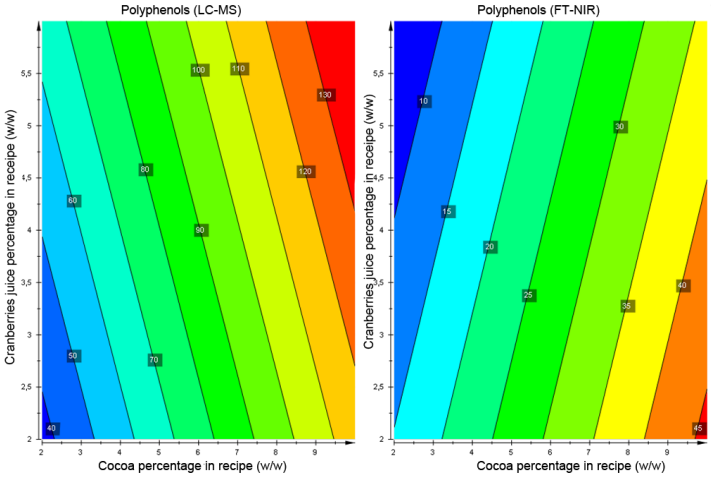

Figure 24 – Contour plot of Polyphenols measures (LC-MS and FT-NIR) against cranberries juice and cocoa added to receipt.

Figure 24 shows the same contour plot in the case of polyphenols. Also in this case the predominant factor is cocoa percentage for both the analysis with a stronger dependency from the cranberries juice concentration again in the case of the FT-NIR analysis. The trends in the two plots are opposite; this can be explained with the composition of the cranberries juice. In the LC-MS case the selectivity of the system is very high and the non-phenolic molecules added to the receipt do not influence significantly the final measure. On the opposite this cannot happen for FT-NIR that is able to detect also the interferent molecules reading a lower (in this case) total concentration of polyphenols inside the sample.

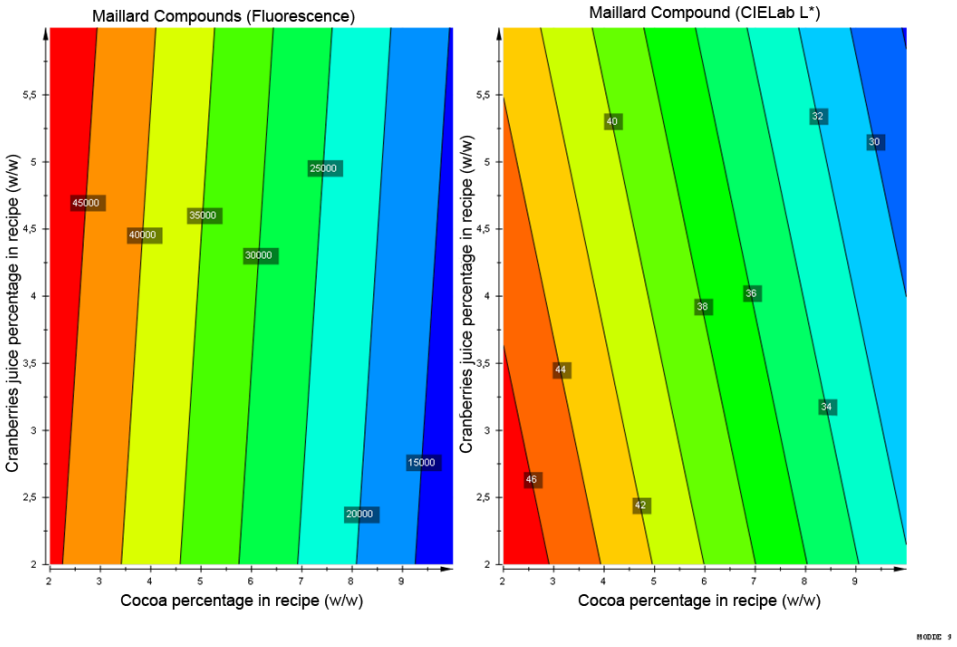

Figure 25 – Contour plot of Maillard compounds measures (fluorescence and CIELab L*) against cranberries juice and cocoa added to receipt.

In figure 25 it is investigated the trend analysis for Maillard compounds formation (with fluorescence and colorimetry) against the cocoa and cranberries juice added to the recipe. On the left it is shown that fluorescence decrease dramatically adding cocoa: opposite correlation between these two parameters. On the other hand L* coordinate has a dependency from both the ingredients but also in this case it decreases mainly at the rising of the cocoa concentration because it influences the overall colour of the sample. Also the cranberries juice is able to bring a change in the final colour of the sample and this fact explain the partial dependency of the L* coordinate.

Figure 26 shows the dependency of the PAA responses toward the ingredients added to recipe. As expected, bitterness increase with both cocoa and cranberries juice but it is more influenced by the first, sign of the strongest bitterness due to the presence of large quantities of xanthines. Sweetness is independent from cocoa concentration but has a strong dependency from the cranberries juice. It can be hypothesized that the polyphenols presents in the juice are able to interact with the sucrose lowering the overall sweet sensation, as previously indicated.

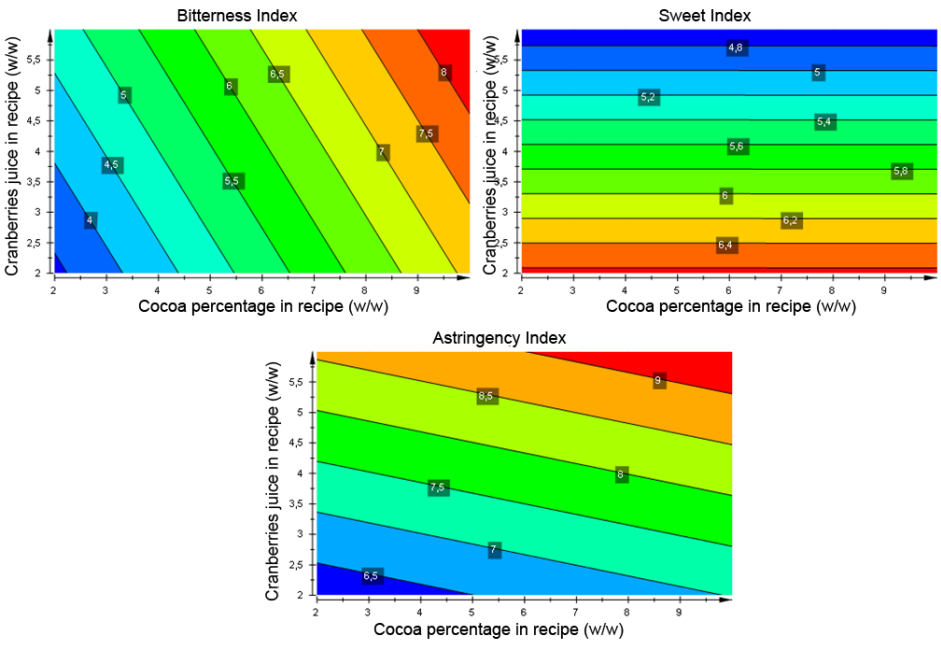

Figure 26 – Contour plot of PAA measures (Bitterness, Sweetness and Astringency Index) against cranberries juice and cocoa added to receipt.

The astringency index shows clearly a strong dependence from the cranberries juice, where the polyphenols are more concentrated.

Baking condition contour plot

In the following contour plots the variables were correlated to the baking time and temperature. The xanthines concentration is less sensible to temperature because this class of molecules are thermally stable in the range used for baking the samples. Instead, polyphenols concentration is strongly influenced by both the baking conditions that favor oxidation and decomposition of these molecules (figure 27).

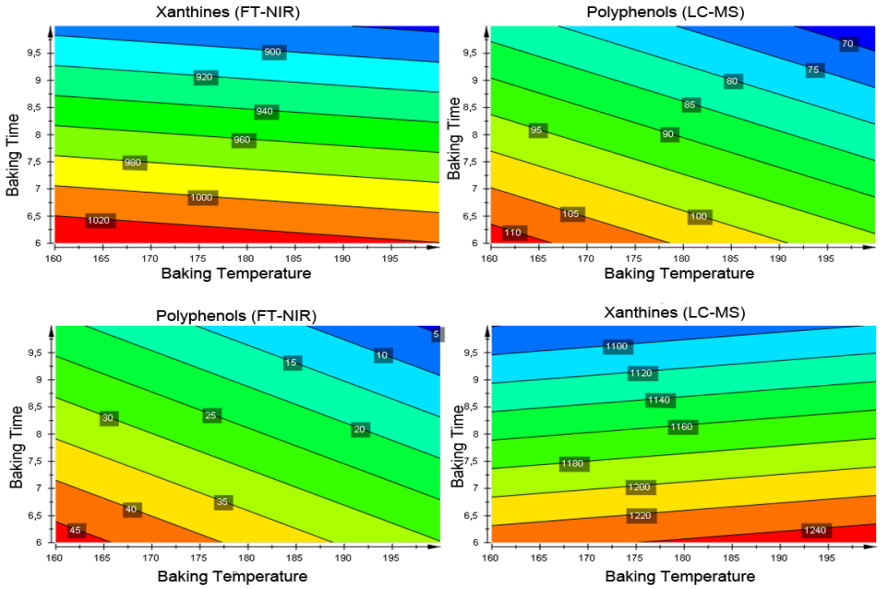

Figure 27 – Contour plot of Xanthines and polyphenols measures against baking conditions.

The bitterness index is influenced by both the factor in the same way and this is probably due to the Maillard compounds formation (figure 28).

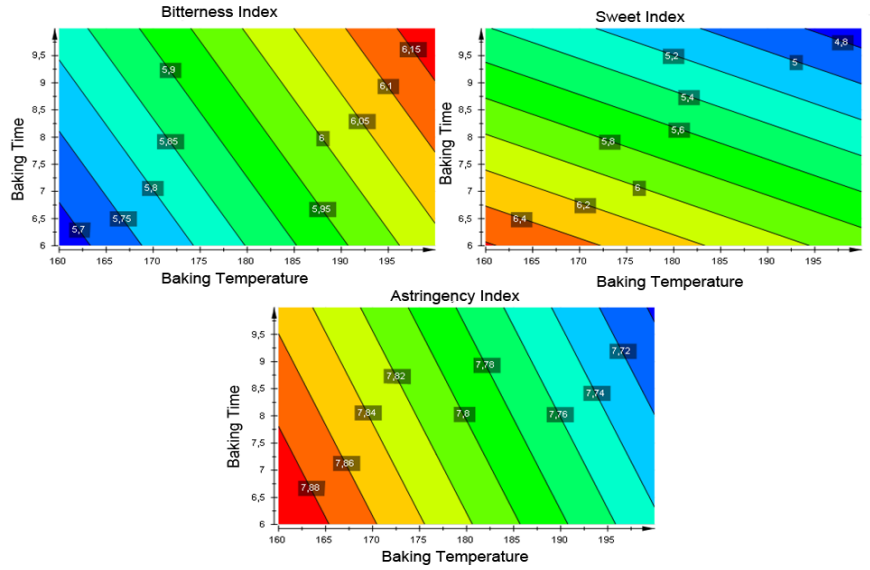

Figure 28 – Contour plot PAA measures against baking conditions.

The sweet index, instead, is influenced dramatically by the baking time due to the caramelisation that occurs partially also at the lowest temperature. Instead, astringency index is influenced by the temperature because it is related mainly to the polyphenols (not necessary only catechins and epicatechins).

5.4 Conclusions

This Design of Experiment evaluated the interactions between biscuits manufacturing parameters and taste molecular markers. All the previously developed protocols were used in order to clarify the role of each class and verify the different hypothesis on the bitter taste molecular origin discussed in chapters 1-4. LC-MS and FT-NIR techniques also proved their potential in the analysis of biscuits together with the PAA to investigate new recipes or to evaluate concurrency products.

Apart the role of Maillard compounds which is still partially unclear due to the lack of a reliable technique able to detect their concentration in solid phase, the DoE proved :

- The direct correlation between polyphenols and xanthines and the overall sensed bitterness.
- The influence of baking condition in the polyphenols thermal degradation and corresponding low astringent taste sensation.
- The congruence between LC-MS data, FT-NIR data and PAA measures.

References

[1] "*Design of Experiment*"; Eriksson L., Johansson E., Kettaneh-Wold N., Wikström C., Wold S.; Umetrics Academy, ISBN 91-973730-0-1.

[2] "*A Brief Introduction to Design of Experiments*"; Telford, J.K.; Johns Hopkins APL Technical Digest; Vol.27, Nr.3, Pg. 224-232 (2007).

[3] "*Chemistry of Browning Reactions in Model Systems*"; Hodge J.E.; Journal of Agricultural and Food Chemistry, Vol. 1, Pg. 928–943 (1953).

[4] "*Action Des Acides Amine´s Sur Les Sucres. Formation Des Melanoidins Par Voie Methodique*"; Maillard L. C.; Compt. Rend. ,Vol.154, Pg. 66–68 (1912).

[5] "*Molecular Structure of Humin and Melanoidin via Solid State NMR*"; Herzfeld J., Rand D., Matsuki Y., Daviso E., Mak-Jurkauskas M., Mamajanov I.; Journal of Physical Chemistry B, Vol. 115, Pg. 5741–5745 (2011).

[6] "*A review of Maillard reaction in food and implications to kinetic modelling*"; Martins S.I.F.S., Jongen W. M.F., van Boekel M.A.J.S.; Trends in Food Science and Technology, Vol. 11, Pg. 364–373 (2001).

[7] "*Fluorescence from the Maillard Reaction and its Potential Applications in Food Science*"; Matiacevich S. B., Santagapita P. R., Buera M. P.; Critical Reviews in Food Science and Nutrition, Vol. 45, Pg. 483–495 (2005).

[8] "*Fluorescence and color as markers for the Maillard reaction in milk–cereal based infant foods during storage*"; Bosch L., Alegrìa A., Farré R., Clemente G.; Food Chemistry, Vol. 105, Pg. 1135–1143 (2007).

[9] "*Instrumental Methods (Spectroscopy, Electronic Nose, and Tongue) As Tools To Predict Taste and Aroma in Beverages: Advantages and Limitations*"; Smyth H., Cozzolino D.; Chemical Review; dx.doi.org/10.1021/cr300076c (2012).

[10] "*Astringency: Mechanisms and Perception*"; Bajec M. R., Pickering G. J.; Critical Reviews in Food Science and Nutrition, Vol. 48, Pg. 858–875 (2008).

[11] "*The chemistry of beer aging – a critical review*"; Vanderhaegen B., H. Neven B., H. Verachtert B., G. Derdelinckx B.; Food Chemistry, Vol. 95, Pg. 357–381 (2006).

[12] "*The Maillard reaction during the ripening of Manchego cheese*"; Corzo N., Villamiel M., Arias M., Jimenez-Perez S., Morales F. J.; Food Chemistry, Vol.71 Pg. 255-258 (2000).

Bitter taste molecular markers detection in Smoothies : FT-NIR vs RAMAN spectroscopy

6

6.1 Introduction

In the previous chapters different techniques are described for the detection of bitter taste molecular markers in bakery products. Similar approaches could be applied toward liquid matrices like milk [1-3], beverages [4-6] or fruit juices [7-10]. An emerging beverage that is progressively more common in the food industry is represented by the smoothies. In recent years the number of products of this type raised, asking for rapid techniques for the quantification of quality control parameters.

6.2 FT-NIR measures on Smoothies

The same method developed for solid sample has been tested on smoothies in order to develop a protocol able to quantify bitter taste molecular markers. First of all we needed to know: (i) the bitter taste index of the samples; (ii) which markers were present; (iii) their concentrations. Five different samples of smoothies, made with different types of fruit (both in the puree and juice form), were chosen for this experiment. A PAA analysis was done in order to score their bitter taste: results summarized in table 1. In this case the absolute score obtained are far lower than the ones obtained for biscuits.

Sample	Bitter taste Index
Sample 1	2
Sample 2	2.5
Sample 3	3.5
Sample 4	2.5
Sample 5	3

Table 1 – PAA analysis on smoothies commercial samples.

In practice, the results show that the average sensation about bitter taste is generally low with little variation between the samples. In this case the molecular markers seem to be less present than in the biscuits case: this hypothesis was checked using the RP-HPLC-MS method developed for biscuit matrices (described in chapter 2). It has been verified that no xanthines are presents inside each smoothie and this is plausible because only particular species of plant, like cocoa and tea, are known to produce this class of molecules in appreciable concentrations [11]. Fruit generally implied in the smoothies production do not contain any xanthine at relevant concentration. In table

2 all the HPLC-MS results are summarized[1]: the analysis reveals the presence of catechin and epicatechin at concentrations of tenths of mg kg^{-1}.

Samples	CATECHIN (mg kg^{-1})	EPICATECHIN (mg kg^{-1})	Total polyphenols (mg kg^{-1})
Sample 1	2.1	5.2	7.3
Sample 2	1.1	11.1	12.2
Sample 3	3.4	14.5	17.9
Sample 4	1.7	13.4	15.1
Sample 5	7.4	8.5	15.9

Table 2 – RP-HPLC-MS analysis of bitter taste molecular markers on smoothies commercial samples.

These concentrations are still in the range on which the calibration curve for polyphenols were built for the biscuit case but here the main problem of measuring water based samples is the impossibility to work in transmittance mode, due to the large absorption of NIR light by the water itself. In addition, in this case there is the problem of the very low concentration of the polyphenols in the samples. In figure 1 an example of a typical spectrum recorded with a Buchi Nirflex-N500 with a 10 mm cuvette holder is reported.

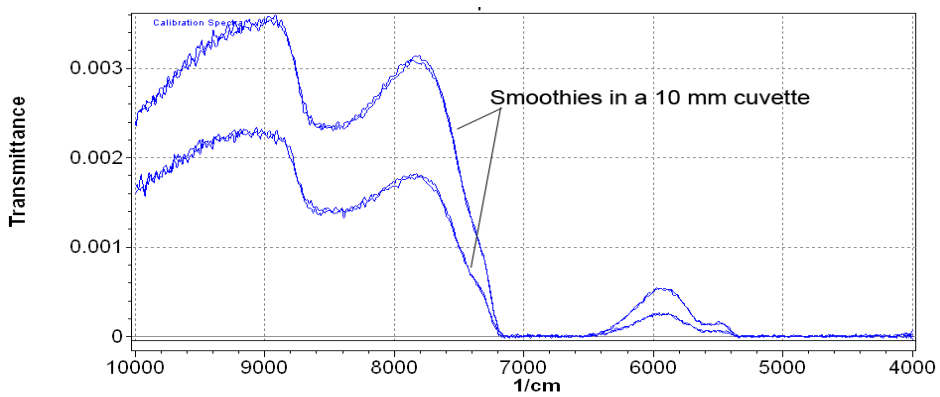

Figure 1 – FT-NIR spectra of smoothie in a 10 mm cuvette.

[1] Similarly to what previously described in chapter 2, sample extractions were performed diluting 2 mL of smoothie in 18 mL of MeOH/H_2O 7/3 at 80°C for 30 minutes in a Teflon sealed tube. The solution was filtered and injected without any further dilution. For chromatographic and mass spectrometry parameters refer again to chapter 2.

The two spectra are related to the same sample and it is possible to see that the transmittance does not exceed the 0.004 value. This phenomenon is due to the large portion of the radiation that is absorbed by water. In fact in the two main regions where water absorptions are localized (4000-5500 cm^{-1} and 6500-7500 cm^{-1}) the transmittance falls to zero. Furthermore the samples result too dense and turbid for a transmittance analysis. Two techniques were therefore tested to remove water :

- Lyophilization.
- Stripping with nitrogen.

In both cases the samples were treated without raising the temperature to overcome the degradation of polyphenols because their thermal instability and susceptibility to oxidation [12]. Water removal was performed placing the sample in a Petri dish. In the case 1 a non homogeneous film was obtained because removal was only partially executed and lyophilization removed water too vigorously. The Petri obtained[2] with this technique was not used for the FT-NIR calibration curve. In the case 2 the Petri dish was put under a constant nitrogen flux for 6 hours at room temperature. This allows to obtain a more homogeneous and reproducible film, removing up to the 85 % of the initial water and concentrating the polyphenols by one order of magnitude (Figure 2).

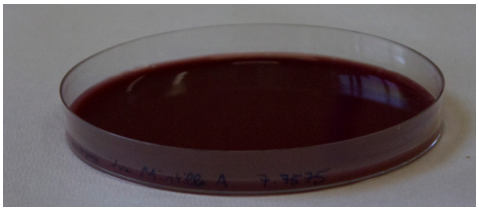

Petri dish filled with 12 g of sample

Petri dish with 3 g of concentrated sample (~ 80 %of water removal)

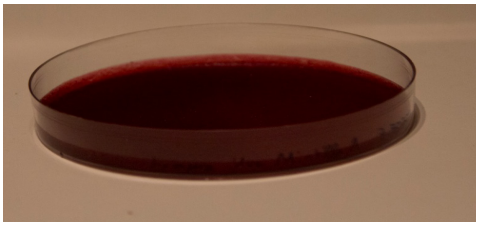

Figure 2 – Sample of smoothie before and after 6 hours of solvent stripping with nitrogen.

[2] The Petri were realized weighting 12 g of smoothie and posing it under a constant nitrogen flux for 12 hours obtaining an overall water loss of at least 10 g.

Table 3 summarizes the relative value of water averagely removed from the different samples subjected to the treatment. The water loss is not the same for all the smoothies and this is due to their starting composition. Repeated water stripping showed that the mean water loss is reproducible for each sample.

Figure 3 shows a gain in the signal intensity of two order of magnitude due to water removal: transmittance pass from an average value of 0.003 to 0.4.

Sample	Water loss (% w/w)
Sample 1	78.93
Sample 2	85.00
Sample 3	85.20
Sample 4	84.30
Sample 5	82.56

Table 3 – Average water loss of the samples dehydrated under nitrogen flux.

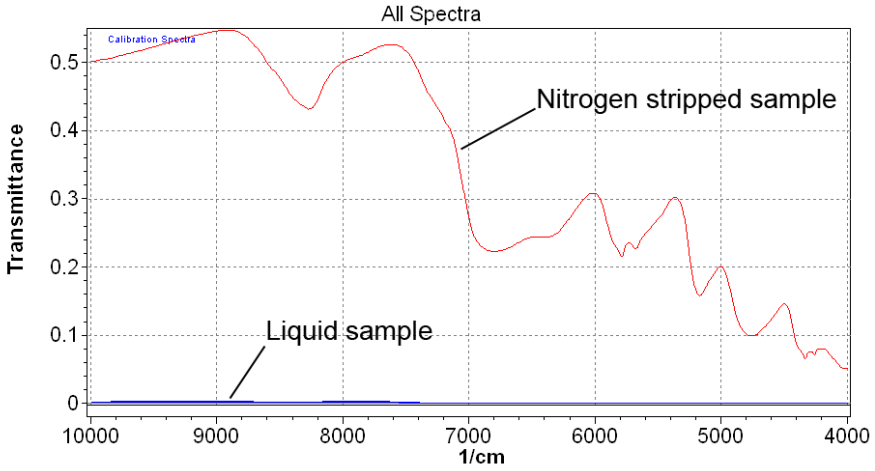

Figure 3 – FT-NIR spectra of smoothie before and after 6 hours of water stripping with nitrogen.

On all the five samples subjected to nitrogen water stripping an HPLC-MS analysis was performed in order to verify if the polyphenols are still present and in which concentration they remain inside the matrix. All the extractions were performed removing the dehydrated film from the Petri dish and extracting it with 10 mL of

MeOH/H_2O (7/3) at 80°C for 30 minutes. Table 4 summarizes all the data for the five categories of smoothies.

Samples	CATECHIN (mg kg^{-1})	EPICATECHIN (mg kg^{-1})	Total polyphenols (mg kg^{-1})	PAA (Bitter Index 0-12)
Sample 1	8	20	27	2
Sample 2	4	47	51	2.5
Sample 3	16	71	87	3.5
Sample 4	7	69	76	2.5
Sample 5	28	32	60	3

Table 4 – LC-MS Polyphenols compositions on the dried smoothies.

The total polyphenols content measured by LC-MS correlates nicely with the PAA bitter taste index. All the results are similar each one with the other in absolute terms, and the differences are lower than the ones encountered in the biscuits case.

6.2.1 FT-NIR calibration curve

All the Petri were used for the calibration of the FT-NIR calibration curve and the results are summarized in figure 4-5 and table 5.

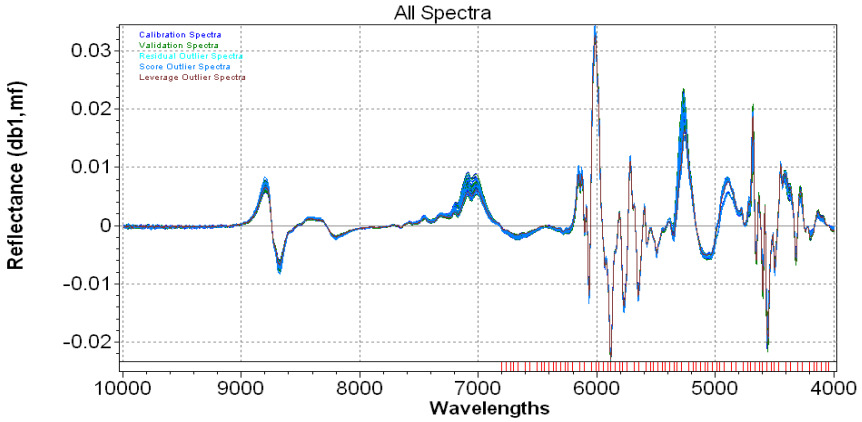

Figure 4 – Smoothies spectra after normalization e 1st derivative.

The calibration curve was built using the PLS algorithm on the spectra normalized and pretreated with the 1st derivative (figure 4). Only a limited set of wavelengths between 4000 and 7000 cm^{-1} were used for the principal component analysis . We limited the calibrations to five concentrations, without preparing any sample in order to fulfill the

concentration gaps, only because the reliability of the procedure was not sufficiently robust and predictive.

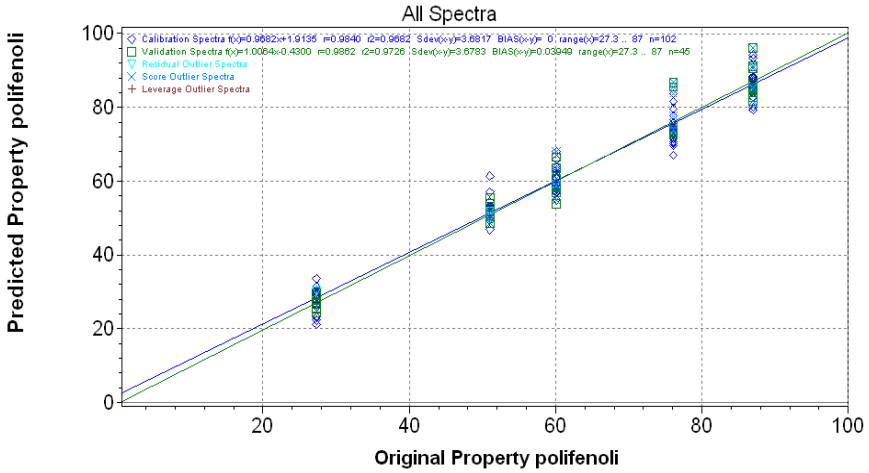

Figure 5 – Polyphenols calibration curve on nitrogen stripped smoothies.

In fact, both the calibration and the validation curve show a good linearity with a R^2 coefficient of 0.97 and 0.96 respectively. The standard errors of calibration and prediction are both equal to 3.7 mg kg^{-1}, leading to an overall consistency of the model (defined as SEC/SEP) close to 1: this means that the calibration curve owns a good robustness.

Compound	*Set*	*N° of Samples*	*Range*	*R^2*	*SEC-SEP*
Polyphenols	**C-SET**	**102**	**27-87 mg kg^{-1}**	**0.97**	**3.68 mg kg^{-1}**
[mg kg^{-1}]	**V-SET**	**45**	**27-87 mg kg^{-1}**	**0.96**	**3.67 mg kg^{-1}**

Table 5 – Polyphenols calibration curve statistical parameters.

Different samples were than dehydrated with nitrogen stripping and then analyzed with this calibration curve. Table 6 shows the results for the quantification on unknown samples, all measures are realized in duplicate.

Sample	**Theoretical polyphenols**	**Measured polyphenols**
Sample 1a	27	100.71
Sample 1b	27	110.54
Sample 2a	51	99.54
Sample 2b	51	101.34
Sample 3a	87	170.23
Sample 3b	87	132.2

Sample 4a	76	110.25
Sample 4b	76	125.38
Sample 5a	60	134.45
Sample 5b	60	154.62

Table 6 – FT-NIR polyphenols detection on smoothies samples dehydrated with nitrogen stripping

The FT-NIR is clearly not able to distinct the samples one by the other and this is probably due to the presence of an amount of water in the Petri dish that is sufficient to act as a strong interferent.

6.2.2 Conclusions

A new FT-NIR methodology for the detection of polyphenols in beverages was developed. The calibration curve shows a good linearity (R^2 = 0.97) and a relatively low SEC (3.68 mg kg^{-1}). The FT-NIR is not able to distinct one sample from the other and this is due to the quantity of residual water still present in the analyzed samples, even after an adequate water removal by nitrogen stripping treatment.

6.3 RAMAN Spectroscopy

The principle behind Raman spectroscopy is based on the light scattering phenomenon. Raman measures the vibration of molecular bonds as in the case of the two other spectroscopic vibrational techniques FT-IR and FT-NIR (described in chapter 4). Raman effect rise from the inelastic scattering of an incident electromagnetic radiation [13].

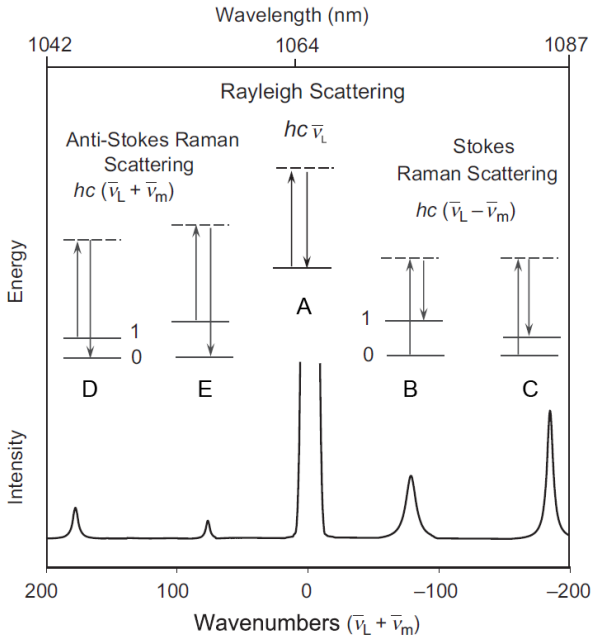

Figure 6 – Different scattering phenomena .

The scattered photons are constituted by two different types of components :

- Rayleigh scattered photons
- Raman scattered photons

During Rayleigh scattering (figure 6 peak a) no energy is lost, the incident radiation and the scattered radiation has the same wavelength; this means that the photons are elastically scattered by the sample and no information about its chemical nature can be recovered. On the other hand there are Raman photons characterized by the different energy of the emitted photons. When the material absorbs energy and the emitted photon has a lower energy than the absorbed photon we have the Stokes

Raman Scattering (figure 6 peaks b and c). Instead when the material absorbs energy and the emitted photon has a higher energy than the absorbed photon we have the Anti-Stokes Raman Scattering (figure 6 peaks d and e). Stokes peaks are more common that Anti-stokes peaks and this is due to the state in which the bond is when the excitation occurs. Stokes peaks are originated from a ground state, more populated level, instead Anti-Stokes peaks are originated from a less populated vibrational level. This difference is the main responsible of the intensities of the two peaks type (figure 8).

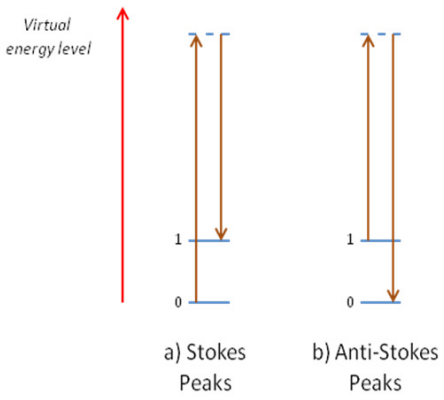

Figure 7 – Stokes and Anti-Stokes peaks.

During a Raman experiment the sample is irradiated with a laser source. The wavelength of the laser can fall both in UV and in the visible region. The choice of the laser is mainly due to the fluorescence phenomena that it is able to generate. Fluorescence is the main interferent in Raman experiments and, for this reason, it is preferred to avoid intense fluorescence in order to obtain sharper Raman peaks. Raman scattering and fluorescence are two competing phenomena with a very similar molecular origin. In Raman the laser photon excite the electrons to a virtual state losing a certain amount of energy necessary to induce vibration of the molecule with a subsequent emission of a new photon at a different wavelength. The overall phenomenon is possible independently by the laser source used to induce the scattering and it happens in the time scale of picoseconds (10^{-12} s). Figure 7 is a graphical illustration of the virtual states that are needed to explain Raman scattering from a quantomechanical point of view. Sometimes it occurs that the laser wavelength or the scattered photons posses the necessary energy to excite an electron between two electronic state originating the fluorescence phenomenon during a Raman

experiment. In this case the relaxation happens in the scale of nanoseconds (10^{-9} s). The fluorescence can be minimized exposing the sample to long exposure to the laser source (for seconds or minutes). This lead to the photobleaching of the analyzed sample with subsequent reduction of the overall fluorescence.

The selection rules for the Raman scattering are different from the ones described in chapter 3 for FT-IR and FT-NIR . Furthermore, selection rules for Raman spectroscopy results complementary to the IR selection rules; this is an important phenomenon because allow us to work in presence of water in large quantities without any direct interference of this molecule itself.
In order to be Raman active a molecule need :

- $\Delta v = \pm 1$, a unit jump in the vibrational quantum number is needed;
- $\left(\frac{d\alpha}{dQ}\right) \neq 0$, a variation of the polarizability of the molecule during the vibration;

The first selection rule is similar to the one encountered for the harmonic oscillator model, instead the second one is obeyed also in the case when the dipole moment doesn't change. This second rules make complementary Raman and IR observed vibrations.

6.4 Raman Spectroscopy for the detection of polyphenols

Raman spectroscopy was widely used in the past for characterization of composites materials or for identification procedures. In recent years the large diffusion of simple statistical software packages made possible to use this technique for quantification of analytes in both inorganic [14-15] and organic [16-17] matrices. Several methods were developed for the food industry, but for the moment Raman diffusion in this sector remains limited. The determination of gustative markers inside liquid products like the smoothies can be achieved using Raman spectroscopy because, as previously mentioned, this technique is water insensitive. This allow us to check the total phenolic content of a beverage with a low consumption of time because no extraction is needed and analysis can be performed in a non-destructive way directly on the sample. In this case different problem arises anyway :

- The low concentration of the total polyphenols in the sample matrix.

- The fluorescence of the background, not avoidable for quantification experiments.

While the first issue cannot be tackled, the second one can be limited searching for the optimal condition that minimize the fluorescence. The spectra were recorded using a DXR Raman Microscope[3] (Thermo Fischer Scientific) and no mathematical pretreatment of the spectra were performed in order to use them for building up a calibration curve. The previous five smoothies were used for the experiment and therefore the total phenolic content remains the one summarized in table 2. Different spectra were recorded in different conditions in order to find the right protocol to minimize the fluorescence. The operative parameters used for quantification are illustrated in table 7.

Laser Wavelenght	780 nm
Power	10 mW
Aperture	0.25 mm pinhole
Filter	Full range
Time of Acquisition	60 s
Number of scans	4
Fluorescence correction	No
Lens	20X LF

Table 7 – Operative parameters for RAMAN analysis.

A red laser with a low power minimizes the fluorescence background. Also the choice of the acquisition time is related to this effect, because it is known that long acquisition times reduced the fluorescence via photobleaching. The instrument available was a microscope and not a bench instrument able to see only the overall sample. This leads to the problem of the homogeneity of the measures performed. Smoothies samples are not a continuous solution but they seems like a slurry suspension.

[3] All the spectra were treated with Omnic TQ Analyst 8.0 software package with no correction of the fluorescence

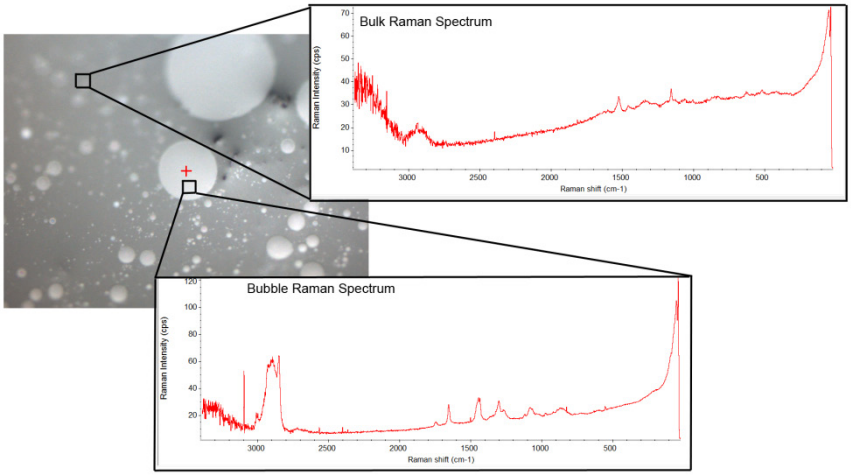

Figure 8 – Raman spectra of bubble and bulk of the same sample.

This make difficult a microscope analysis because only small portion of the sample can be analyzed in each session so a large number of areas must be covered in order to obtain a representative spectra. In figure 8 there is a typical image recorded with the Raman microscope where the red cross represent the area hit by the laser (around 1 μm^2) that is effectively too small to be representative of all the sample. Furthermore the analysis enlighted the difference between the signal recordend on bubble and on the bulk of the sample in terms of background fluorescence and signals intensities. It is possible to notice the evident differences between the two zones. Analyzing deeply the bulk Raman spectrum it is possible to see an intense fluorescence, despite the long time of photobleaching used, and the relatively low intensity of all the signals present. On the other hand, bubble Raman spectrum shows sharper peaks with a good intensity. The background shows a limited fluorescence that drift the baseline between 1700 and 0 cm^{-1}. The main drawback in this second type of analysis is the impossibility to record spectra on small bubbles because the power supplied by the laser source is able to heat up locally the solution, generating micro movements in the fluid mass, and moving out of the focal plane the bubble. Furthermore, the distribution of bubbles in liquid sample is not homogeneous and, before performing the analysis, bubbles with the correct shape must be searched. Figure 10 shows an example of two different types of bubbles commonly seen in the five smoothies analyzed: picture A shows an analyzable bubble with a circular shape; instead , picture B shows a collapsed bubble easily recognizable by the iridescent pattern.

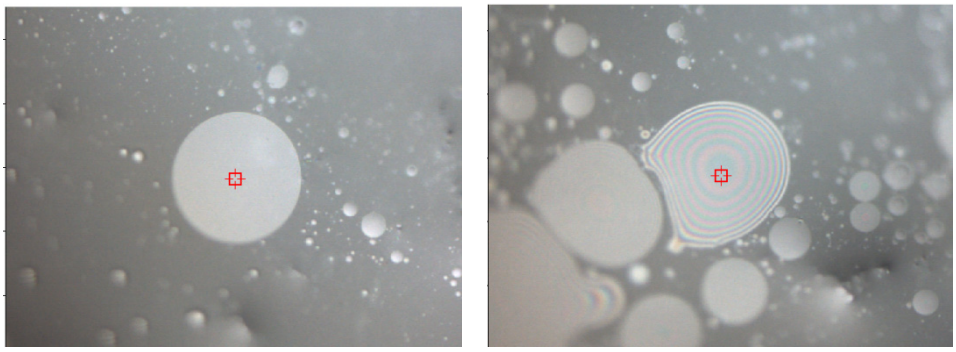

A) Recordable bubble B) Collapsed bubble

Figure 10 – Different types of bubbles.

In order to achieve a more precise description of the overall sample both zones spectra must be recorded: for each analyzed sample 3 different bulk spectra and 3 different bubble spectra were recorded; the same concentration of polyphenols was attributed to them in the calibration curve building phase. Two different sets of spectra were recorded in order to achieve large variability and full coverage of the investigated concentration range:

- Pure smoothies samples.
- Binary mix of smoothies samples.

Table 8 summarizes the polyphenols concentration of all the mix realized and checked with HPLC-MS.

Sample	Polyphenols mg kg^{-1}
MIX 1	16.6
MIX 2	13.7
MIX 3	14.1
MIX 4	11.7
MIX 5	17.0
MIX 6	9.7
MIX 7	11.2
MIX 8	12.6
MIX 9	15.1
MIX 10	15.5
MIX 11	9.5
MIX 12	8.5

Table 8 – Polyphenols concentrations of mixes used for Raman calibration curve.

Combining the spectra obtained from both mixes and common samples it is possible to calculate a calibration curve for the polyphenols in the smoothies matrix as shown in figure 11.

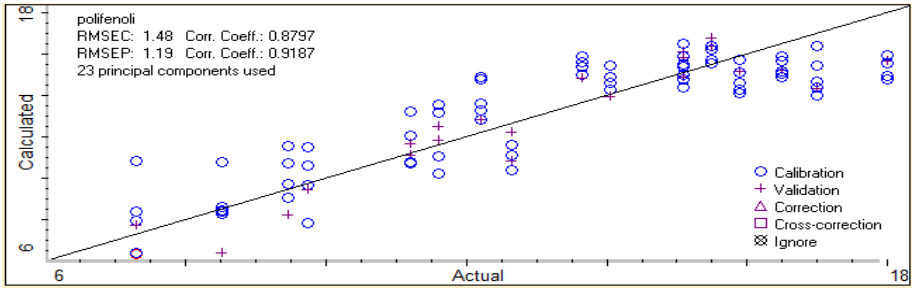

Figure 11 – Calibration curve for polyphenols using Raman spectra.

Compound	*Set*	*N° of Samples*	*Range*	R^2	*SEC-SEP*
Polyphenols	**C-SET**	102	7.3-18.0 mg kg^{-1}	0.88	1.5 mg kg^{-1}
[mg kg^{-1}]	**V-SET**	45	7.3-18.0 mg kg^{-1}	0.92	1.2 mg kg^{-1}

Table 9 – Raman polyphenols calibration curve statistical parameters.

The calibration curve was obtained with the PLS algorithm and the resulting validation and calibration set scored a R^2 coefficient of 0.88 and 0.92 respectively. These values are minor that the one calculated in the FT-NIR case but the respective standard error are smaller: 1.48 mg kg^{-1} for calibration and 1.19 mg kg^{-1} for validation (table 9). The residue, graphically reported in figure 12, shows a good progress until the 15-18 mg kg-1 region.

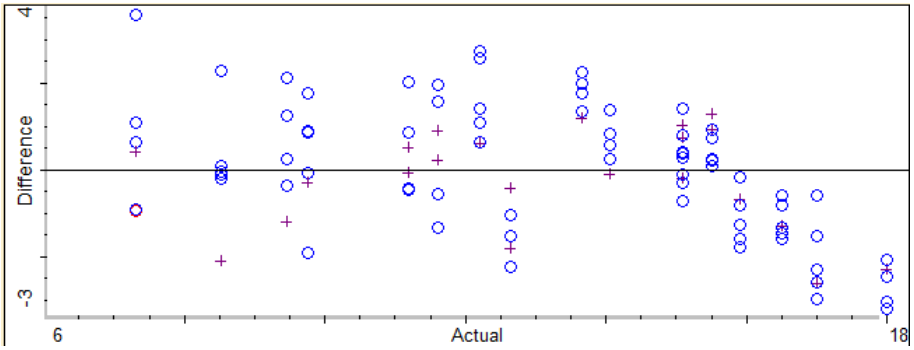

Figure 12 – Residues of the calibration curve for polyphenols.

Then the calibration curve was used for checking the total polyphenols content in real smoothies samples. All the results were summarized in table 10. Results on test samples show that the average error is still high if referred to the known concentration of polyphenols inside the beverage. Samples 4 and 5 show acceptable errors under the mg kg^{-1} and for these samples Raman spectroscopy shows to be a good solution for polyphenols content detection. Samples 1, 4 and 5 show higher errors. It is very difficult to obtains samples with a large number of readable bubbles also because, as already mentioned, the laser irradiation in a small spot generate a high density of power able to move the bubble outside the focal plane resulting in an altered spectra; this means that the laser beam result to be defocused and it excite a larger area than the one targeted at the start of the measure. This problem may be overcome using an instrument able to record the spectra of the overall sample, like the NIRFLEX N500 used for FT-NIR measurements: the future work of this research field will be focused to evaluate these different instrumental solutions.

Sample 2	**Measured polyphenols (mg kg^{-1})**	**Theoretical polyphenols (mg kg^{-1})**	**Δ (mg kg^{-1})**
Bubble 1	18,6	12,2	6,4
Bubble 2	16,1	12,2	3,9
Bubble 3	15,8	12,2	3,6
Bulk 1	15,4	12,2	3,2
Bulk 2	15,8	12,2	3,6
Bulk 3	15,3	12,2	3,1
		Average error	4.0

Sample 3	**Measured polyphenols (mg kg^{-1})**	**Theoretical polyphenols (mg kg^{-1})**	**Δ (mg kg^{-1})**
Bubble 1	15,7	18.0	-2,3
Bubble 2	16.0	18.0	-2,0
Bubble 3	16,8	18.0	-1,2
Bulk 1	16,6	18.0	-1,4
Bulk 2	15,4	18.0	-2,6
Bulk 3	16.0	18.0	-2,0
		Average error	-1,9

Sample 4	Measured polyphenols (mg kg^{-1})	Theoretical polyphenols (mg kg^{-1})	Δ (mg kg^{-1})
Bubble 1	15,5	15,1	0,4
Bubble 2	16,8	15,1	1,7
Bubble 3	15,6	15,1	0,5
Bulk 1	15,2	15,1	0,1
Bulk 2	16,5	15,1	1,4
Bulk 3	14,8	15,1	-0,3
		Average error	0,6

Sample 5	Measured polyphenols (mg kg^{-1})	Theoretical polyphenols (mg kg^{-1})	Δ (mg kg^{-1})
Bubble 1	14,8	15,9	-1,1
Bubble 2	18,3	15,9	2,4
Bubble 3	15,3	15,9	-0,5
Bulk 1	16,8	15,9	0,9
Bulk 2	14,8	15,9	-1,1
		Average error	0,1

Sample 1	Measured polyphenols (mg kg^{-1})	Theoretical polyphenols (mg kg^{-1})	Δ (mg kg^{-1})
Bubble 1	12.0	7,3	4,7
Bubble 2	14,2	7,3	6,9
Bubble 3	10,3	7,3	3,0
Bulk 1	9,7	7,3	2,4
Bulk 2	8,2	7,3	1.0
Bulk 3	4,9	7,3	-2,4
		Average error	2,6

Table 10 – Overall results on real samples.

6.5 Conclusions

The analysis of bitter taste molecular markers in inhomogeneous beverage like smoothies appears to be very difficult. FT-NIR is not able to discriminate between samples because the reflected NIR light has a too low intensity due to water absorption. Stripping water with nitrogen lead to a series of samples in which the residual moisture content is till to relevant to permit a further reproducible FT-NIR measurement. Raman microscopy shows the possibility to see the polyphenols in the mg kg^{-1} range, but errors are still high for recording the real sample concentration.

Raman spectroscopy is promising, but its use with the smoothies requires an instrument able to make bulk measurements.

6.6 Acknowledgements

The author would like to thank Massimiliano Rocchia (Thermo-Fischer) for help and fruitful discussions.

References

[1] "Melamine detection by mid- and near-infrared (MIR/NIR) spectroscopy: A quick and sensitive method for dairy products analysis including liquid milk, infant formula, and milk powder"; Balabin R. M., Smirnov S. V.; Talanta, Vol. 85, Pg. 562–568 (2011).

[2] "Issues in development of NIR micro spectrometer system for on-line process monitoring of milk product"; Brennan D., Alderman J., Sattler L., O'Connor B., O'Mathuna C.; Measurement, Vol. 33, Pg. 67–74 (2003).

[3] "Rapid Determination of Tetracycline in Milk by FT-MIR and FT-NIR Spectroscopy"; Sivakesava S., Irudayaraj J.; Journal of Dairy Science, Vol. 85, Pg. 487–493 (2002).

[4] "Determination of ethanol in fuel ethanol and beverages by Fourier transform (FT)-near infrared and FT-Raman spectrometries"; Mendes L. S., Oliveira F. C.C., Suarez P. A.Z., Rubim J. C.; Analytica Chimica Acta, Vol. 493, Pg. 219–231 (2003).

[5] "Classification of distilled alcoholic beverages and verification of adulteration by near infrared spectrometry"; Pontes M.J.C., Santos S.R.B., Arau´ jo M.C.U., Almeida L.F., Lima R.A.C., Gaia˜o E.N., Souto U.T.C.P.; Food Research International, Vol. 39 Pg. 182–189 (2006).

[6] "Comparison of non-invasive NIR and Raman spectrometries for determination of alcohol content of spirits"; Nordon A., Mills A., Burn R. T., Cusick F. M., Littlejohn D.; Analytica Chimica Acta, Vol. 548, Pg. 148–158 (2005).

[7] "Rapid analysis of sugars in fruit juices by FT-NIR spectroscopy"; Rodriguez-Saona L. E., Fry F. S., McLaughlin M. A., Calvey E. M.; Carbohydrate Research, Vol. 336, Pg. 63–74 (2001).

[8] "PLS-NIR determination of total sugar, glucose, fructose and sucrose in aqueous solutions of fruit juices"; Rambla F.J., Garrigues S., de la Guardia M.; Analytica Chimica Acta, Vol. 344, Pg. 41-53 (1997).

[9] "Differentiation of apple juice samples on the basis of heat treatment and variety using chemometric analysis of MIR and NIR data"; Reid L. M., Woodcock T., O_Donnell C. P., Kelly J. D., Downey G.; Food Research International, Vol. 38, Pg.1109–1115 (2005).

[10] "Nondestructive measurement of the internal quality of bayberry juice using Vis/NIR spectroscopy"; Y. Shao, Y. He; Journal of Food Engineering, Vol. 79, Pg.1015–1019 (2007).

[11] "Biosynthesis of purine alkaloids in *Camellia* plants."; Ashihara H., Kubota H.; Plant Cell Physiology, Vol**.** 28, Pg**.** 535–539 (1987).

[12] "Plant Polyphenols: Chemical Properties, Biological Activities, and Synthesis"; Quideau S., Deffieux D., Douat-Casassus C., Pouysegu L.; Angewandte Chemie International Edition, Vol. 50, Nr. 3, Pg. 586–621 (2011).

[13] "Infrared And Raman Spectroscopy Principles And Spectral Interpretation"; Larkin P.; ISBN: 978-0-12-386984-5, Elsevier (2011).

[14] "A Quantitative Raman Spectroscopic Signal for Metal−Phosphodiester Interactions in Solution**";** Christian E. L., Anderson V. E., Carey P. R. and Harris M. E.; *Biochemistry*, Vol. 49, Nr.13, Pg. 2869–2879 (2010).

[15] "Quantitative Raman analysis of free carbon in polymer-derived ceramics"; Jiang T., Wang Y., Wang Y., Orlovskaya N., An L.; Journal of the American Ceramic Society, Vol. 92, Nr.10, Pg. 2455-2458 (2009).

[16] "Visible micro-Raman spectroscopy for determining glucose content in beverage industry"; Delfino I., Camerlingo C., Portaccio M., Della Ventura B., Mita L., Mita D.G., Lepore M.; Food Chemistry, Vol. 127, Nr. 2, Pg. 735–742 (2011).

[17] "Quantitative Analysis of the Banned Food Dye Sudan-1 Using Surface Enhanced Raman Scattering with Multivariate Chemometrics"; Cheung W., Shadi I. T., Xu Y., and Goodacre R.; Journal of Physical Chemistry C, Vol. 114, Pg. 7285–7290 (2010).

TNT taggants sensing in the gas phase

7

7.1 INTRODUCTION

An explosive is a material, either a pure single substance or a mixture of substances, which is capable of producing an explosion by its own energy [1]. Generally explosives are thermodynamically unstable and, when exposed to heating or shocks, they start exothermic reactions of decomposition. For common organic explosives the deflagration starts in presence of oxygen producing water, nitrogen oxides and carbon oxides [2].

All the explosives can be subdivided into two categories on the basis of their sensibility to shock and energy produced:

- **Primary Explosives**, explode or detonate when they are heated or subjected to shock without burning.

- **Secondary Explosives**, detonate under the influence of the shock of the explosion of a suitable primary explosive. They do not function by burning; in fact, not all of them are combustible, but most of them can be ignited by a flame and in small amount generally burn safely and can be extinguished easily.

Generally primary explosives are used as detonator and they are present in low concentration in the final device. On the other hand secondary explosives are present in large quantities because they are the main constituent of the explosive charge.

In the last decade the interest in the development of new analytical techniques able to detect secondary explosives in trace level increased. This is due to three major tasks concerning explosives : (i) the detection of explosives in sensible locations like airports; (ii) the monitoring of soil near explosives depot or near sites were the explosives are buried (minefield for example); (iii) the identification explosives in suspicious objects. Traditional security measures used in airports are focused on the detection of weapons or metallic objects using metal detectors in combination with X-ray. These techniques have the major problem that cannot be used for the direct detection of the explosives and in recent years explosives were manufactured avoiding metallic parts in order to elude the baggage screening systems. So the principal systems for the detection of explosives are based on the analysis of the volatile organic compounds presents in the air. A new issue arose using these techniques and it is due to the low vapor pressure generally shown by explosives. In order to solve this problem during sampling, different materials, selective toward a specific class of molecules, can be used to concentrate explosives trace in air.

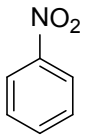

Nitrobenzene
(NB)
B.P. 210-211°C

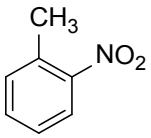

2-Nitrotoluene
(2-NT)
B.P. 222 °C

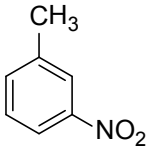

3-Nitrotoluene
(3-NT)
B.P. 231.9 °C

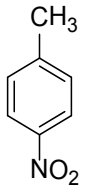

4-Nitrotoluene
(4-NT)
B.P. 238 °C

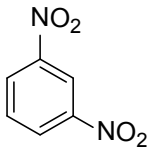

1,3-Dinitrobenzene
B.P. 301.5 °C

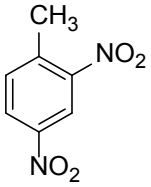

2,4-
Dinitrotoluene
(2,4-DNT)
B.P. 331.5 °C

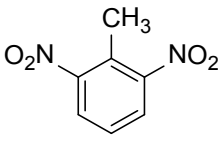

2,6-Dinitrotoluene
(2,6-DNT)
B.P. 278.2 °C

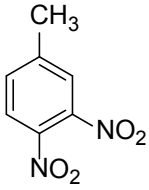

3,4-
Dinitrotoluene
(3,4-DNT)
B.P. 350.8 °C

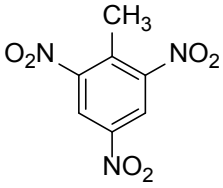

2,4,6-Trinitrotoluene
(TNT)
B.P. 409.9 °C

Figure 1. Taggant molecules present inside TNT based explosive and their boiling points

Most of the energetic materials used by military as explosives are organic compounds containing nitro groups bounded to aliphatic or aromatic scaffolds. Different classes of these substances were synthesized in the last century, but one the most employed explosive is TNT (2,4,6-trinitrotoluene). The reasons concerning its large diffusion are mainly its thermal stability in absence of oxidizers and its simple handling, due to the

low melting point (80°C), which make possible to melt it and handle it in safety to fill ammunitions of different dimensions. It can be found in various composite explosives in combination with inorganic salts or other nitroaromatic explosives like RDX (1,3,5-Trinitroperhydro-1,3,5-triazine) or HMX (Octahydro-1,3,5,7-tetranitro-1,3,5,7-tetrazocine). More in general explosives with this structure can be found in soil, as contaminant, near artillery crater or in proximity of the explosives manufacturing site or ammunition warehouse. Detecting TNT using a simple GC is a difficult task due to the low vapor pressure (0.0004 torr at 25°C [3]). Commonly explosive are filled with inert molecules (taggant) that don't participate to the deflagration, but are used for tracing the explosive itself in case that it will be used for illicit purposes [4]. The taggant molecules presents inside the TNT are mononitrotoluenes (2-NT, 3-NT and 4-NT) and dinitrotoluenes (2,4-DNT and 2,6 -DNT). They posses also high boiling points (Figure 1) and they can be concentrated using dynamic headspace sampling (DHS) techniques before injecting the sample in the GC. Many articles can be found in literature about detection of TNT using appropriate materials for the preconcentration phase like, for example, molecular imprinted polymers (MIP) [5-6] or SPME fibers [7-9]. All of these materials own the ability to concentrate the taggant but they have not sufficient selectivity toward a specific class of molecules. In order to enhance the selectivity toward the taggants appropriate receptors, tailored on the general structure of nitroaromatic compound like TNT or DNTs, must be synthesized. A receptor able to interact via multiple weak interaction can be used to enhance the selectivity toward nitroaromatic compounds. The supramolecular approach to analytical chemistry is particularly appealing due to the possibility of designing selective receptors in function of the analytes to be detected. Previous studies, made in our laboratories, proved the possibilities to enhance the selectivity of a common SPME fiber through the use of specifically designated supramolecular receptors [10]. The same approach can be used, combined with the rational design of the receptor itself, to enhance the sensibility and the specificity of the trapping device toward nitroaromatic compounds. A covalent approach in the detection would result in an irreversible saturation of receptors. Instead the use of multiple weak interaction makes possible to obtain reversible interactions used to develop a material provided of reversibility of responses. This new receptor can be used as trapping material to concentrate explosive taggants in a gas stream or can be used in a sol-gel to develop a new more specific coating for SPME.

7.2 Receptor design

The design of an appropriate receptor for TNT taggants has been based on our first experience in selective detection of aromatic compounds with tetraquinoxaline-

bridged cavitands (4QxCav). The molecular recognition properties of 4QxCav toward aromatic hydrocarbons like benzene and toluene are well documented both in the gas phase [11] and in the solid state [12]. In both cases π-π and CH-π interactions [13] are responsible for the observed complexation, both with the quinoxaline cavity walls [14] and with the resorcinarene scaffold [15]. These multiple weak interactions, made possible by the complete confinement of the guest within the cavity, render 4QxCav cavitands the receptor of choice for selecting aromatic over aliphatic hydrocarbons. The transfer of these complexation properties at the gas-solid interface has been already proven with QxCav in gas sensing [16] using both mass [17] and surface plasmon resonance transducers [18]. Extraction of micro pollutants from water using 4QxCav in pure form has also been demonstrated [19]. In the latter case, selectivity in the inclusion has been attributed to the hydrophobicity of the guest, which prefers cavity inclusion to water solvation. SPME gel-coating based on 4QxCav as receptor has also been developed and proposed as a valid alternative to commercial fibers for selective determination of benzene and chlorobenzene at ultra-trace levels in environmental air and water samples.

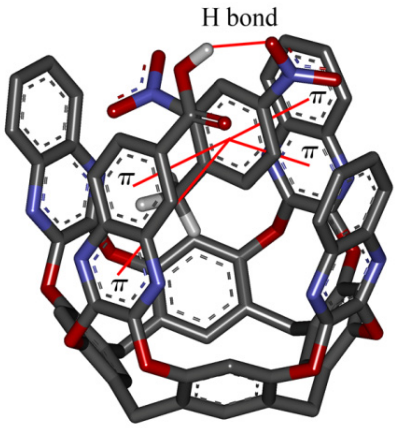

4QxCOOHCav

Figure 2. Proposed interaction mode between the designed receptors and a TNT taggant (2,4 DNT)

The CH-π interactions alone are not able to grant sufficient selectivity to the receptor toward TNT taggants. In order to accomplish this task a second weak interaction must be added to the receptor (Figure 2). The presence of the COOH introduces an additional synergistic H-bonding interaction with the NO_2 group of the guest. The carboxylic acid can be placed as fourth bridge in the cavitand skeleton

(3QxCOOHCav, figure 3d) or directly attached to one of the quinoxaline walls (4QxCOOHCav, figure 3c). Previous studies demonstrated that 3QxCOOHCav was a good trapping material for TNT taggants. However its reduced thermal stability near the desorption temperatures made impossible to use it as reusable trapping material. Decomposition started with the decarboxylation of the COOH present as fourth bridge in the cavitand upper rim.

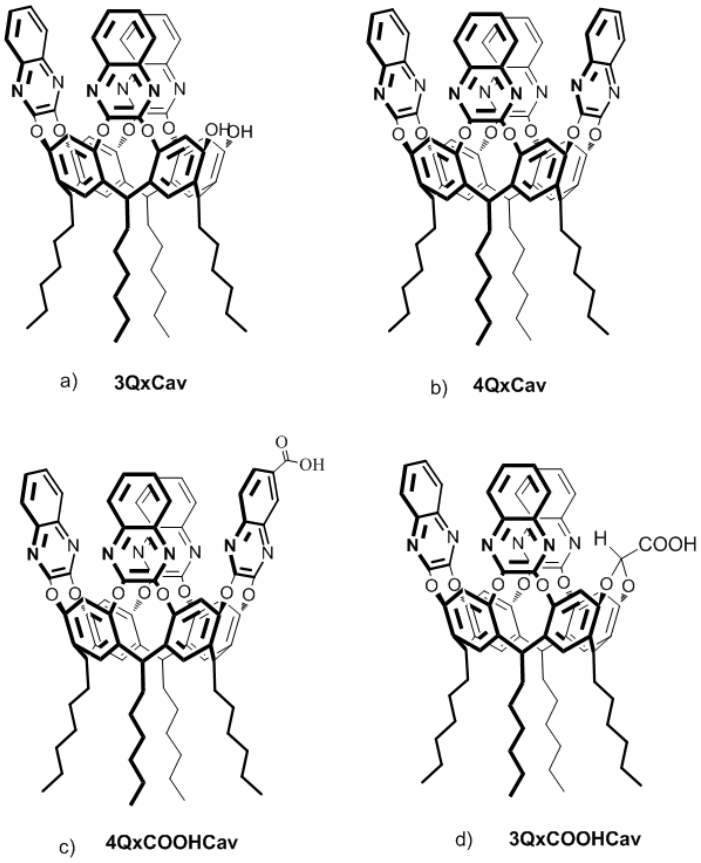

Figure 3. Target receptors a) 3QxCav, b) 4QxCav, c) 4QxCOOHCav, d) 3QxCOOHCav.

This problem can be overcome moving the COOH group on top of the QxCav cavity, directly attached to one of the quinoxaline wall. The presence of the acid directly attached to the quinoxaline ring will improve the thermal stability, suppressing thermal decarboxylation. In figure 2 the proposed complexation mode of a typical TNT taggant (2,4 DNT) is shown for 4QxCOOHCav.

All the synthesized receptors have been tested with DHS and SPME sampling techniques in order to verify their selectivity toward TNT taggants. In particular receptors 3QxCav and 4QxCav (Figure 3a and 3b) are used as references, in the purge and trap experiments, because they do not have H-bonding donor groups but only quinoxaline walls able of π-π and CH-π interactions. The comparison of the behavior of these two cavitands with the 4QxCOOHCav is important to highlight if the presence of carboxyl group enhances the taggants complexation. 4QxCOOHCav will be compared with commercial DHS and SPME trapping material commonly used in forensic studies.

7.3 Receptors synthesis

The preparation of the target molecules involve a multistep process starting from the synthesis of 4QxCav.

All the receptors were synthesized starting from a triquinoxaline cavitand (3QxCav) whose synthesis is reported in the literature [21]. This reaction was carried out following the established procedures for the preparation 4QxCav of homo-bridged cavitands (scheme 1). Resorcin[4]arene was treated with 2,3-dichloroquinoxaline in the presence of K_2CO_3 to give tetraquinoxaline-bridged cavitand (4QxCav) in good yield (80%).

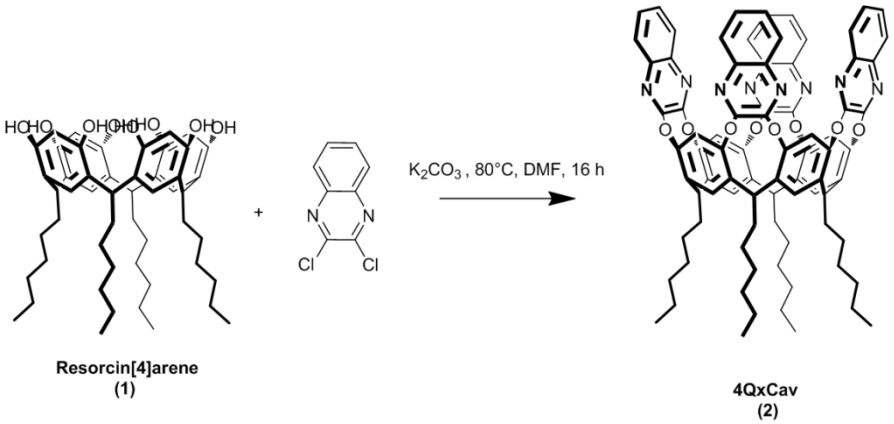

Scheme 1 – Synthesis of 4QxCav

In the second step the triquinoxaline resorcinarene **3** was made following the procedure reported in literature for the selective excision of quinoxaline units from tetraquinoxaline cavitand [21]. This reaction requires the use of a stoichiometric amount of catechol in the presence of CsF as base and provide a selective removal of a quinoxaline moiety with yield around 50 %. This reaction is preferred instead the direct

synthesis using 2,3 dichloroquinoxaline and resorcin[4]arene due to the high overall yield (50 % instead of 20 %) and the easy of purification.

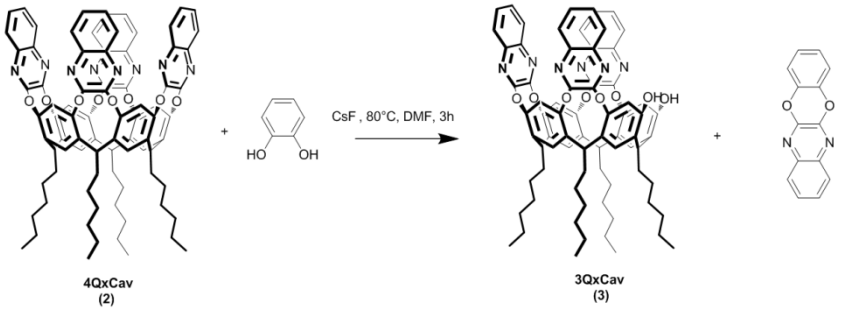

Scheme 2 – Synthesis of 3QxCav by Quinoxaline excision reaction

In order to synthesize 4QxCOOHCav a 2,3-dichloroquinoxaline bearing a carboxylic acid **5** is required. According to scheme 3 the quinoxaline was synthesized starting from 3,4-diaminobenzoic acid and oxalic acid reacted in acid media obtaining the corresponding dioxoquinoline **4a** in a quantitative yield. **4a** is then reacted with thionyl chloride in presence of catalytic amount of dimethylformamide (DMF). Compound **4b** is not isolated, but it is reacted with a large excess of water resulting in the formation of 2,3-dichloroquinoxaline-6-carboxylic acid **5** with a 90 % yield.

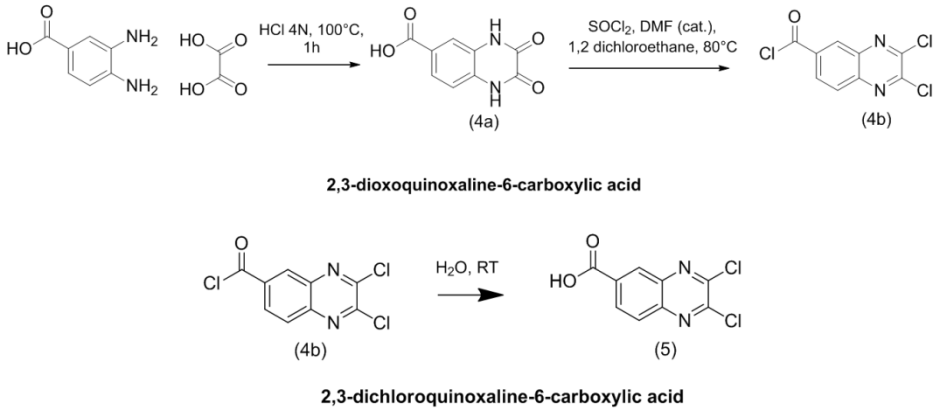

Scheme 3 – Synthesis of 2,3-dichloroquinoxaline-6-carboxylic acid

Compound **5** is then reacted with the resorcinarene **3** in presence of K_2CO_3 to give the cavitand **6** in 20 % yield according to scheme 4. The unreacted **3** is recovered and further reacted leading to a quasi-quantitative yield over several passages.

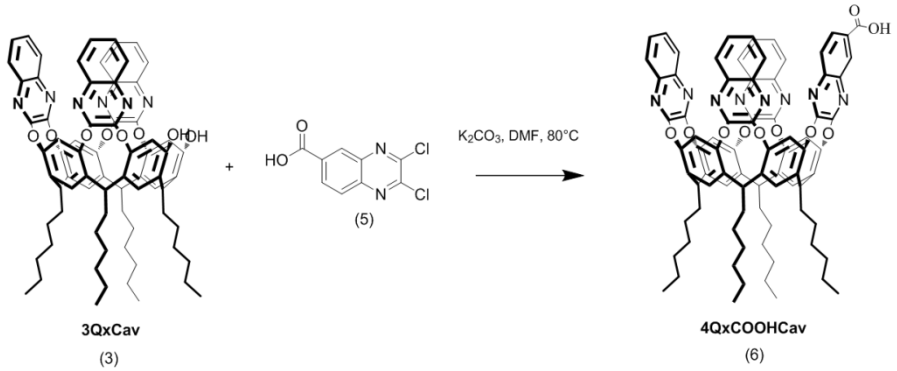

Scheme 4 – Synthesis of 4QxCOOHCav

This reaction leads to the formation of two enantiomers (planar chirality). The formation of **6** is confirmed on the basis of the ^{1}H NMR shown in Figure 4. The signals relative to the three aromatic protons of the substituted quinoxaline are present at low field. The triplet at 5.7 ppm is diagnostic of presence of the vase conformation in solution [22]. Therefore the installment of the COOH group on the top of the cavity does not alter cavity shape and dimensions.

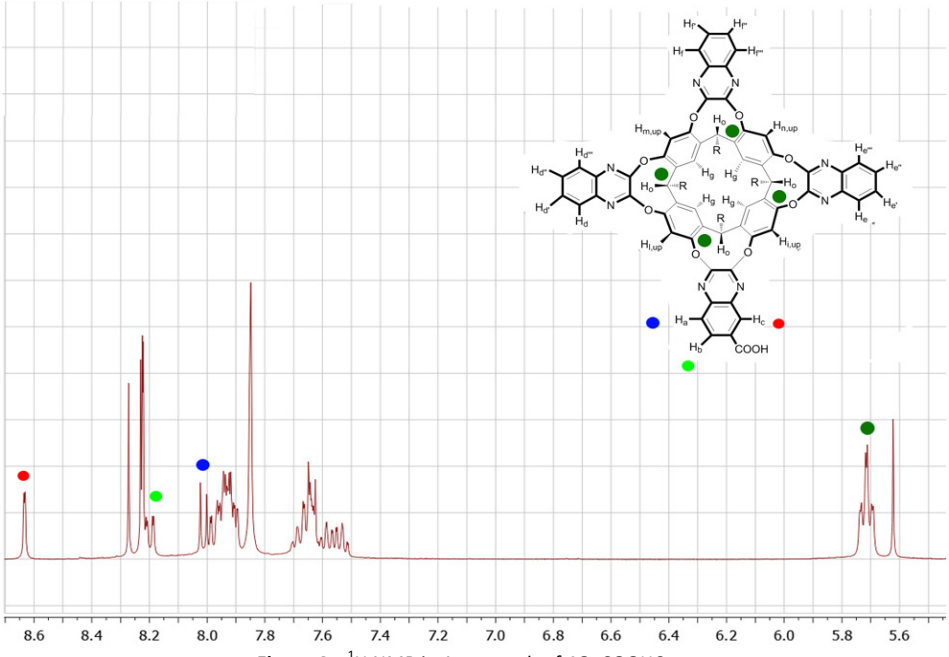

Figure 4 – ^{1}H NMR in Acetone-d_6 of 4QxCOOHCav

Also the exact mass spectrum (Figure 5) recorded with a LTQ Orbitrap XL confirm the synthesis of the cavitand **9**. The expect mass for the molecular ion was 1371.59204 m/z and the found one is 1371.59137 m/z with a difference between the two values below 0.5 ppm.

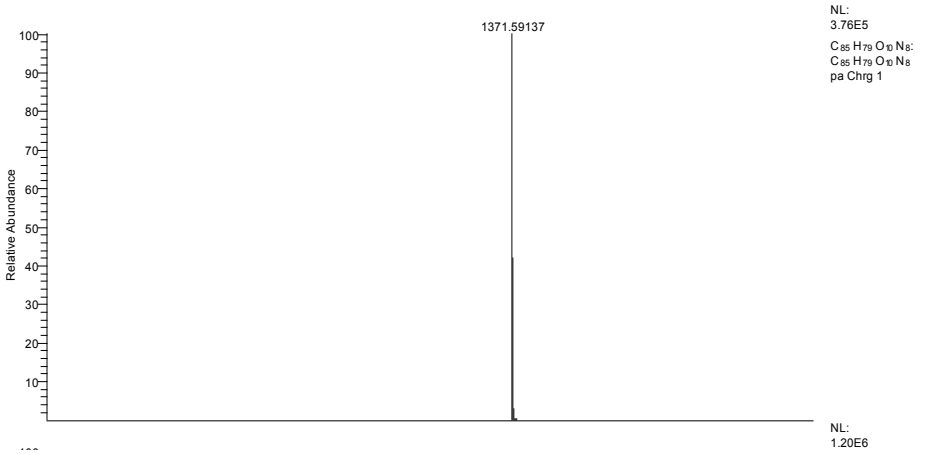

Figure 5 – Exact mass of 4QxCOOHCav

7.3.1 Thermo gravimetric analysis (TGA)

At this point, the thermal stability of 4QxCOOHCav was assessed via TGA. The thermal desorption experiment uses temperature cycles spanning from 50 °C to 200 °C typical of purge and trap experiments. Previous study conducted in our laboratory showed that cavitands bearing a carboxylic acid on the fourth bridge (3QxCOOHCav, figure 3d) are thermally unstable due to the decomposition that starts around 100 °C leading to an overall weight loss of 10%. The main problem encountered with this cavitand is its thermal instability in the operative range at which the thermal desorption trap operates. This means that it can be used only once for the determination of the presence of explosive taggants because when the temperature of thermal desorption are reached also decomposition of the cavitand takes place.

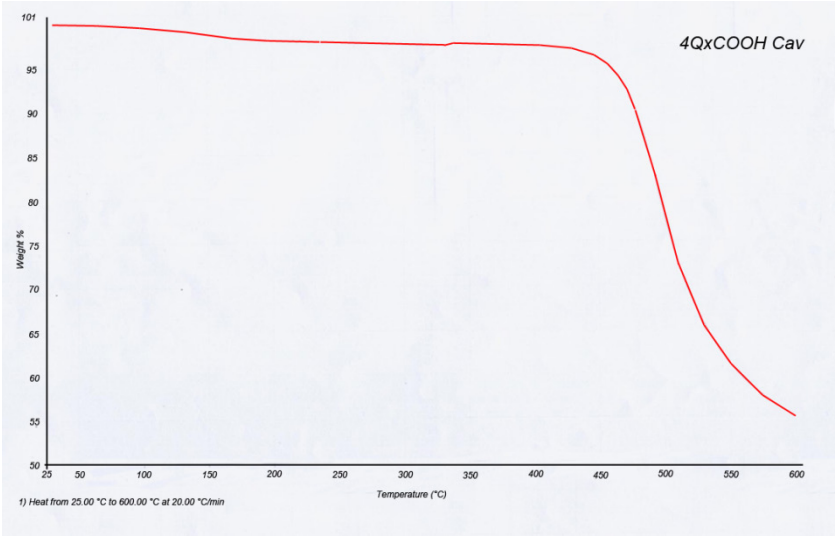

Figure 8 – TGA of cavitand 4QxCOOHCav (6); temperature scan rate : 20°C/min in air atmosphere.

The thermal stability of the receptor increased up to 450°C, as shown by TGA (Figure 8). This improvement is due to the conjugation of the carboxylic moiety with the aromatic ring of a quinoxaline wall, that suppresses decarboxylation at purge and trap working temperatures. The analysis is repeated also for the references 3QxCav and 4QxCav that remain both stable up to 450 °C and be can be used several time without incurring in decomposition.

7.4 Purge and trap experiments

The aim of this part of the work is the analytical testing of new materials that can be used for trapping nitroaromatic taggant molecules. Two different techniques for the taggant detection were used:

- Dynamic Headspace (DHS)
- Solid Phase Micro Extraction (SPME)

The DHS technique [23] (Figure 9) is based on the continuous transfer of volatile compounds present in a condensed phase into a gas phase (headspace). The volatiles are purged from the headspace with a flow of inert gas and can either be analyzed directly [24] or, more commonly, they are trapped [25] either cryogenically or on a solid adsorbent. Then the trapped compounds are rapidly desorbed raising the

temperature up to 250 °C an injected in the GC for the detection and the quantification. DHS allows to use directly the cavitand in the trap without any further derivatization or immobilization on surfaces. In this way the complexing capabilities of the cavitands bearing carboxylic acid are compared to reference cavitands bearing four and three quinoxaline walls. The major limitation of this technique is due to the volatility of the analyzed compounds. Only molecules with a relatively low boiling point like mononitrotoluenes (MNTs) can be analyzed.

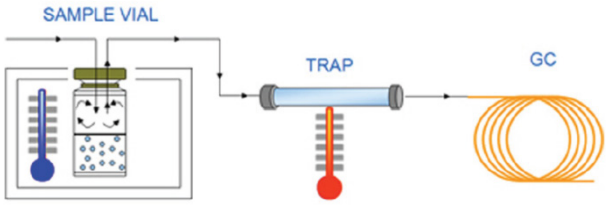

Figure 9 – Scheme of Dynamic Headspace apparatus.

The second approach used to test the complexing capability of 4QxCOOHCav is based on SPME (figure 10). The trapping device previously used is now replaced by the fiber itself coated with the cavitand **6**.

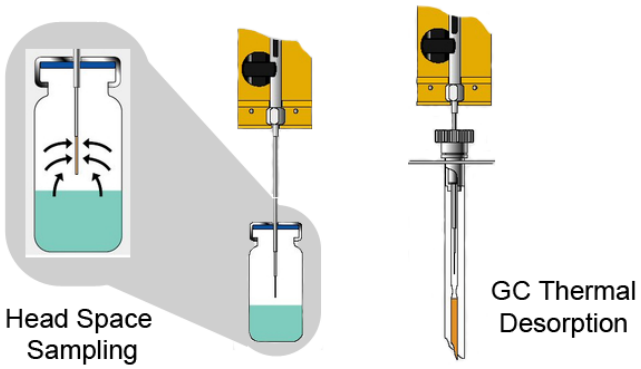

Figure 10 – SPME apparatus and procedure.

The fiber is realized attaching the cavitand, in the form of a fine powder, to a silicon needle with the help of a epoxy glue. The cavitand is only physiadsorbed on the surface of the polymeric matrix and not covalently linked to the resin. Analysis in this

case are performed closing a sample (both liquid and solid samples can be analyzed) in a sealed vial. The fiber is inserted in the headspace of the vial and then heated at 75 °C for 30 minutes. Then, the fiber is introduced in the GC inlet for thermal desorption and for the chromatographic run. This technique allows us to analyze all the taggant molecules (dinitrotoluenes and mononitrotoluenes) and the TNT itself in a single chromatographic run.

7.4.1 GC-DHS analysis (Mononitroaromatics)

The complexing capabilities of 4QxCOOHCav are tested for nitroaromatics detection with respect to 3QxCav and 4QxCav in order to verify the importance of the presence of a carboxylic group. The analyses conducted with DHS are focused on the detection of MNTs. A solution containing toluene, nitrobenzene, 2-nitrotoluene, 3-nitrotoluene and 4-nitrotoluene at the concentration of 50 µg/L (in pentane) is used as test solution. The toluene is used because is a typical guest molecule for quinoxaline based cavitand and in this case its presence is used to demonstrate the selectivity toward nitroaromatics molecules. Different desorption temperatures (50, 100, 150, 200, 250°C) were used in order to identify the best temperature to promote the analytes desorption. The releasing of the analytes at low temperature indicates a low complexing capacity of the cavitand. Also at low temperature all the molecules not retained inside the cavity but adsorbed via weak dispersion interactions out of the cavity are released. On the opposite, release at high temperatures indicates the inclusion of the target molecule inside the cavity.
All the three cavitands were tested separately at different temperatures. Results obtained with 4QxCav (Figure 11) show that at 50 °C all the analytes are retained inside the cavity and temperatures between 100 and 150 °C are needed for the desorption. At these temperatures nitrobenzene and 2-nitrotoluene are released with good selectivity and this is due to their relatively high volatility. As previously mentioned this indicates a low specificity toward nitroaromatic because only π-π stacking interaction and CH-π are possible. At higher temperature also the less volatile taggant (3- and 4-nitrotoluene) are released.

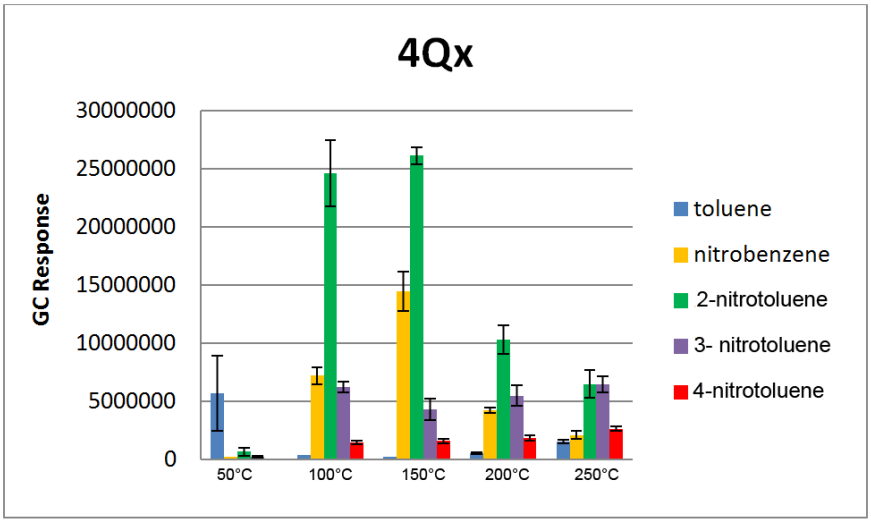

Figure 11 – DHS analysis at different temperature for 4QxCav.

The other reference cavitand tested is 3QxCav (Figure 12); in this case the releasing pattern of the analytes is the has similar behavior for all the analytes up to 250°C. In absolute terms all the response are lower than in the previous case and this fact indicates a very low selectivity toward nitroaromatics but also toluene. This different behavior is due to the open cavity that does not allow the analytes inclusion.

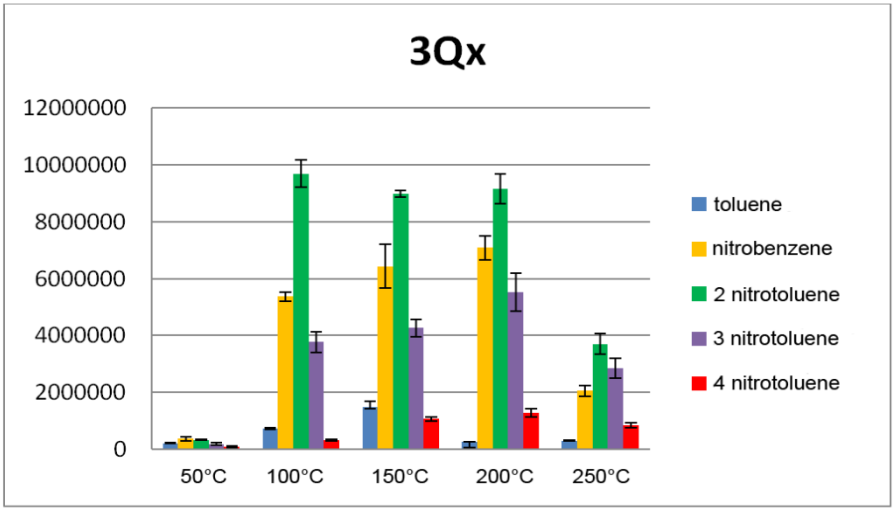

Figure 12 – DHS analysis at different temperature for 3QxCav.

3QxCav present an open conformation with only three quinoxaline walls at the upper rim. The lack of a quinoxaline wall as fourth bridge jeopardizes the retention of the TNT taggants and the presence of two hydroxyl groups rim is not sufficient to guarantee H-bonding for taggants complexation. These two aspects contribute to an overall performances lower that the one obtained with 4QxCav.

The behavior of 4QxCOOHCav is completely different (Figure 13). No release of the adsorbed molecules before 100°C is observed. The best results are obtained at 200°C and in this case the peaks area of the analytes is 20 times higher than the ones recorded at the same temperature with 4QxCav. The presence of a carboxylic acid at the upper rim enhances the selectivity toward nitroaromatics compound making 4QxCOOHCav a good candidate for the development of taggant trapping materials.

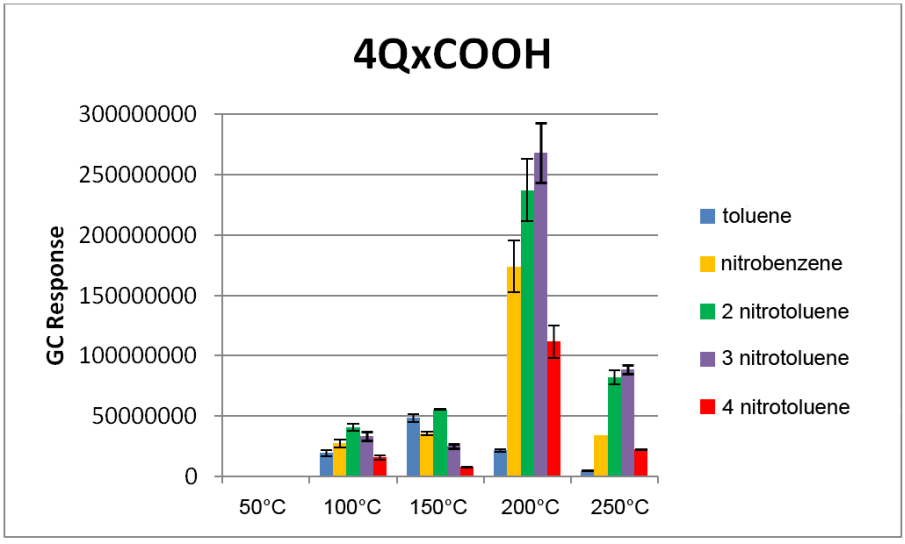

Figure 13 – DHS analysis at different temperature for 4QxCOOHCav.

In figure 14 the desorption of the three cavitands are compared at the same temperature in order to compare the trapping capabilities of the three receptors.

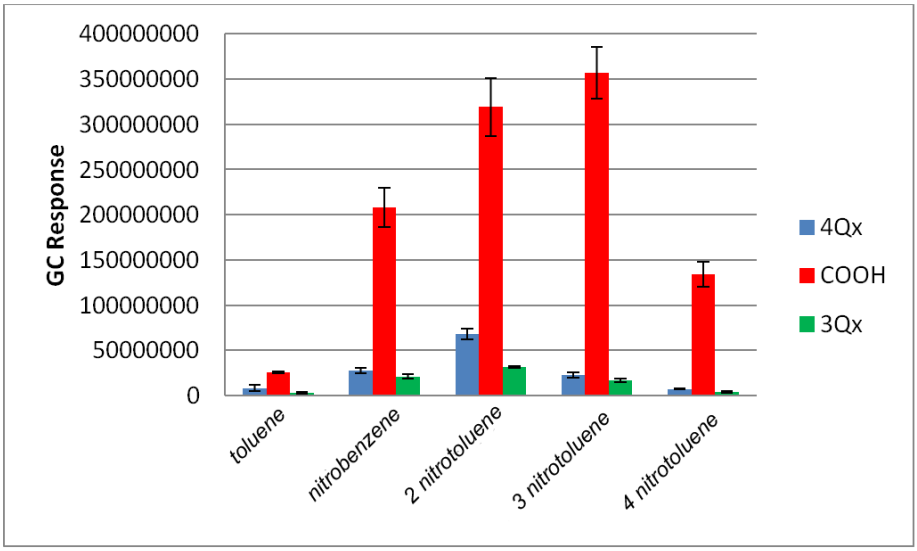

Figure 14 – Comparison of 4QxCav, 3QxCav and 4QxCOOHCav at 250°C.

The cavitand 4QxCOOHCav (red bars) retains the largest quantities of all the analytes with respect to the other two control cavitands 3QxCav (green bars) and 4QxCav (blue bars). In all cases the analyte less retained is toluene since it does not present a nitro group available to H-bonding and it is the lowest boiling point. the presence of a single nitro group able to interact with the carboxylic moiety via hydrogen bonding in MNTs boosts complexation by 4QxCOOHCav. Interestingly, among MNTs, p-nitrotoluene is the less retained despite of its higher boiling point. This bias cannot be explained at this point in the absence of crystal structure of the complexes.

7.4.2 DHS analysis of hydrocarbons

In order to verify the selectivity of the cavitand 4QxCOOHCav and its reference 4QxCav a trapping test in presence of different hydrocarbons was done. Linear hydrocarbons are the major interferents present in air. A solution of 5 different hydrocarbons at the concentration of 500 µg/L was used for this experiment. The extraction was repeated for every cavitand at different temperature form 50 °C to 250 °C with step of 50°C. Competitive experiments with both taggants and hydrocarbons showed that the two classes of analytes do not interfere in the desorption experiments.

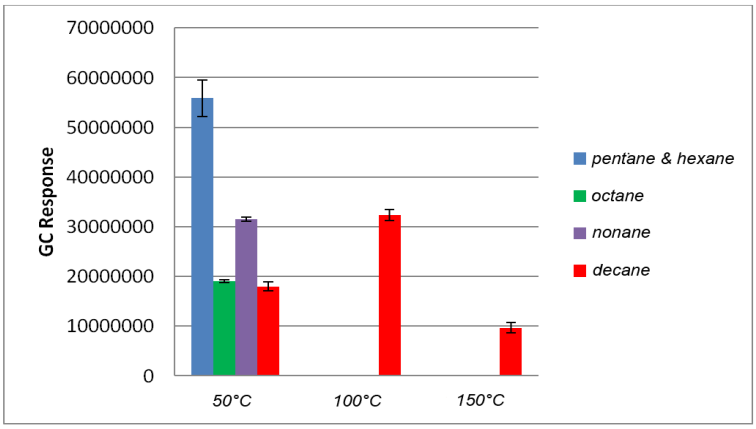

Figure 15 – Complexation of hydrocarbons at different temperature made by 4QxCav.

The results for 4QxCav are shown in figure 15. The hydrocarbons are totally released already at 50°C; decane is the only one with a significant value at 100°C. Results for higher temperature are not shown because no hydrocarbons are revealed.
4QxCOOHCav shows a similar behavior with retention of all the hydrocarbons at 50°C. The pentane is the most absorbed in both cases because it is the solvent of the solution so its concentration is far higher than the others analytes. At temperature higher than 200°C no hydrocarbons retention is seen. These experiments suggest that linear hydrocarbons are partially retained outside the cavity by the multiple weak dispersion interaction with the apolar chain at the lower rim of the cavitand. The higher retention of decane can be explained with its boiling point (174°C).

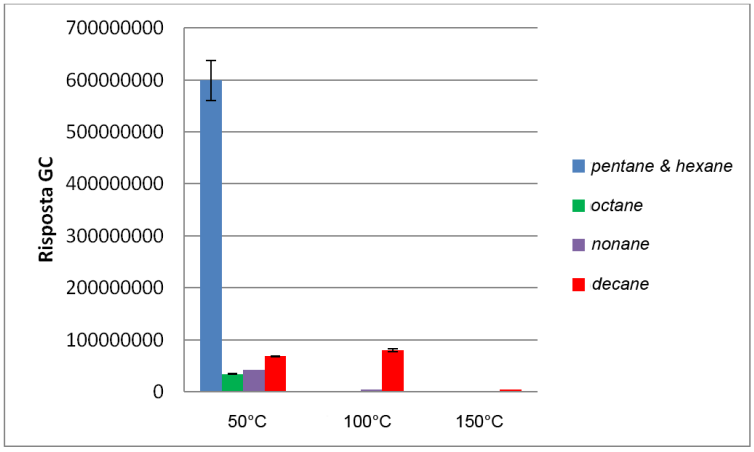

Figure 16 – Complexation of hydrocarbons at different temperature made by 4QxCOOHCav.

Therefore the hydrocarbon interference can be avoided by desorbing first at 50-100°C to remove hydrocarbons and then raising to 250°C to desorb the desired analytes retained in the trap.

7.4.3 DHS analysis (Comparison with commercial traps)

The two cavitands (4QxCav and 4QxCOOHCav) are compared with a commercial polymer matrix commonly used for explosives detection based on 2,6-diphenylene dioxide (TENAX®). In this experiment three different traps filled respectively with 4QxCav, 4QxCOOHCav and TENAX® are compared in DHS desorbing at 250°C (Figure 17).

The results highlighted a lower response of the commercial polymer and 4QxCav compared to 4QxCOOHCav. The response toward nitrotoluenes is at least 30 times higher compared to the one obtained with TENAX®. This is a great advantage because taggants in explosives are present in very low concentration and an analytical technique able to detect them requires first of all low LOD (limit of detection).

Overall, the trap formed by 4QxCOOH turned out to be at the same time very selective and highly sensitive to nitroaromatics, by far better than commercially available traps (Figure 17).

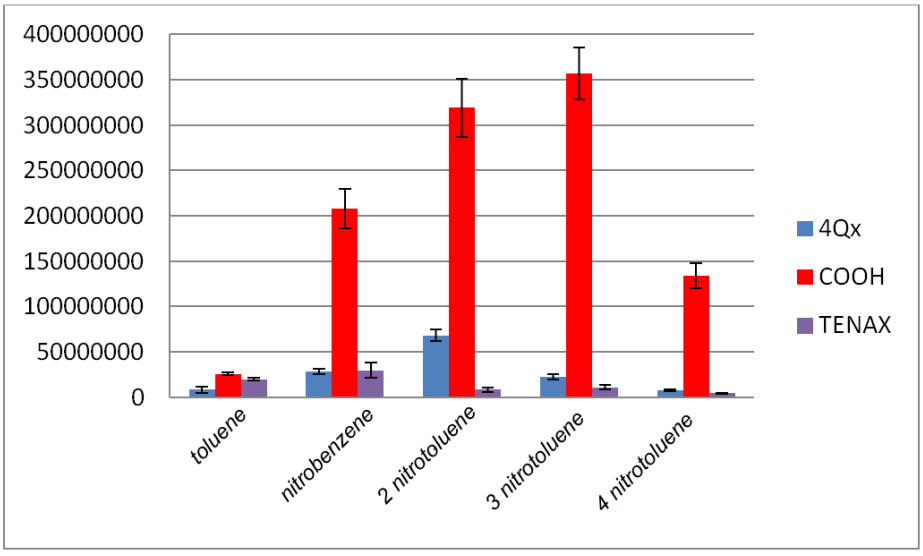

Figure 17 – Comparison between 4QxCav, 4QxCOOHCav and TENAX at 250°C.

The main limit consists in the DHS sampling that force to detect only volatile molecules like MNTs. In order to overcome this limit a SPME method is needed.

7.4.4 SPME analysis (4QxCOOHCav and 4QxCav based fibers)

The 4QxCOOHCav is placed on a SPME fiber in order to expand the application to dinitrotoluenes and TNT detection.

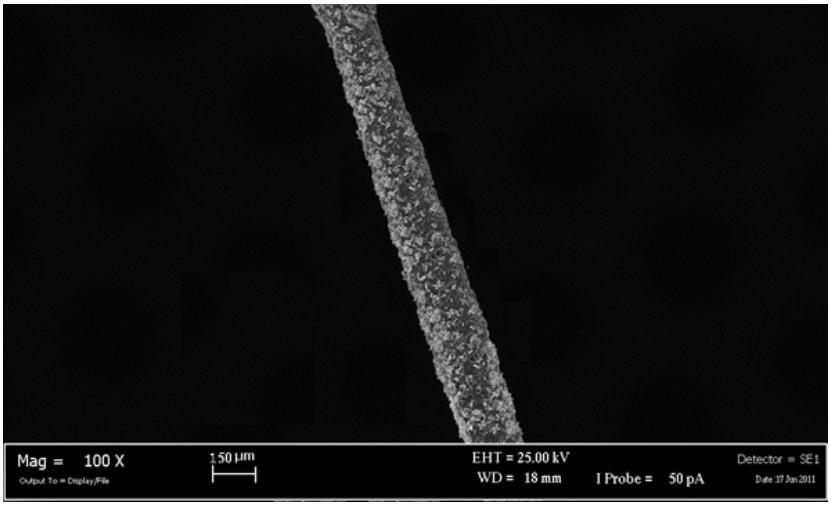

Figure 18 – 4QxCOOHCav coated silicon support for SPME.

The cavitand, in fine powder form, is placed on a silicon support with the help of an epoxy glue resistant at high temperature. In Figure 18 a SEM image of the coating recorded with a LEICA CAMBRIDGE 430i with EDX OXFORD ISIS working at 25 kV at distance of 18mm is shown. The dispersion of the cavitand on the surface is homogeneous and the calculated average thickness of the film is 50±4 µm. Working in DHS it is not possible to analyze DNTs; the presence Si-OH groups in the glass tube used for the analysis, in the connection between the trap and the GC, retain all these molecules via multiple H-bonds with nitro groups. This problem can be overcome using a silicon fiber for sampling because no more connection is needed for the GC injection.
In this case we used a test solution containing toluene, nitrobenzene, 2-nitrotoluene, 3-nitrotoluene, 4-nitrotoluene, 1,3-dinitrobenzene, 2,4-dinitrotoluene, 2-6-dinitrotoluene, 3,4-dinitrotoluene e 2,4,6-trinitrotoluene at the concentration of 50 ng/L (3 order of magnitude lower than the one analyzed in DHS).
The extractions are performed on the headspace of a 10 mL vial at 75°C for 30 minutes and the two fibers made with 4QxCOOHCav and 4QxCav are compared.

The results are showed in Figure 19. This experiment confirmed the higher retention capacity of 4QxCOOHCav also towards DNTs and TNT itself (Figure 19).

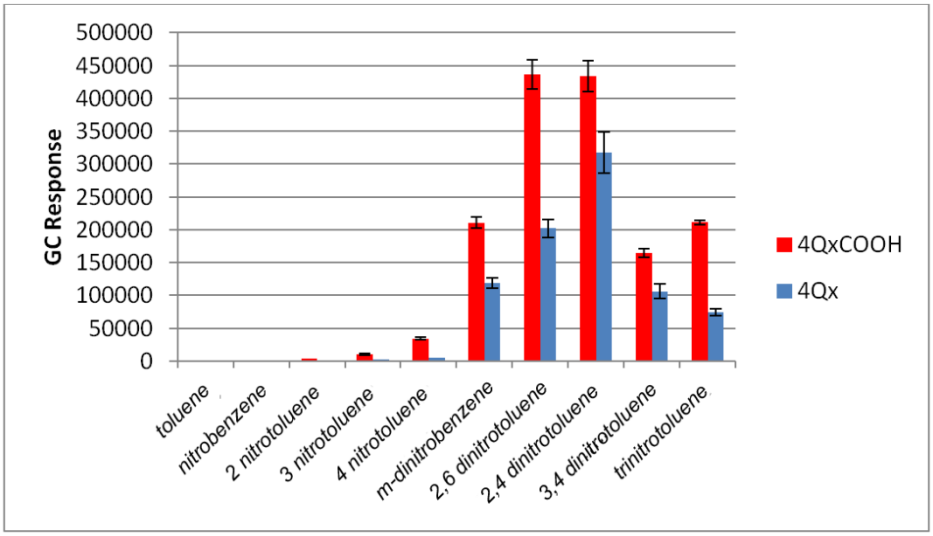

Figure 19 – Comparison between 4QxCOOHCav and 4QxCav coated silicon support for SPME with desorption at 200°C.

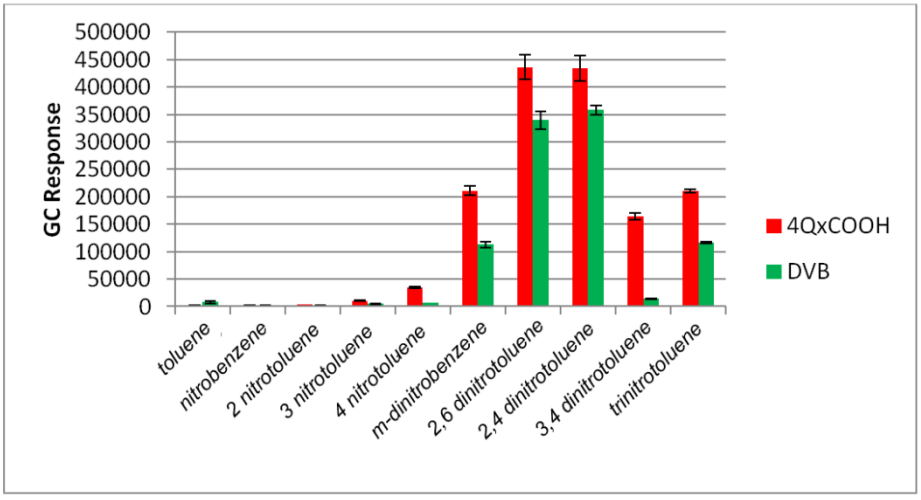

Figure 20 – Comparison between 4QxCOOHCav and PDMS-DVB with desorption at 200°C.

Also in this case the 4QxCOOHCav fiber was compared with a commercial one: PDMS-DVB (poly dimethylsiloxane and divinilbenzene copolymer) with a 65 µm thickness. This commercial fiber chosen for its affinity toward aromatic compounds due to the π-π stacking interaction between the aromatic ring of the polymer and the ones of the taggants. In the case of the comparison with DVB coated SPME fiber, the 4QxCOOHCav fiber is more sensitive than the commercial one (Figure 20).
The analytes are absorbed with relative responses 1 to 12 times higher than the commercial fiber. The one based on PDMS-DVB gives better results only in the case of toluene were the response is 20 time higher than the cavitand.

7.4.5 SPME analysis (Unknown explosive sample)

The last experiment was performed on unknown explosive sample provided by RIS (Reparti Investigazioni Scientifiche) of Parma. The solid was analyzed with the 4QxCOOHCav fiber in SPME and in the same conditions of desorption. In Figure 21 the results are shown. The chromatographic results show the presence of TNT and mainly the 2,4 DNT and 2,6 DNT as taggant. These two compounds are byproducts of the explosive manufacturing.

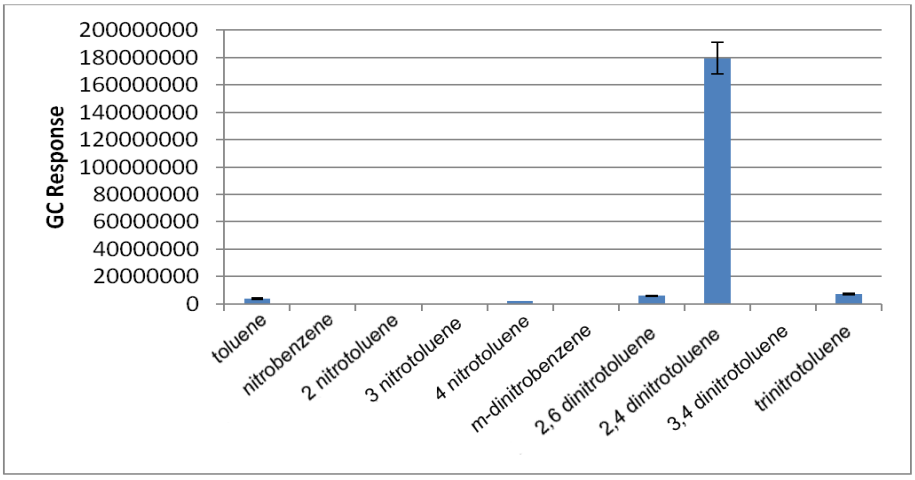

Figure 21 – Analysis of an explosive sample with 4QxCOOHCav fiber with desorption at 200°C.

Traces of 4-nitrotoluene are also present. The correct attribution of the unknown sample underlines the potential of 4QxCOOHCav in supramolecular analytical chemistry.

7.5 Conclusions

In this work a new receptor for the TNT taggants was synthesized and characterized. Its thermal stability up to 450°C in air was demonstrated by TGA. This result led to the possibility to use this receptor in purge and trap experiments in order to determine the selective uptake of both MNTs and DNTs. Preliminary studies executed on standard solutions showed that 4QxCOOHCav cavitand is a good supramolecular receptor for nitroaromatic compounds.
Further studies, focused on the comparison of the trapping capabilities of 4QxCOOHCav and commercially available materials, demonstrated the selective uptake of TNT taggants classes at trace level.

7.6 Acknowledgements

Special thanks to Dr. Federica Bianchi of the University of Parma and Nicolò Riboni for DHS/SPME studies and also to Andrea Sartori of the University of Parma.

7.7 Experimental Section

7.7.1 Material and Chemicals.

Resorcinol (98% purity), 2,3-Dichloroquinoxaline (96% purity), Catechol (99% purity, recrystallized from toluene), 3,4-Diaminobenzoic acid (99% purity), Oxalic acid (99% purity), Ethyldichloroacetic acid (99% purity), Sodium Hydroxide (99% purity), Potassium carbonate (99% purity), Thionyl chloride (99% purity), o-Dichlorobenzene (99% purity), Dimethylformammide (99% purity) were purchased by Sigma Aldrich.

7.7.2 Synthesis of Quinoxaline based cavitands

For the synthesis, all solvents were dried over 3 and 4 Å molecular sieves. Resorcinarene Res[C_6H_{13}, H]) was prepared according to a literature procedure [21] ^{1}H NMR spectra were recorded on a Bruker Avance 300 (300 MHz) spectrometer (Bruker, Karlsruhe, Germany), on a Bruker Avance 400 (400MHz) and on a Varian Inova 600 (600MHz) spectrometer and all chemical shifts (δ) were reported in parts per million (ppm) relative to proton resonances resulting from incomplete deuteration of NMR solvents. The electrospray (ESI) mass spectra were acquired on a Waters ACQUILITY SQD detector equipped with an ESCi multimode-APCI/ESI-ionization (Waters, Milford, MA). Exact mass spectra were recorded using a LTQ Orbitrap XL Thermo**.** Column chromatography was performed using silica gel 60 (Merck 70-230 mesh).
All the receptors were synthesized starting from a triquinoxaline-bridged resorcinarene (3QxCav) whose synthesis is reported in the literature[21].

Cavitand 2 (4QxCav)

To a solution of resorcinarene (R= C_6H_{13}) (1.60 g, 1.95 mmol) in dry DMF (36 mL), 2,3-dichloroquinoxaline (1.71 g, 8.58 mmol) and K_2CO_3 (3.20g, 23.00 mol) were added. The mixture was heated and stirred for 16 h at 80°C. The reaction was quenched by addiction of acidic water (with HCl) and the precipitate was filtered, washed with water, and dried. The crude product was crystallized from ethyl acetate: chloroform (9:1 v/v) to afford the pure product as white solid (1.30 g, 51%).

^{1}H NMR ($CDCl_3$, 300 MHz): δ= 8.15 (s, 4H, ArH_{up}), 7.79 (m, 8H, Ar*H* AA' part of an AA'BB' system), 7.46 (m, 8H, Ar*H* BB' part of an AA'BB' system), 7.21 (s, 4H, ArH_{down}), 5.57 (t, 4H, ArC*H*, J=7.9 Hz), 2.26 (m, 8H, ArCHCH_2), 1.48-1.31 (m, 32H, -CH_2-), 0.93 (t, 12H, -CH_3, *J=6.8*);

ESI-MS: *m/z* 1330 $[M+H]^+$.

Resorcinarene 3 (3QxCav)

A solution of tetraquinoxaline cavitand **2** (1.85 g, 1.39 mmol) and CsF (4.23 g, 30.00 mmol) in dry DMF (250 mL) heated to 90°C, catechol (0.16 g, 1.45 mmol) was added. The mixture was heated and stirred for 3 h at 90°C. The reaction was quenched by pouring into 300 mL of ice-cold brine, and the precipitate was filtered, washed with water, and dried. The crude product was purified by column chromatography (SiO_2, gradient from 100% CH_2Cl_2 to 90/10, CH_2Cl_2:EtOAc, v/v) affording triquinoxaline resorcinarene **3** as a pale yellow solid (886 mg, 53%).

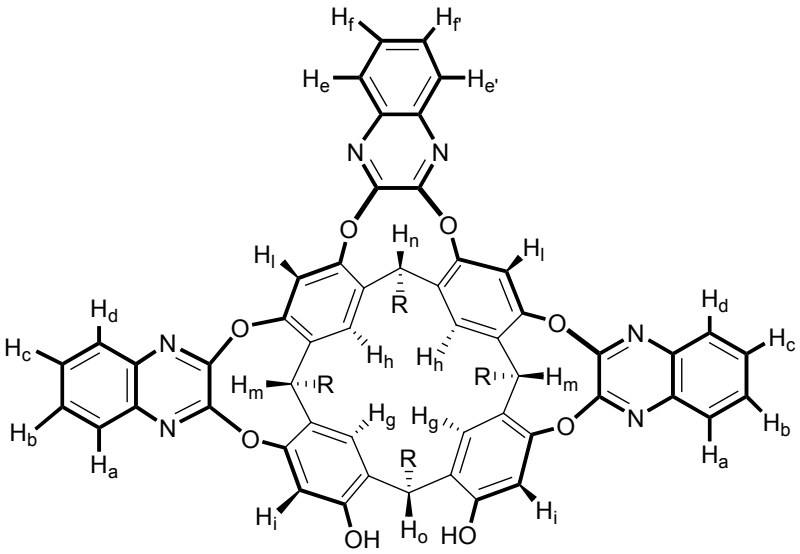

^{1}H NMR ($CDCl_3$, 300 MHz) δ= 8.25 (s, 2H, Ar$H_{l,up}$), 7.94 (m, 2H, H_d part D of an ABCD system), 7.82 (m, 2H, H_e e $H_{e'}$ part AA' of an AA'BB' system), 7.68 (m, 2H, H_a part A of an ABCD system), 7.58 (m, 2H, H_c part C of an ABCD system), 7.54-7.46 (m**,** 4H, H_f e $H_{f'}$ part BB' of an AA'BB'system + H_b part B of an ABCD system), 7.28 (s, 2H, Ar$H_{i,up}$), 7.14 (s, 2H, Ar$H_{h,down}$), 7.09 (s, 2H, Ar$H_{g,down}$), 5.60 (t, 1H, ArCH_n, J=8.2 Hz), 5.53 (t, 2H, ArCH_m, J=8.1 Hz), 4.26 (t, 1H, ArCH_o, J=8.2 Hz), 2.17 (m, 8H, ArCHCH_2-), 1.57-1.23 (m, 32H, -CH_2-), 0.90 (m, 12H, -CH_3);

ESI-MS: m/z 1203 $[M+H]^+$, m/z 1225 $[M+Na]^+$, m/z 1241 $[M+K]^+$.

2,3-dioxoquinoxaline-6-carboxylic acid (4a)

A solution of 3,4-diaminobenzoic acid (4 g, 26.3 mmol) dissolved in 30 mL of HCl 4N was added to a solution of oxalic acid (2.64 g, 29.3 mmol) dissolved in 30 mL of HCl 4N.

The resulting mixture was heated at reflux overnight. The reaction was quenched pouring into 100 mL of ice-cold water and the precipitate was filtered, washed with water, and dried affording 2,3-dioxoquinoxaline-6-carboxylic acid in a quantitative yield as purple solid.

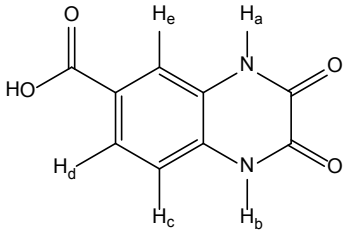

^{1}**H NMR** (DMSO, 400 MHz) δ= 12.19 (s, 1H NH_a), 12.07 (s, 1H, NH_b), 7.73 (s, 1H, H_e), 7.65 (d, 1H, H_d, *J=8.32Hz*), 7.17 (d, 1H, H_c, *J=8.32Hz*)

2,3-dichloroquinoxaline-6-carboxylic acid (5)

To a solution of **4a** (1.000 g, 0.617 mmol) and DMF (0.100 mL) dissolved in 30 mL of o-dichlorobenzene thionyl chloride (5.869 g, 4.93 mmol) was added dropwise. The resulting solution was heated at 80°C overnight. The reaction was cooled to room temperature and 15 mL of distilled water were added. The two-phase solution was stirred for 30 minutes and then the organic layer was collected and dried with Na_2SO_4. The solvent was removed under vacuum affording 2,3-dichloroquinoxaline-6-carboxylic acid with a 90% yield as tan grey solid.

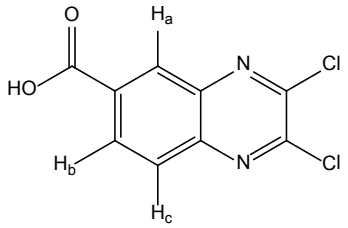

^{1}**H NMR** (DMSO, 400 MHz) δ= 10.18 (bs, 1H, COOH), 8.52 (d, 1H, H_a, J_{meta}=3.24 Hz), 8.34 (dd, 1H, H_b , J_{orto}=8.32Hz, J_{meta}=3.24 Hz), 8.16 (d, 1H, H_c, J_{orto}=8.32Hz).

Cavitand 6 (4QxCOOHCav)

To a stirred solution of triquinoxaline resorcinarene **3** (0.40 g, 0.33 mmol) and K_2CO_3 (0.16 g, 1.15 mmol) in dry DMF (11 mL), 2,3-dichloroquinoxaline-6-carboxylic acid (0.088 g, 0.36 mmol) was added. The mixture was heated at 80°C overnight and then

quenched in acidic water (HCl 1N). The precipitate obtained was filtered and washed to neutrality. The crude product was purified by column chromatography (SiO_2, 9/1, CH_2Cl_2/ EtOH, v/v) affording **6** (96 mg) as a white solid. The recovered resorcinarene **3** is further reacted, bringing the overall yield is close to 100%.

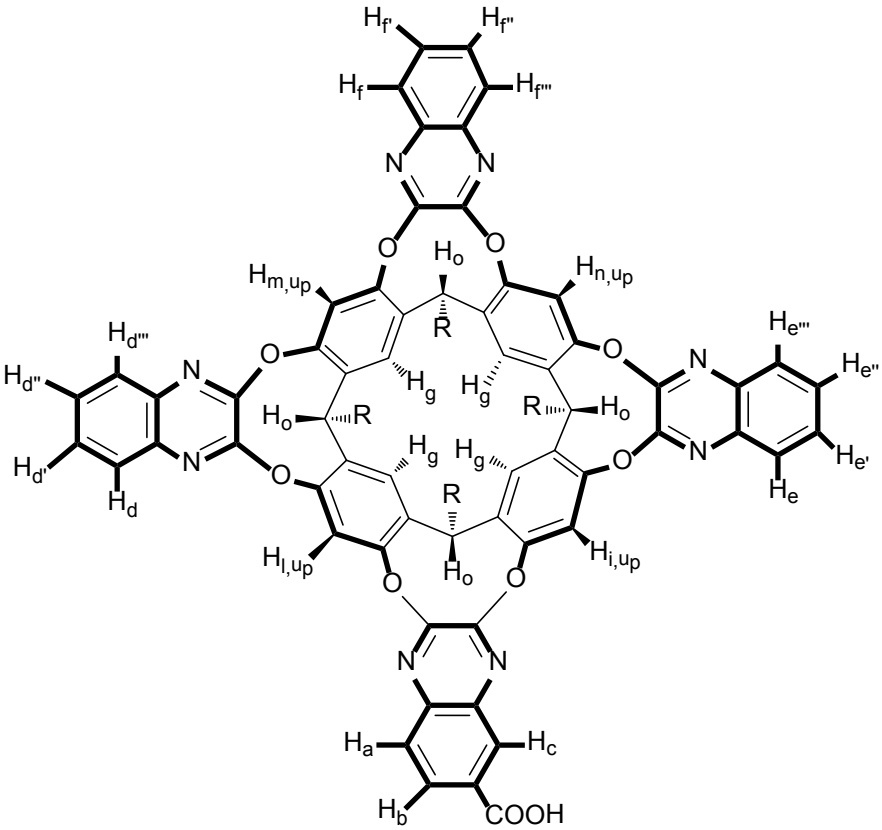

^{1}H NMR (DMSO, 400 MHz) δ= 8.63 (d, 1H, H_c, J_{meta}= 4.1Hz), 8.27 (s, 1H, $H_{i,up}$), 8.23 (s, 1H, $H_{l,up}$), 8.22 (m, 2H, $H_{m,up}$ + $H_{n,up}$), 8.20 (dd, 1H, H_b, J_{orto}=8.2Hz, J_{meta}=4.1 Hz), 8.01 (d, 1H, Ha, J_{orto}=8.2 Hz), 7.99-7.89 (m, 8H, H_d + $H_{d'}$ + $H_{d''}$ + $H_{d'''}$ + H_e + $H_{e'}$ + $H_{e''}$ + $H_{e'''}$), 7.85 (s, 4H, $H_{g,down}$), 7.70-7.51 (m, 4H, H_f + $H_{f'}$ + $H_{f''}$ + $H_{f'''}$), 5.71 (t, 4H, H_o, J=8.2 Hz), 2.46 (m, 8H, $ArCHCH_2$-), 1.57-1.23 (m, 32H, $-CH_2$-), 0.94 (m, 12H, $-CH_3$).

Exact mass: m/z calculated for $C_{85}H_{79}O_{10}N_8[M-H]^-$: 1371.59191 found: 1371.59137

7.7.3 Traps preparation and conditioning

Traps were prepared by introducing 54 mg of each cavitand (**3QxCav, 4QxCav and 4QxCOOHCav)** in glass tubes (l= 16 cm, i.d.= 3.5 mm). Fiberglass was put at the edges and the tubes were closed with Swagelock caps.
The traps were conditioned in the injector of the gas chromatograph at 140°C for about 14 hours under nitrogen

7.7.4 Dynamic Headspace (DHS)

Pre-concentration of the analytes:
The analytes were purged for 30 minutes with a flow of nitrogen (40 mL/min) from the headspace of a 50 mL flask containing stirred solution at 70°C.
Thermal desorption:
The analytes were desorbed in the GC injector using a thermal desorber (Tekmar, TD800, Fisons Instruments, MI, Italy).
The desorption process has required four steps:
- pre cooling: the cryogenic trap was cooled down using liquid nitrogen at -120°C;
- desorption: the carrier gas (He, 10 mL/min) was flown into the trap kept at the temperature of 50°C or 250°C and the desorbed analytes were transported into the cryogenic trap;
- injection: the cryogenic trap was quickly heated and the analytes were injected into the GC in 0.6 minutes through a transfer line keep at high temperature;
- bake : the cryogenic trap was heated and cleaned by flowing carrier gas in the opposite way as before.
Commercial Polymer used for comparison experiment: Tenax® 20/35 Mesh, Superchrom (Milano, Italia)

7.7.5 Solution preparation

Solutions of toluene, nitrobenzene, 2-nitrotoluene, 3-nitrotoluene, 4-nitrotoluene, 1,3-dinitrobenzene, 2,4-dinitrotoluene, 2-6-dinitrotoluene, 3,4-dinitrotoluene e 2,4,6-trinitrotoluene at the concentration of 1000 mg/L were obtained from pure compounds in 1 mL vials using acetonitrile as solvent. Solutions of pentane, hexane, heptanes, octane, nonane and decane at the concentration of 500 mg/L were obtained from pure compounds in 1 mL vials using n-pentane as solvent. Working solutions at the concentration of 50 µg/L and 50 ng/L were obtained by dilution from the stock solutions.

7.7.6 SPME Sampling

Preparation of the fiber: The cavitand, in fine powder form, is placed on a silicon support with the help of an epoxy resin resistant at high temperature. SEM image of the coating is recorded with a LEICA CAMBRIDGE 430i with EDX OXFORD ISIS working at 25 kV at distance of 18mm.

Extraction in Headspace: A solution containing each analyte at 50 ng/L is placed in 10 mL vial at 75°C for 30 minutes in the presence of the Fiber.

Commercial Fiber used for comparison experiment: StableFlex™ , 65µm PDMS-DVB, Supelco (Milano, Italia).

7.7.7 GC-MS analysis

Gas-chromatograph HP 6890 Series Plus, Agilent Technologies (Milano, Italia):
- Column: HP5-MS (l=30 m, i.d.=0.25 mm, d.f.=0.25 µm) (Agilent Technologies);
- Carrier gas: helium
- Carrier gas flux: 1 mL/min
- Carrier gas pressure: 70 KPa.
- Injector Temp: 200°C
- Injection mode: splitless
-Temperature program : 50°C for 2 minutes (10°C/min until 200°C are reached) and then 200°C for 5 minutes (10°C/min until 260°C are reached)

Mass Spectrometer **MSD 5973, Agilent Technologies**:
- Source Temperature: 200°C;
- Transfer Line temperature: 200°C;
- Ionization: E.I. (70 eV);
-Voltage: 2200 V;
-Acquisition modality: Time scheduled monitoring;
-Solvent delay: 0.5 minutes;
- Monitored ions:

from 0.5 to 5 min:	m/z 91 e 92 per toluene
from 5 to 11 min:	m/z 51,77,123 per nitrobenzene
	m/z 65,92,120 per 2-nitrotoluene
	m/z 65,91,137 per 3-nitrotoluene
	m/z 65,91,137 per 4-nitrotoluene
from 11 to 28 min:	m/z 76,122,168 per 1,3-dinitrobenzene

m/z 89,119,165 per 2,4-dinitrotoluene
m/z 89,148,165 per 2,6-dinitrotoluene
m/z 78,89,182 per 3,4-dinitrotoluene
m/z 89,193,210 per 2,4,6 trinitrotoluene

The Mass Spectrometer has been tuned using Perfluorotributylamine and the analytes were identified on the base of the retention time of standards solution and the MS spectra reported in NIST Library (National Institute of Standards and Technology).

References

[1] "*Sensors—An effective approach for the detection of explosives*"; Singh S.; Journal of Hazardous Materials, Vol.144, Pg. 15-28 (2007).

[2] "*The scientific foundation and efficacy of the use of canines as chemical detectors for explosives*"; Furton K.G., Meyers L.J.; Talanta, Vol. 54, Pg.487-500 (2001).

[3] "*Vapour And Trace Detection Of Explosives for Anti-Terrorism Purpose*"; Krausa M., Reznev A.A., Kluwer Academic Publishers, (Dordrecht, The Nederland), p.23 (2004), ISBN 1-4020-2715-1.

[4] Convention on the Marking of Plastic Explosives for the Purpose of Identification, Montreal, 1 March 1991.

[5] "*Detection of Nitroaromatic Explosives Using a Fluorescent-Labeled Imprinted Polymer*"; Stringer R. C., Gangopadhyay S., Grant S. A.; Analytical Chemistry, Vol. 82, Pg. 4015–4019 (2010).

[6] "*Microreactor-Based Synthesis of Molecularly Imprinted Polymer Beads Used for Explosive Detection*"; Roeseling D., Tuercke T., Krause H., Loebbecke S.; Organic Process Research & Development, Vol. 13, Pg. 1007–1013 (2009).

[7] "*Identification of volatile chemical signatures from plastic explosives by SPME-GC/MS and detection by ion mobility spectrometry*"; Lai H., Leung A., Magee M., Almirall J. R.; Analytical and Bioanalytical Chemistry, Vol. 396, Pg. 2997–3007 (2010).

[8] "*Analysis of the volatile chemical markers of explosives using novel solid phase microextraction coupled to ion mobility spectrometry*"; Guerra P., Lai H., Almirall J. R.; Journal of Separation Science, Vol. 31, Pg. 2891-2898 (2008).

[9] "*Evaluating Headspace Component Vapor_Time Profiles by Solid-Phase Microextraction with External Sampling of an Internal Standard*"; MacCrehan W., Moore S., Schantz M.; Analytical Chemistry, Vol.83, Pg. 8560–8565 (2011).

[10] "*Innovative Cavitand-based Sol-gel Coatings for the Environmental Monitoring of Benzene and Chlorobenzenes via Solid-phase Microextraction*"; Bianchi F., Mattarozzi M., Betti P., Bisceglie F., Careri M., Mangia A., Sidisky L., Ongarato S., Dalcanale E., Analitical Chemistry, Vol.80, Pg. 6423-6430 (2008).

[11] "*Host-Guest Complexation in the Gas Phase by Desorption Chemical Ionization Mass Spectrometry*"; Vincenti M., Dalcanale E., Soncini P., Guglielmetti G., Journal of the American Chemical Society, Vol. 112, Pg. 445-446 (1990).

[12] "*Cavitands as Versatile Molecular Receptors*"; Soncini P., Bonsignore S., Dalcanale E., Ugozzoli F., Journal of Organic Chemistry*, Vol. 57*, Pg. 4608- 4612 (1992).

[13] "*Aromatic interactions*"; Hunter C. A., Lawson K. R., Perkins J., Urch C.J., Journal of the Chemical Society Perkin Transaction 2, Pg.651-669 (2001),

[14] "*Host-guest Complexation in the Gas Phase. Investigation of the Mechanism of Interaction between Cavitands and Neutral Guest Molecules*"; M. Vincenti, E. Dalcanale; Journal of the Chemical Society, Perkin Transaction 2, Pg. 1069-1076 (1995).

[15] "*Cavitands as Superior Sorbents for BTX Detection at Trace Level*"; Bianchi F., Pinalli R., Ugozzoli F., Spera S., Careri M., Dalcanale E.; New Journal of Chemistry*,* Vol. *27*, Pg. 502-509 (2003).

[16] "*A Supramolecular Approach to Sub-ppb Aromatic VOC Detection in Air*"; Zampolli S., Betti P., Elmi I., Dalcanale E.; *Chemical Communications,* Pg. 2790-2792 (2007).

[17] "*Chemical Sensing with Cavitands. Influence of Cavity Shape and Dimensions on the Detection of Solvent Vapors*" ; Hartmann J., Hauptmann P., Levi S., Dalcanale E.; Sensors and Actuators B, Vol. 35, Pg. 154-157 (1996).

[18] "*Influence of Cavity Depth on the Responses of SPR Sensors Coated with Self-Assembled Monolayers of Cavitands*"; Feresenbet E.B., Busi M., Ugozzoli F., Dalcanale E., Shenoy D.K.; Sensor Letters, Vol. 2, Pg. 186-193(2004).

[19] "*Removal of Organic Pollutants from Water via Molecular Inclusion within a Cavitand*"; Dalcanale E., Costantini G., Soncini P.; Journal of Inclusion Phenomena in Molecular Recognition Chemistry, Vol. 13, Pg. 87-92 (1992).

[20] "*In-Liquid Sensing of Chemical Compounds by QCM Sensors Couplet with High-Accuracy ACC Oscillator*"; Ferrari M., Ferrari V., Marioli D., Taroni A., Suman M., Dalcanale E.; IEEE Transaction on Instrument and Measurement, Vol. 55, Pg. 828-834 (2006).

[21] "*Quinoxaline Excision: A Novel Approach to Tri- and Diquinoxaline Cavitands*"; Castro P. P., Zhao G., Masangkay G. A., Hernandez C., Gutierrez-Tunstad L. M., Organic Letters, Vol. 3, Pg. 333-336 (2004).

[22] "*Vases and Kites as Cavitands*"; Moran J.R., Ericson J.L., Dalcanale E., Bryant J.A., Knobler C.B., Cram D.J.; Journal of the American Chemical Society, Vol. *113*, Pg. 5707-5714 (1991).

[23] C.F. Poole, and S.K. Poole, *Chromatography Today*, Elsevier,Oxford, 1991, p. 818.

[24] "*Volatile Organic Compound Analysis by an inertial Spray Extraction interface Coupled to an ion Trap Mass Spectrometer*"; St-Germain F., Mamer O., Brunet J., Vachon B., Tardif R., Abribat T., Rosiers C.D., Montgomery J.; Analytical Chemistry, Vol. 67, Pg. 4536-4541 (1995).

[25] "*Isolation and preconcentration of volatile organic compounds from water*"; Namiesnik J., Gorecki T., Biziuk M., Torres L., Analytica Chimica Acta, Vol. *237*, Pg. 1-60 (1990).

[26] "*Cavitands receptor for chiral recognition and fluorescent sensing*"; Maffei F.; Ph.D. Thesis (university of Parma, Italy).

About the author

09/1985	Born in Castelnuovo né Monti (RE), Italy
07/2004	High school diploma : “Liceo Dall’Aglio”, Castelnuovo né Monti (RE), Italy
10/2007	Bachelor in Industrial Chemistry, University of Parma, Supervisor : Enrico Dalcanale
10/2009	Master in Science and Technology of the Industrial Chemistry, University of Parma, Supervisor : Enrico Dalcanale
01/2010-12/2012	Ph.D. Research with Prof. Enrico Dalcanale (University of Parma, Italy) and Michele Suman (Barilla S.p.A., Italy)